Bhushan Taskar

The Effect of Waves on Marine Propellers and Propulsion

Thesis for the degree of Philosophiae Doctor

Trondheim, May 2017

Norwegian University of Science and Technology
Faculty of Engineering
Science and Technology
Department of MarineTechnology

NTNU
Norwegian University of
Science and Technology

NTNU
Norwegian University of Science and Technology

Thesis for the degree of Philosophiae Doctor

Faculty of Engineering
Science and Technology
Department of MarineTechnology

ISBN 978-82-326-2284-9 (printed version)
ISBN 978-82-326-2285-6 (electronic version)
ISSN 1503-8181

Doctoral theses at NTNU, 2017:106

Printed by Skipnes Kommunikasjon as

Abstract

Ship design is evolving around ever-increasing market demands in quest of competitive and cost-effective solutions. The global increase of shipping activities has raised concerns regarding the environmental impact of sea operations- transportation, fishing and exploitation of offshore resources. These conditions have driven naval architects to look for novel and energy efficient ship designs. Currently, there is increasing demand to optimize ships for actual environmental conditions i.e. in the presence of wind, waves, etc.

The work in this thesis explores the effect of waves on ship propulsion; it consists of two major parts. First, the analysis of propulsion system in the presence of waves where the effects of added resistance, wake variation, propulsion losses and propeller-engine interactions have been studied on engine efficiency, propulsion efficiency, power and RPM fluctuations in waves. It was found that the effect of waves on engine performance is relatively small, for the studied cases, however; wake variation and propulsion losses can cause considerable changes in vessel performance.

The second part deals with propeller performance in terms of cavitation, pressure pulses and efficiency in the presence of waves. The effects of wake change, speed loss, RPM variation and ship motions have been investigated. It was found that wake variations in waves has by far the largest impact on pressure pulses. Therefore, it is recommended to consider wake variation in waves while designing propellers. Due to the practical difficulties in doing this, which mainly are related to determining the wake variations, the recommended compromise is to consider the wake variation in one regular wave of length close to the ship length.

A framework of systematic analysis laid out in this thesis would be useful for analyzing different propulsion systems and propeller designs in the presence of waves. Methods and tools used in the work can be further incorporated into the optimization process to consider the effect of waves. The investigation in this thesis will help the optimization as various factors affecting the propulsion have been recognized and their effect has been quantified.

Acknowledgments

I would like to express my sincere gratitude towards Prof. Sverre Steen, for being an excellent supervisor. He provided me the freedom to explore, support when required and guidance when my steps faltered. I have enjoyed all our discussions, which were always productive and informative.

I would sincerely thank Mr. Leif Vartdal, who has played a significant role in shaping my work by providing vital inputs from the industry perspective. His support and feedback have indeed enriched my research. I also thank Mr. Jonas Eriksson for timely help and informative discussions related to CFD simulations.

I am grateful to Prof. Rickard Bensow for providing me an opportunity to work at the Chalmers University of Technology, which proved very successful. I thank Rolls-Royce University Technology Centers at Chalmers and NTNU for supporting my research stay at Chalmers. I also thank Dr. Florian Vesting and Prof. Carl-Eric Janson for the whole-hearted help.

I would like to express my gratitude towards everyone at Rolls-Royce AB for providing me the information and resources related to propeller design. Mr. Björn Schröder has been very kind and patient in answering my numerous questions about propeller design procedure.

I thank Prof. Moustafa Abdel-Maksoud whose questions, suggestions and comments were always insightful. I am pleased to have interacted with him on several occasions. I am also grateful to Prof. Bjørn Egil Asbjørnslett, Prof. Eilif Pettersen and my co-supervisor Prof. Bjørnar Pettersen for help and encouragement. I would also like to thank Kevin and Drazen for successful collaboration, which helped me extend the boundary of my research.

My parents and my sister are the very pillars of my strength. Their endless love and firm support throughout the journey has been vital. Thanks to my friends and colleagues at the Department of Marine Technology for creating lively and motivating atmosphere.

Finally, yet importantly, I would like to extend the vote of thanks to this beautiful country, Norway, which was home to me during my PhD and my motherland, India, to whom I will always be indebted.

List of Publications

The following papers are included as a part of this thesis.

1. Taskar B., Steen S., Analysis of propulsion performance of KVLCC2 in waves. Proceedings of Fourth International Symposium on Marine Propulsors (SMP'15), Austin, Texas, USA, 2015.
2. Taskar B., Yum K.K., Pedersen E., Steen S., Dynamics of a marine propulsion system with a diesel engine and a propeller subject to waves. Proceedings of 34th International Conference on Ocean, Offshore and Arctic (OMAE2015), St. John's, Newfoundland, Canada, 2015.
3. Taskar B., Yum K.K., Steen S., Pedersen E., The effect of waves on engine-propeller dynamics and propulsion performance of ships. Ocean Engineering. 2016; 122: 262-77.
4. Taskar B., Steen S., Bensow R.E., Schröder B. Effect of waves on cavitation and pressure pulses. Applied Ocean Research. 2016; 60: 61-74.
5. Taskar B., Steen S., Eriksson J., Effect of waves on cavitation and pressure pulses of a tanker with twin podded propulsion. (Accepted for publication in the Journal of Applied Ocean Research)

The PhD work also resulted in contributions to the following papers, which are not regarded as a part of this thesis, since the author's contributions were somewhat limited. In these papers, the author assisted in the modeling of propeller thrust and torque to provide correct environmental loading to the propulsion machinery in different wave conditions.

a. Yum K.K., Taskar B., Pedersen E., Steen S., Simulation of a two-stroke diesel engine for propulsion in waves. International Journal of Naval Architecture and Ocean Engineering. 2016.
b. Yum K.K., Skjong S., Taskar B., Pedersen E., Steen S., Simulation of a hybrid marine propulsion system in waves. Proceedings of 28th CIMAC World Congress, Helsinki, June 2016.

List of Variables

λ	Wavelength
A	Wave amplitude
L	Ship length
w	Taylor wake fraction
t’	Thrust deduction fraction
ω_e	Wave encounter circular frequency
ξ_a	Surge amplitude with phase delay of ζ_ξ
ζ_ξ	Phase delay
ω	Wave circular frequency
h_a	Wave amplitude
k	Wave number
U	Ship speed
$(x_P, 0, z_P)$	Propeller co-ordinates
t	Time
T	Wave encounter period
X	Wave encounter angle (0 for following sea; 180 for head sea)
α	Coefficient representing effect of wave amplitude decrease at the stern
w_P	Effective wake fraction
V_{mean}	Time averaged wake velocity considering the effect of pitching motion
V_{total}	Total wake velocity considering mean increase as well as wake fluctuations
x	Longitudinal distance of the propeller from the center of gravity of the ship
$\Delta\bar{p}$	Pressure gradient below the bottom of the ship due to pitching motion
η_5	Pitch amplitude
N	Propeller RPM
D	Propeller diameter (m)
Z	Number of blades
d	Distance from r/R = 0.9 to a position on the submerged hull when the blade is at the top dead center position (m)
R	Propeller radius (m)
w_{Tmax}	Maximum value of the Taylor wake fraction in the propeller disc

w_e	Mean effective full-scale Taylor wake fraction
h	Depth to the shaft center line
p_0	Non-cavitating contribution to pressure pulses
p_c	Cavitating contribution to pressure pulses
p_z	Total pressure pulses
a_1	Friction coefficient for the main engine[1]
a_2	Friction coefficient of the propulsion shaft[1]

Note: Notation of some variables is different in appended papers. Please refer the list of variables in each paper for the correct representation of variables.

[1] Variables used in Paper 2

Contents

1. Introduction

1.1 Background and Motivation

Global warming due to the anthropogenic emissions of greenhouse gases poses a serious threat. To limit this problem, a steep reduction in the emission of greenhouse gases is necessary. Shipping industry being a major contributor to the global CO_2 emissions will have to face this challenging task of reducing the emissions even though global trade is increasing.

The industry is striving for higher efficiency and lower emissions as a result of competition in the market combined with environmental regulations, like the EEDI and emission control areas. The challenge is to increase the efficiency and reduce the emissions while still assuring a high level of safety and reliability. This challenge is addressed by researchers, ship designers and ship builders, as well as ship owners and operators. One such research effort is the Low Energy and Emission Design of Ships (LEEDS) project sponsored by the Research Council of Norway (grant number 216432/O70), Rolls-Royce MARINE and DNV-GL. The work in this thesis is a part of LEEDS project.

Traditionally, ships have been optimized for calm water operation, because this is the intended condition during the contractual sea trials, and probably also because one has not had the knowledge and tools to optimize ships properly for operations in waves. Ships have of course been designed to be safe in all operational conditions they are supposed to be used in, but not to be optimally efficient in the typical operating condition, which for most ships is not calm water. Optimization for operation in waves is increasingly viable, and so it is expected that more energy-efficient and economical ships can be designed if conditions in waves are taken into account in the design optimization.

Propellers have traditionally been optimized for calm water conditions, partly because of insufficient knowledge about the conditions in waves and partly due to unavailable tools to optimize propellers for operations in waves. However, with increasing environmental concerns and emission regulations, there is growing demand to optimize the ships for the actual operating conditions, which typically include waves. Also with advancements in the technology, it is increasingly viable to analyze propeller performance in a complex environment like waves. In this regard, propulsion design approach should also be revisited to explore the possibility of optimizing propellers not just in calm water but also in the presence of waves. Initially, the effect of waves on existing propulsion systems should be analyzed. Substantial wake variation observed in the presence of waves by Wu [1] using CFD and by Kim [2] using PIV experiments are strong motivations for such an analysis, since the wake field is a very important input to the propeller design process.

1.1.1 Change of propulsion factors in waves

Currently, propellers are designed using wake, thrust deduction and relative rotative efficiency obtained in calm water conditions. Moor *et al.* [3] have shown through model tests of multiple ship hulls that wake, thrust deduction, and propeller efficiency vary in the presence of waves. In their work, propulsion factors have been presented for three different ships in loaded and ballast condition in the presence of head waves with wavelength varying from λ/L = 0.5 to 3.0. Thrust deduction, wake fraction, and propeller efficiency varied notably in the presence of waves as compared to their calm water values.

In the experiments performed by Nakamura *et al.* [4], self-propulsion factors were found to vary considerably especially when wavelength to ship length ratio was lower than 0.5. Moreover, the amount of these variations was larger in the case of low ship speed. In the range of λ/L = 0.9 to 1.3, where ship motions are severe, values of (1-*w*) and (1-t') were larger than the calm water values. Here, *w* is Taylor wake fraction and t' is thrust deduction fraction. (1-*w*) had a tendency to increase with the increase in waveheight whereas the variation of (1-t') with waveheight was comparatively small. However, (1-*w*) did not show as remarkable tendencies in irregular waves as observed in regular head waves. Further investigations into the wake in the presence of waves revealed that time averaged wake velocities were higher in the presence of waves than in calm water, especially when ship motions were severe. Forced pitch oscillation tests performed to investigate this phenomenon led to the conclusion that increase in mean (1-*w*) in waves compared to still water is mainly due to the magnitude of pitch motion. The radial distribution of circumferentially averaged wake also changed due to waves and ship motion, and the change was more pronounced at inner radii (close to the hub) of the propeller as compared to outer radii.

Guo *et al.* [5] simulated KVLCC2 advancing in head waves using an unsteady RANS code. Along with ship motions and added resistance, wake distributions were obtained in the presence of waves. The numerical calculation for wake flow was performed with wavelength λ/L = 0.9171, and wave height H = 0.138 m. Maximum change in time-averaged axial velocity was as large as 35% of the ship speed, which occurred close to the propeller shaft. First order axial velocity also showed large amplitude at the lower part of the propeller disc, where the maximum value was about 35% of the ship speed. Therefore, the effect of waves on the wake was found to be surprisingly strong.

Wu [1] computed the added resistance, ship motions and wake field of the KVLCC2 hull in head waves using the code CFDShip-Iowa v4.5, which uses overset block structured CFD solver designed for ship applications. Simulations were performed with free and fixed surge conditions and added resistance. Ship motions were validated by the experiments. Wakes computed using CFD simulations matched well with those obtained by Kim [2] using 3D Particle Image Velocimetry (PIV). PIV experiments were carried out at Fr=0.142 in calm water and in head waves with λ/L = 0.6 to 2.0 for fully loaded and λ/L = 0.3 to 2.0 for ballast condition using a 1:100 scale model of the ship. Significant wake variation was observed in the presence of waves, especially in λ/L = 1.1 and 1.6 as bilge vortices created due to ship motions affect the wake in waves.

Albers *et al.* [6] investigated the wake in the presence of waves using Laser-Doppler Velocimetry (LDV). The effects of undisturbed wave orbital motion, ship motion and disturbance due to the presence of the hull have been separated. Propeller loading and cavitation calculations have been performed for various conditions in the unsteady wake. Variation in cavitation number was found to be smaller in the presence of waves whereas variation in the angle of attack of propeller blade section increased. To maintain the ship speed in the presence of waves, RPM had to be increased which led to propeller sections experiencing lower cavitation numbers and higher angles of attack. It was concluded that the complete picture of the influence of waves and ship motions on wake velocity and local pressures is necessary for the assessment of cavitation in the presence of waves. Adaption of the propeller based on the environmental conditions in the area of operation of the ship was suggested to improve the long-term cavitation performance.

Chevalier *et al.* [7] and Jessup *et al.* [8] studied the cavitation of a propeller operating in waves by calculating wake velocities using potential flow calculations and observed a drop in the cavitation inception speed of the vessel in waves.

1.1.2 Importance of cavitation and pressure pulses

Due to increasing demand for efficiency, it is no longer common to design the propellers for operating entirely without cavitation. Cavitation can lead to erosion on the propeller blades. Moreover, the pressure pulses can cause vibration in the ship structure, thus affecting passenger comfort and in severe cases damage the structural integrity of the hull. In merchant ships, bearing forces cause about 10% of the propeller-induced vibrations, whereas approximately 90% are due to pressure fluctuations, or hull surface forces[9]. Pressure amplitudes at blade pass frequency of 1 to 2, 2 to 8 and over 8 kPa at a point directly above the propeller can be categorized as low, medium, and high, respectively. However, the pressure amplitude above the propeller is not alone adequate to characterize the excitation behavior of a propeller. Therefore, no universally valid limits can be stated for pressure fluctuation amplitudes. Whether these excitation forces result in high vibrations, depends on the dynamic characteristics of the ship's structure and can only be judged based on a forced vibration analysis. Moreover, lowering the pressure pulses comes at the expense of efficiency. Thus, accurate estimation of pressure pulses in realistic operating condition can help us maximize the efficiency while still avoiding the unwanted consequences.

Survey of 47 ships with vibration problem has shown that around 80% of the cases could be traced back to pressure pulses as a source of vibration problems [10]. Further, cases suffering from local deck vibration were twice as frequent as those where global vibration is the problem. However, the vibration of a superstructure is tough and expensive to solve when found on a ship in service.

The vibration level necessary to cause fatigue cracks in a superstructure is approximately ten times of that causing complaints from the crew. Such damages are therefore mostly experienced close to the excitation source and particularly in the aft peak. Based on reported cracks in the aft peak of 20 ships, fatigue damages in the afterbody strongly correlated with the amplitude of pressure pulses at blade harmonic frequency. Hence, it is necessary to avoid high pressure

pulses even when the cavitation is present, which is achieved by adapting the propeller design to calm water wake, as cavitation and pressure pulses depend on the wake distribution. However, given the substantial wake change occurring in the presence of waves, it is essential to investigate the performance of the propeller in the presence of waves.

1.1.3 Engine-propeller interaction

Propulsion plants are optimized for calm water operation while off-design conditions like rough weather are taken care of by adding a simple sea margin to the required power. The sea margin is typically 15 to 25% of the power needed in calm water condition. However, to optimize the installed engine size, the sea margin should be accurately calculated to ensure acceptable performance in average operating conditions or frequently encountered weather conditions. Accurate estimation of sea margin would require precise calculation of added resistance as well as propulsion performance in the presence of waves.

The dynamics of the propulsion system in the presence of waves is yet to be clearly understood. The system of engine and propeller react to the time varying flow field encountered in waves, and it would be useful to observe the effect of waves on the engine-propeller system dynamics. Propulsion losses may occur in the presence of waves due to events like propeller emergence. It is essential to evaluate the importance of such events and engine response to decide if it should be taken into account in the design phase of a ship. From the weather routing point of view, it is essential to correctly predict if propeller emergence will occur in any particular sea condition as it can lead to both voluntary and involuntary speed loss.

Changes in flow field explained previously cause fluctuations in propeller thrust and torque as noted by Nakamura *et al.* [4], Lee [11] and Amini [12]. Moreover, waves cause surge motions and periodic change in propeller submergence due to heave and pitch. Such changes in propeller submergence, surge motion, and occasional propeller emergence give rise to fluctuating loads on the engine, which may affect engine performance as well as propeller performance due to shaft speed variations. Therefore, engine and propeller should be studied together as a system to simulate the interaction between them. Kyrtatos [13] suggested that ship and propeller dynamics should be taken into account while optimizing the control strategy of the machinery.

From the industry perspective, there is a certain interest to study engine dynamics in the presence of rough weather as it is thought to affect the engine performance. The experience of Rolls-Royce in vessel design and operation suggests that the specific fuel consumption of marine diesel engines can be significantly affected by dynamic engine loading, for engines operating at relatively low load. Unsteady environmental loads are thought to be one of the many culprits leading to the drop in propulsion performance. Therefore, for the better understanding of the engine-propeller coupled dynamics, its effect on efficiency should be investigated.

Kyrtatos [13] simulated engine-propeller coupled model in a sea state of about 8 BF. Variation of engine power and speed was studied with speed control and fuel control governor settings. In addition to engine-propeller interaction in the presence of waves, crash stop maneuvers were also studied. Use of such simulations to optimize the control of marine engines operating in adverse condition and undergoing severe load transients has been suggested.

Kayano *et al.* [14] studied the effect of environmental conditions like wind and waves on the propulsion performance using full-scale trials. DHP (Delivered Horse Power) measured in full-scale experiments in the presence of wind and waves was higher and propulsive efficiency lower than the estimated value. As a result, the need for predicting the power curve more precisely considering the effect of wind and waves was proposed.

For the study of coupled dynamics of the vessel-propulsion-diesel engine system, Kyrtatos *et al.* [15] conducted a simulation of propeller – diesel engine dynamics and applied a PI governor. They demonstrated the model's reliability to test the governor in different transient loads. Livanos *et al.* [16] and Theotokatos *et al.* [17] studied coupled dynamics for a vessel-propeller-diesel engine system. Livanos *et al.* [16] studied the case with a controllable pitch propeller under maneuvering operation with a primary interest in the engine system response like shaft speed, turbocharger speed and power development under transient load. Ship acceleration with propeller pitch increase, rapid deceleration with pitch decrease and crash astern maneuvers were simulated. The engine model used was a mean value model, derived from their phenomenological model. The engine model was found to be capable of capturing dynamic response in different maneuvers by comparing the results with experimental measurements. Theotokatos *et al.* [17] have investigated the variation of performance and emission parameters of a merchant vessel for the given operating profile due to the effect of added resistance. They have demonstrated that the coupled model of ship-engine-propeller can be used to minimize the fuel consumption and CO_2 emission for a typical ship route by adjusting the ship speed.

Campora *et al.* [18] have presented the mathematical model for the dynamic simulation of ship propulsion system. Departure maneuver, arrival maneuver and crash stop have been simulated. Pitch, shaft speed, ship speed variations etc. have been compared with full-scale measurements. Good agreement between simulations and measurements was observed.

el Moctar *et al.* [19] have studied engine-propeller interaction in case of maneuvering by coupling Computational Fluid Dynamics (CFD) analysis with a dynamic engine model. Such a tool can be used in the final stage of ship design; however, due to the computational intensiveness of CFD calculations, it is difficult to utilize it as a tool for the wider search of design parameters.

All the above studies investigate engine-propeller-vessel dynamics with varying level of detail. They consider the effect of different maneuvering operations on the propulsion system. These studies help while building the engine model so that relevant dynamics can be simulated with required accuracy. However, the cyclic load variations that engine and propeller would experience in the presence of waves have not been included in these studies. The formulation for EEDI favors reducing the installed power of the main engine, which might tempt the designers to do so without applying innovative designs [20]. If so, the vessel may not have sufficient power to maintain its maneuverability in harsh weather. On the other hand, adding a design margin for possible off-design conditions without a proper analysis may be a costly solution. In this regard, finding the optimal power rating of a propulsion plant has become more important.

1.2 Thesis outline

This thesis is written as a collection of articles, which are appended in full-length after the main section. These articles represent the research contributions of this work, while the main section is meant to provide a concise overview of the work including important outcomes and conclusions from the study. The remaining part of the thesis has been organized as follows:

Chapter 2 contains objectives of the study further divided into sub goals.

Chapter 3 describes different methods used for the calculations of pressure pulses as pressure pulses play a pivotal role in the analysis of propeller performance in waves.

Chapter 4 highlights important results from each article along with additional calculations performed to support or extend the analysis further.

Chapter 5 lists the contributions of this work, highlights the conclusion and suggests the possible ways for future work.

Appended papers are as follows:

Paper 1: Analysis of propulsion performance of KVLCC2 in waves.

Paper 2: Dynamics of a marine propulsion system with a diesel engine and a propeller subject to waves.

Paper 3: The effect of waves on engine-propeller dynamics and propulsion performance of ships.

Paper 4: Effect of waves on cavitation and pressure pulses.

Paper 5: Effect of waves on cavitation and pressure pulses of a tanker with twin podded propulsion.

2. Objectives

The overall purpose of this work is to study the effects of waves on the propulsion performance of ship, so that the propulsion system can be optimized for realistic operating conditions. Objectives of this study can be broadly divided into two parts.

The first objective is to explore the possibility of optimizing the propulsion system of ships taking into account the conditions in waves. Therefore, a coupled model of engine, propeller, and vessel should be developed to simulate the propulsion system in waves. This model can be used to assess the effect of waves on propulsion performance. The influence of torque load variations on engine operation and its subsequent effect on propeller performance can also be studied. The study should also clarify which effects should be considered for improving the performance prediction of propulsion in waves as accurate performance prediction in different environmental conditions could lead to further optimization of installed engine power. In short, following sub-goals have been identified-

- Build engine-propeller coupled model considering relevant effects in the presence of waves.
- Simulate ship in the presence of different wave conditions.
- Observe the effect of waves on engine and propeller performance.
- Study engine-propeller dynamics and its effects on vessel operation in waves.
- Identify the effects of waves crucial for the accurate speed and power prediction.
- Evaluate the importance of coupled model in vessel performance prediction and optimization of engine power.

The second objective is to study the propeller performance in the presence of waves to explore the possibility of optimizing the propellers considering the effect of waves. Especially given significant wake variation in the presence of waves, one would expect the propeller performance to change significantly, as propeller designs are adapted for calm water wake. The first step would be to find out different ways in which waves can affect propeller performance and the performance parameters that are affected due to waves. The effect of each factor should then be quantified to recognize which factors should be taken into account while designing the propellers. These objectives can be further divided into following sub-goals-

- Simulate propeller in the presence of waves.
- Recognize the factors affecting propeller performance in waves.
- Find out which performance parameters get affected.
- Quantify the effect of different factors influencing propeller in the presence of waves.
- Identify critical factors to be considered to optimize propellers in the presence of waves.

3. Calculation of Pressure Pulses – Methods

Pressure pulses can be estimated using different methods. These methods differ in the level of complexity, uncertainty and sensitivity. For the current study, the method should be sensitive enough to reveal the differences in pressure pulses in different wake fields in waves. Different methods available for the calculation of pressure pulses have been reviewed in this section, since the calculation of pressure pulses in waves have played an important role in the definitive conclusion that pressure pulses tend to increase in the presence of waves.

3.1 Holden's Method

Holden's method is an empirical method for the calculation of pressure pulses. It is based on the full-scale measurements performed on 72 ships before 1980. The method is intended as a first estimate of likely hull surface pressures using a conventional propeller design [21, 22]. The following regression-based formula was proposed for non-cavitating and cavitating contributions of pressure pulses respectively:

$$p_0 = \frac{(ND)^2}{70}\frac{1}{Z^{1.5}}\left(\frac{K_0}{\frac{d}{R}}\right) N/m^2 \quad (1)$$

$$p_c = \frac{(ND)^2}{160}\frac{U(w_{Tmax}-w_e)}{\sqrt{(h+10.4)}}\left(\frac{K_c}{\frac{d}{R}}\right) N/m^2 \quad (2)$$

and K_0 and K_c are given respectively by the relationships:

$$K_0 = 1.8 + 0.4\left(\frac{d}{R}\right) \; for \frac{d}{R} \leq 2 \quad (3)$$

$$K_c = \begin{cases} 1.7 - 0.7\left(\frac{d}{R}\right) & for \frac{d}{R} < 1 \\ 1.0 & for \frac{d}{R} > 1 \end{cases} \quad (4)$$

The total pressure impulse, which combines both the cavitating and non-cavitating components of equation acting on a local part of the submerged hull, is then found from equation-

$$p_z = \sqrt{(p_0^2 + p_c^2)} \quad (5)$$

This method gives results with a standard deviation of the order of 30% when compared to the base measurement set from which it was derived. Thus, results from this method should not be regarded as a definitive prediction of pressure pulses.

Holden's method is used in the initial design stage of propeller design. However, it is not appropriate for current analysis since it only considers a few key parameters related to wake

distribution and therefore fails to capture the effects due to minor variations in wake structure (as observed in paper 4).

3.2 Cavity Volume Variation

Skaar *et al.* [23] developed an expression, which provides further insight into the relation between cavity volume and pressure pulses.

$$p_c = \frac{\rho}{4\pi}\frac{1}{R_P}\frac{\partial^2 V}{\partial t^2}\ N/m^2 \qquad (6)$$

where V is the total cavity volume.

Cavitating pressure signature is proportional to the second derivative of the total cavity volume with respect to time. Hence the pressures encountered upon the collapse of the cavity is usually more violent than those experienced during cavity formation.

The above expression can be applied to obtain pressure pulses at a distance of R_P from the cavity, if time history of cavity volume is known. Methods like lifting surface or vortex lattice can be used for the calculation of cavity volume variation on the propeller in a given wake. Unsteady lifting surface theory is the basis for many advanced theoretical approaches in this field [21]. This method would have been sufficient for the comparative study of pressure pulses in different conditions as cavity volume variation was available from MPuF-3A calculations, which is based on vortex lattice theory [24]. However, HullFPP, which is potential based boundary element method [25], was used for the analysis, as it is more accurate.

Plots of cavity volume variation are presented in paper 4. Cavity volume variation along with its second derivative has been plotted in Figure 3.1 and Figure 3.2 to highlight the aspects of cavity volume variation that are important from the pressure pulse point of view. Interestingly, volume maxima create broad negative peaks in second derivative, while blade angles at which cavity forms and collapses lead to narrow positive peaks in the second derivative.

In, Figure 3.2 the left peak of the second derivative is wider and smaller than the peak on the right-hand side. Since the blade travels from negative blade angles to positive, the left peak corresponds to cavity formation whereas the right one is due to cavity collapse. As we know, cavity collapse is responsible for larger pressure pulses than the cavity formation. Figure 3.1 and Figure 3.2 depict the importance of the wake peak as the peak of cavity volume creates large negative peaks in the second derivative of cavity volume. Narrower wake peak would have led to sharper cavity variation close to the peak thus causing a larger negative peak in the second derivative of cavity volume.

Figure 3.1 Cavity volume variation and its second derivative in calm water wake.

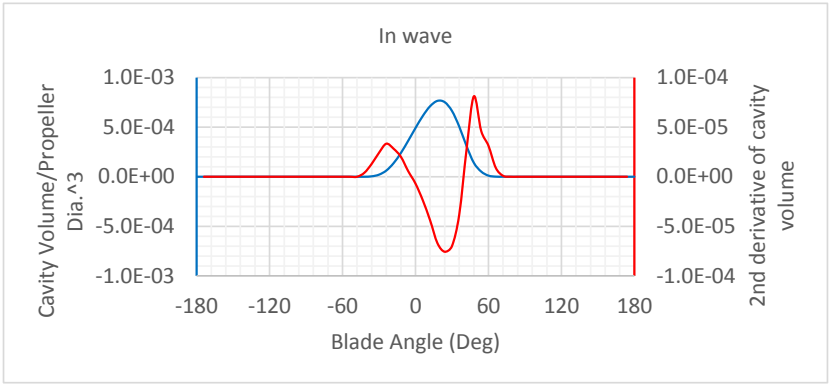

Figure 3.2 Cavity volume variation and its second derivative in the presence of wave.

3.3 Field Point Potential

This method has been used in the analysis where time history of cavity volume is obtained using MPuF-3A calculations, and pressure pulses are calculated using HullFPP. The time history of cavity volume variation is used to derive the field point potential induced by the cavitating propeller. The solid boundary factor is calculated by solving the diffraction potential on the hull using a potential-based boundary element method. Fluctuating pressure on the hull is then determined by multiplying free-space pressures by the solid boundary factor. In this method, the solid boundary factor can be calculated based on the geometry of the hull. Moreover, in addition to pressure pulse amplitudes, the phase of pressure pulses is also obtained, which could be useful for hull vibration analysis.

4. Summary of Papers and Supporting Work

4.1 Overview

This is a paper-based PhD thesis, so most of the work done in this PhD is reported in a total of five papers. Analyses performed in different papers, important outcomes and how the analysis in one paper led to the research in another has been illustrated in Figure 4.1. The figure also depicts the interconnection between the papers.

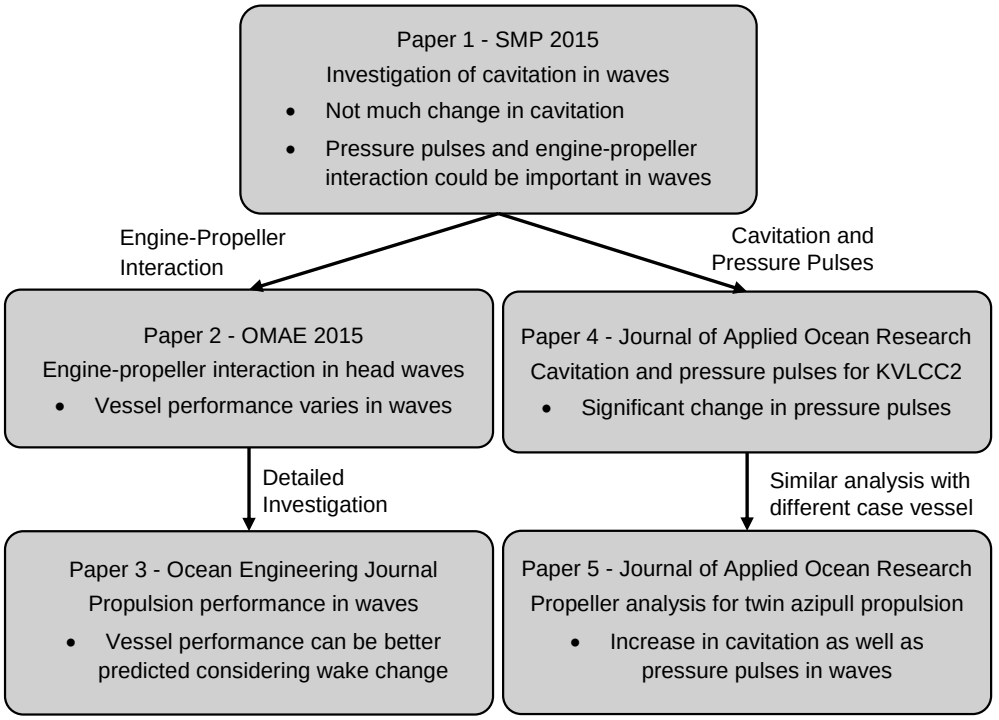

Figure 4.1 An overview of interlinks between research papers.

4.1.1 Paper 1: Analysis of propulsion performance of KVLCC2 in waves

Paper 1 focuses on the performance of a propeller in the presence of waves. As we know, propellers are wake adapted for acceptable noise and vibration characteristics. However, wake adaption is done considering the calm water wake. Hence, wakes in the presence of waves were examined using BSRA wake criteria to see if the conditions in the presence of waves are more or less favorable as compared to calm water as far as cavitation induced noise is concerned. It was observed by using an unsteady panel method that the amount of cavitation does not change much despite the considerable variation in the wake (Figure 4.2). However, the wake gradient increases in the presence of waves as compared to calm water. Since the primary goal of wake adaption is to reduce the level of pressure pulses, it was concluded that although the amount of cavitation shows minimal change, cavitation induced pressure pulses should be examined in the presence of waves as increased pressure pulses can cause detrimental noise and vibrations.

Propeller analyzed at constant RPM in different wake fields in the presence of waves showed substantial fluctuations in thrust and torque coefficients (Figure 4.3). Therefore, further investigations were required to study engine-propeller interaction in the presence of waves for possible dynamics and performance changes in a rough sea.

Further analysis has been divided into two parts:

1. Study of engine-propeller dynamics in the presence of waves
2. The effect of waves on cavitation and pressure pulses

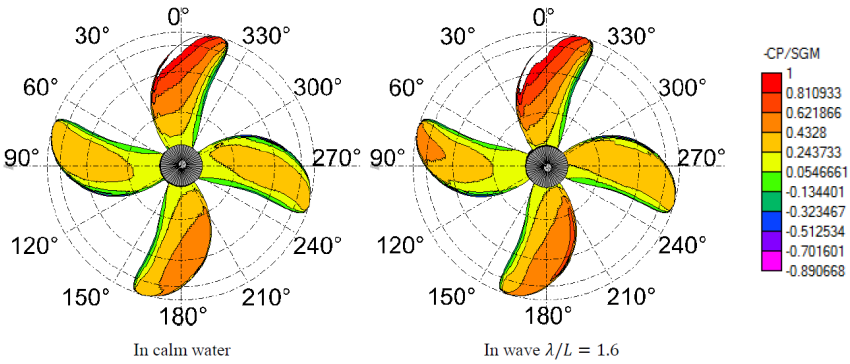

Figure 4.2 Maximum cavitation in calm water and the presence of waves.

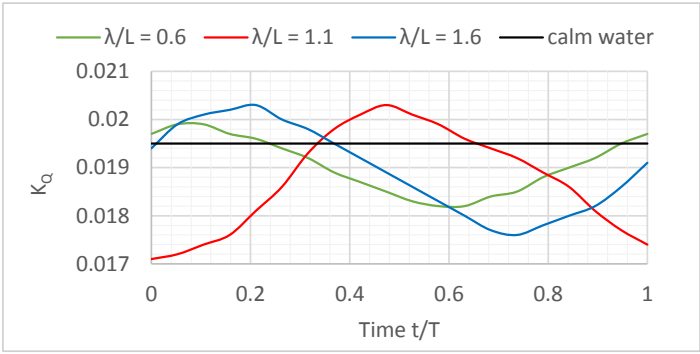

Figure 4.3 K_Q variation in the presence of waves.

4.2 Engine-Propeller Dynamics

4.2.1 Paper 2: Dynamics of a marine propulsion system with a diesel engine and a propeller subject to waves

Due to notable fluctuations in thrust and torque in the presence of waves, it was necessary to investigate if load fluctuations affect the propulsion performance of the vessel. The experience of the industry also supported the notion that engine performance may change in the presence of large torque variations in the presence of waves. Therefore, in paper 2, engine and propeller models were coupled to obtain the realistic response of the propulsion machinery to observe the interaction between engine and propeller. Paper 2 investigates the effects of head waves on the propulsion performance of a ship regarding propulsive efficiency and engine performance. Simulations performed at constant ship speed indicated that the power, RPM and fuel consumption increase in the presence of waves (Figure 4.4, Figure 4.5) due to wake change even when added resistance is not included in the simulation since wake variation causes a change in hull and propeller efficiency. Consequently, in addition to added resistance, wake change, out-of-water effect and dynamic engine response are important in the calculations of power demand and fuel consumption in waves. However, further investigations are required to separate the influence of each of these factors to pinpoint the cause of performance drop.

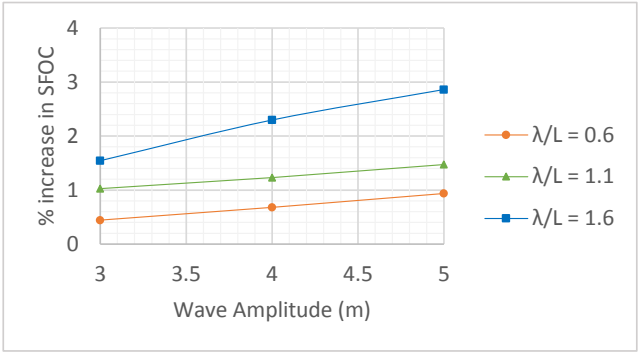

Figure 4.4 Percent increase in SFOC in the presence of waves as compared to that in calm water (without added resistance).

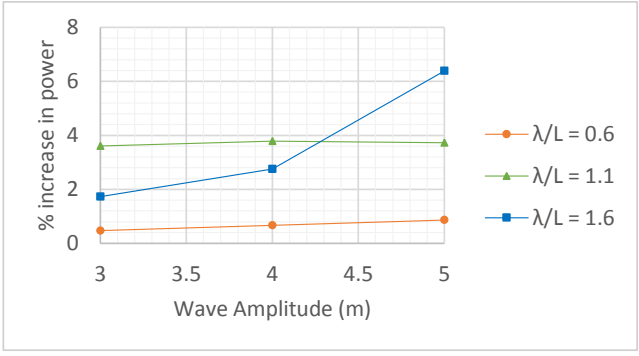

Figure 4.5 Percent increase in engine power in the presence of waves as compared to that in calm water (without added resistance).

4.2.2 Paper 3: The effect of waves on engine-propeller dynamics and propulsion performance of ships

The detailed investigations were performed in paper 3 to study the effects of wake change, engine-propeller dynamics, and propulsion losses in waves on vessel performance. Coupled model of engine, propeller, and vessel was extended to be able to simulate the vessel in waves with different heading angles. Average wake in waves was obtained considering the effect of pitch and surge motion of the ship along with wave-induced particle motion. The following formula was used for the computation of wake velocities utilizing the works of Ueno *et al.* [26] and Faltinsen *et al.* [27]-

$$V_{total} = \Big((1-w_P)\{U - \omega_e \xi_a \sin(\omega_e t - \zeta_\xi)\} + \alpha\omega h_a \exp(-kz_P)\cos X \cos(\omega_e t - kx_P \cos X)\Big)\sqrt{\left(1 - \frac{\Delta\bar{p}}{0.5\rho U^2}\right)} \quad (7)$$

Simulations were performed in three different waves coming from five different directions for three wave amplitudes. Quasi-propulsive efficiency dropped in the presence of waves due to change in hull and propeller efficiency as a result of wake variation (Figure 4.6 and Figure 4.7). It should be noted that since the wake distribution is mainly of interest for cavitation and related effects, only the time-variation of the circumferentially averaged wake was considered in this study. Simulations with engine-propeller coupling were compared with those assuming constant RPM without using engine model to observe the importance of engine-propeller dynamics in the vessel performance prediction. Similarly, the importance of wake change was also studied.

Combined effect of modeling engine-propeller coupling, wake variation, thrust and torque in waves caused maximum 40% change in quasi-propulsive efficiency as compared to simulations without considering these effects (Figure 4.8). However, modeling the wake change and propulsion losses brought down this change to maximum 4% that too only in cases where the engine is operating close to MCR (Figure 4.9). Hence, considering wake variation is more important for accurate prediction of vessel performance as compared to engine-propeller coupling.

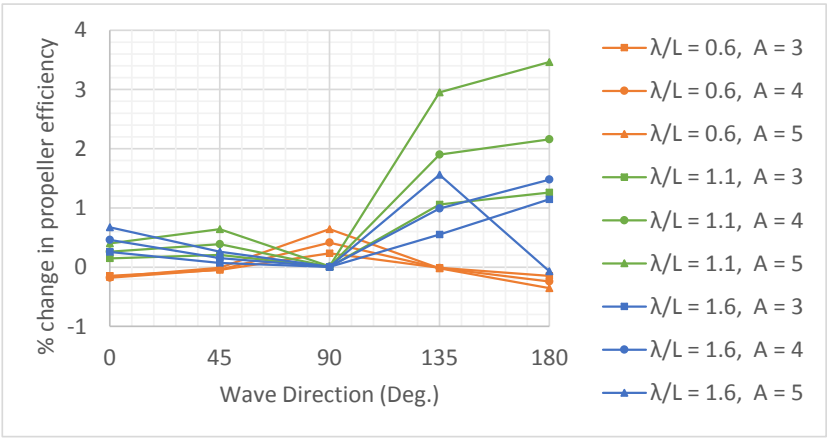

Figure 4.6 Change in propeller efficiency in different wave conditions due to time-varying flow field.

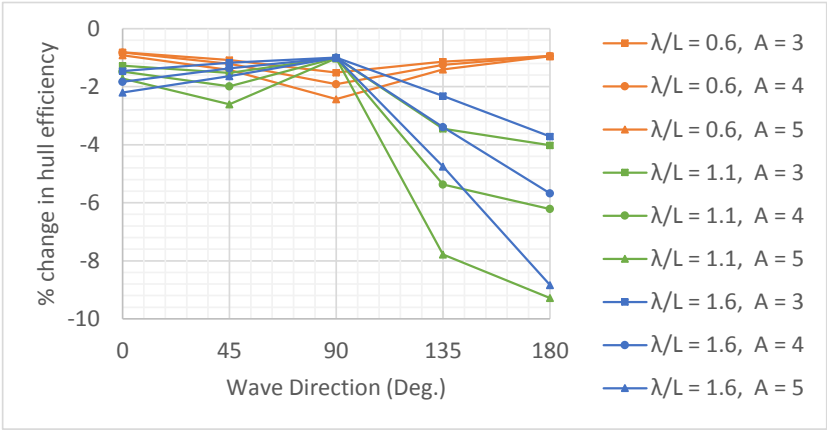

Figure 4.7 Change in hull efficiency due to time varying wake in waves.

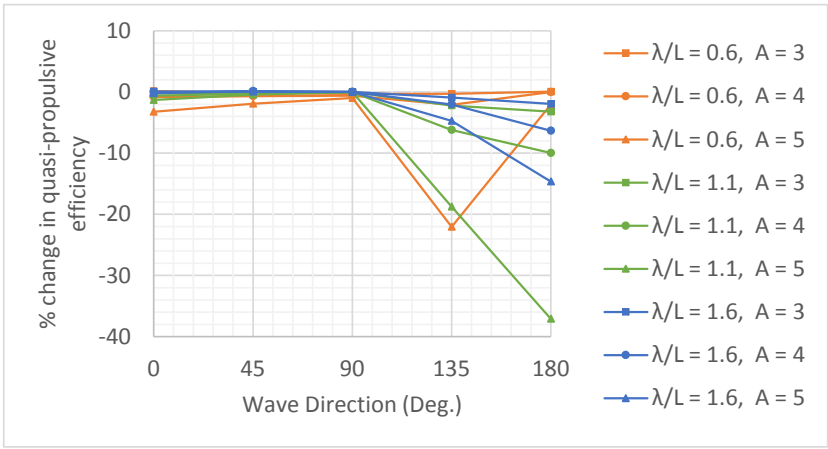

Figure 4.8 Percentage change in quasi-propulsive efficiency due to the use of engine model as compared to that without engine model without considering wake change and changes in thrust and torque.

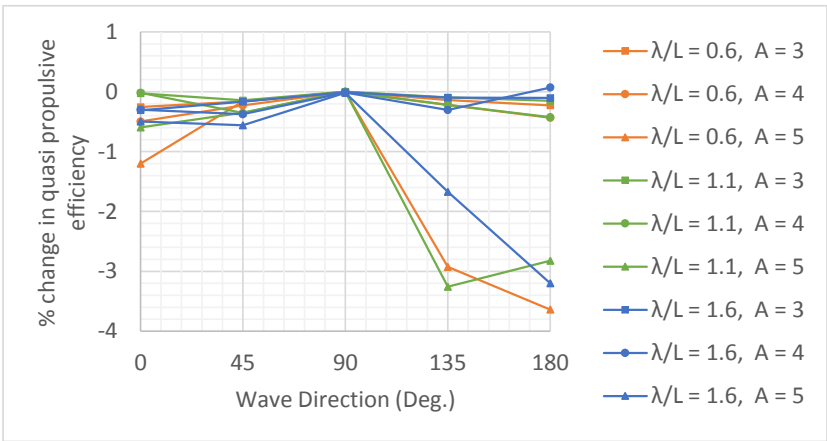

Figure 4.9 Percentage change in quasi-propulsive efficiency due to the use of engine model as compared to that without engine model (including wake change, thrust and torque loss calculations).

Despite significant load fluctuations, relatively small changes in engine performance were observed in most of the cases. Engine fuel consumption was mainly dependent on engine power and RPM, irrespective of the load fluctuations. Moreover, investigations performed by Yum *et al.* [28] also support that the effect of load fluctuations on engine fuel consumption is negligible.

Coupling the engine, propeller, and vessel dynamics can improve the prediction of ship speed and ship motions, since ship motions depend on ship speed, which is dependent on propulsion losses; and propulsion losses and wake variation are again a function of ship motions. As a result, such a tool can be effectively used to assess vessel performance in any environmental condition and not just the possibility of propeller emergence, but also the amount of propeller racing can be predicted. Effective weather routing of ships can be achieved using such a tool. Coupled simulations can be effectively used for the development of a safe and efficient control system by assessing its performance in different weather conditions beforehand. Individual components of the propulsion system, like the propeller shaft can also be examined in greater details with realistic inputs from both engine and propeller side.

4.2.3 Supporting work

4.2.3.1 Parameters affecting mean wake change

In the engine-propeller coupled simulations, the propulsion performance of the ship changes in waves mainly due to change in time-averaged wake fraction. Thus, the factors that influence change in mean wake fraction have been investigated in more detail. The change in time averaged wake velocity, as explained in paper 3, is assumed to be due to the pitching motion of the ship. Mean wake velocities can be estimated as [27]:

$$V_{mean} = \sqrt{\left(1 + \frac{\omega_e^2 |\eta_5|^2 x^2}{2U^2}\right)}\, U \qquad (8)$$

At constant ship speed, ω_e (wave encounter frequency) would decrease with increase in wavelength in case of head waves. Whereas η_5 (Pitch amplitude) will tend to increase with increase in wavelength. Relative contribution and the variation of these two parameters towards mean change in wake can be assessed from Figure 4.10 in the presence of different head waves at the design speed of the ship.

In addition to ω_e and η_5, mean wake also depends on the ship speed, therefore, percentage change in mean wake has been computed at different ship speeds in different wavelength of head waves in Figure 4.11. Comparing Figure 4.10 with Figure 4.11, the maximum of mean increase in wake occurs at wavelengths lower than that showing largest pitch amplitude. The effect of mean wake change due to pitching motion of the ship is largest when wavelength to ship length ratio is between 1 and 1.5. Notably, ship speed or Froude number affects the percentage increase in the mean wake. When ship speed was reduced to half of design speed, the increase in mean wake changed from 2.5% at design speed to 15% at half of the design speed. It could be concluded that the effect of mean wake change could be more pronounced in the case of slow speed ships.

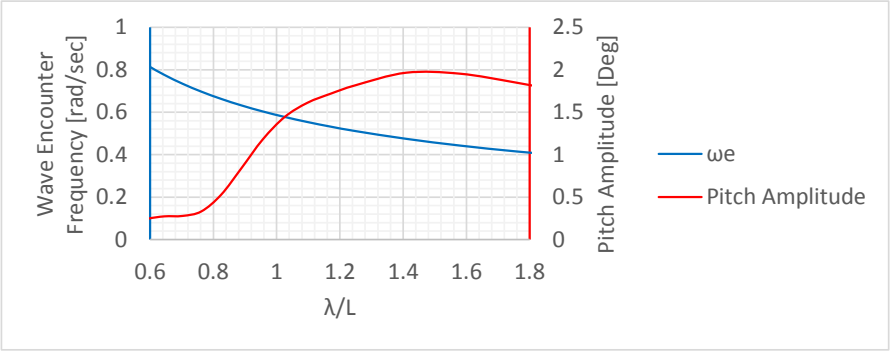

Figure 4.10 Variation of ω_e and η_5 in the presence of different wavelength of waves at constant ship speed.

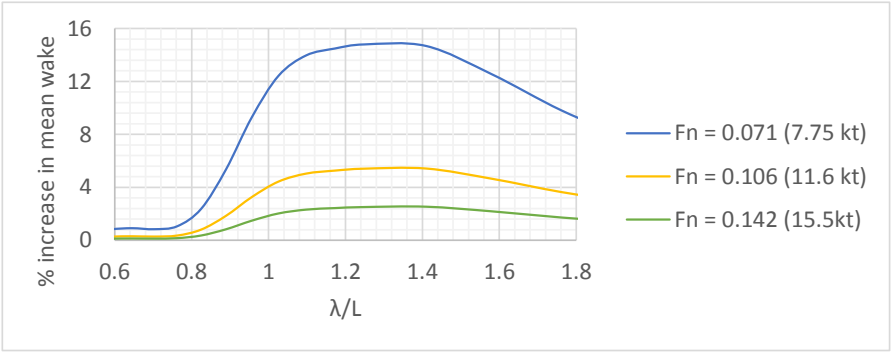

Figure 4.11 Froude number dependence of percentage increase in mean wake.

4.2.3.2 Factors affecting wake fluctuation

Surge and wave-induced velocities are major contributors to the wake fluctuations in waves [26]. In order to compare the effect of these two factors, wake fluctuation due to surge was compared with the wake fluctuation due to wave-induced particle velocities in the case of head waves as seen in Figure 4.12. Variation of surge induced wake fluctuation with wavelength follows surge RAO as expected. Wave-induced wake fluctuation shows hardly any change with wavelength. Wave-induced wake fluctuation depends on various factors. In case of head waves, the effect of the hull is large for shorter waves thus causing significant amplitude reduction as they reach the propeller. Also in shorter waves, amplitude reduction with depth is stronger. However, smaller waves have a higher frequency, which leads to higher induced velocities. Due to the combination of these two effects, wave induced wake fluctuation remains almost constant with wavelength.

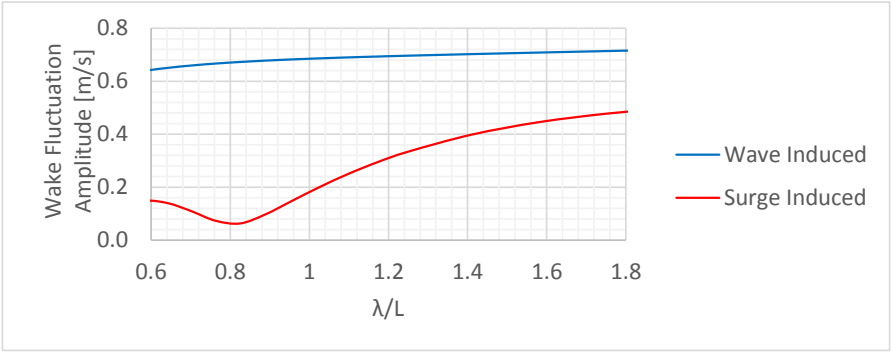

Figure 4.12 Comparison of the contribution of wave induced and surge induced fluctuation in the wake fluctuation.

4.2.3.3 Mean wake estimation using different methods

As mentioned earlier, wake has been estimated using simple methods, which do not take into account the effect of hull shape on the wake. Faltinsen's method used to estimate mean wake change assumes hull as a flat plate while Ueno's method used for computing wake fluctuations uses a reduction factor for wave amplitude at the propeller to take into account the effect of wave diffraction. Therefore, for the accurate estimate of the variation in mean wake, potential flow methods like Shipflow can be used.

KVLCC2 was simulated in the presence of head waves in Shipflow [29] and average potential wake was extracted; mean wake change and wake fluctuations were compared with those obtained from Ueno [26] and Faltinsen's method [27] along with those observed in CFD simulations of KVLCC2 in waves [1].

Figure 4.13 and Figure 4.14 show that all three methods give slightly different results. These figures are also meant to depict possible uncertainty in the estimation of mean increase and fluctuations in the average wake. It is also clear that simple methods also perform well in approximating wake in waves.

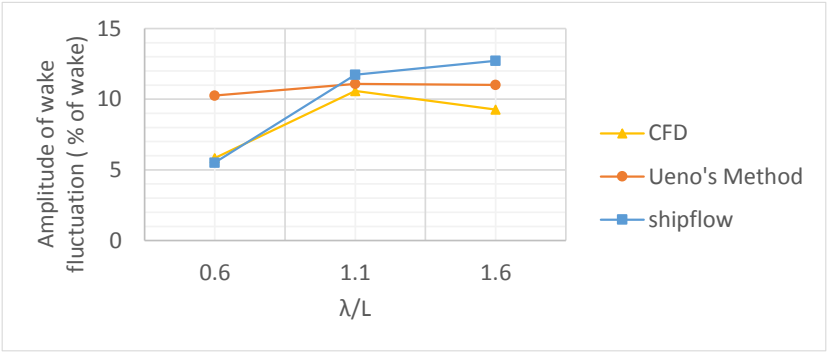

Figure 4.13 Comparison of the amplitude of wake fluctuations using different methods.

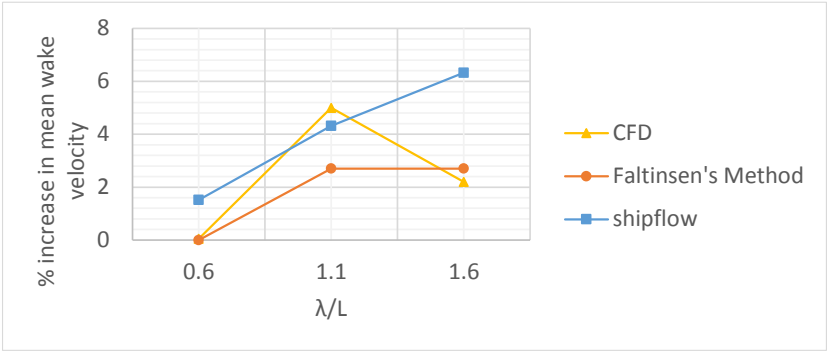

Figure 4.14 Comparison of increase in mean wake using different methods.

4.2.3.4 Cause of change in engine performance

Only small change was observed in fuel efficiency due to the effects of torque fluctuations in the presence of waves (less than 1% in most of the cases). Only in the following wave condition with λ/L=0.6 and A=5m, increase in fuel consumption was notable (around 2.5%). Further investigations into this particular case revealed that it was the effect of what is commonly known as 'turbo-lag'.

In the case of following sea, waves directly affect the propeller unlike in head sea where the propeller is partly shielded from waves due to the presence of the hull in front of it. So, wake fluctuations are larger in following waves, which cause large fluctuations in engine power. During the fluctuations when engine power is rising, turbocharger revs-up slower than the engine power due to turbo lag. Therefore, at a certain point, the amount of compressed air is insufficient to burn the amount of fuel as per the fuel rack position commanded by the controller. At this point, the smoke limiter function of the engine controller (governor) comes into play by limiting the amount of fuel as per the available compressed air, causing a drop in

shaft speed and a saturation of thrust (Figure 4.15). As a result, engine performance gets affected in terms of engine power and fuel efficiency. Further details about this can be found in [30].

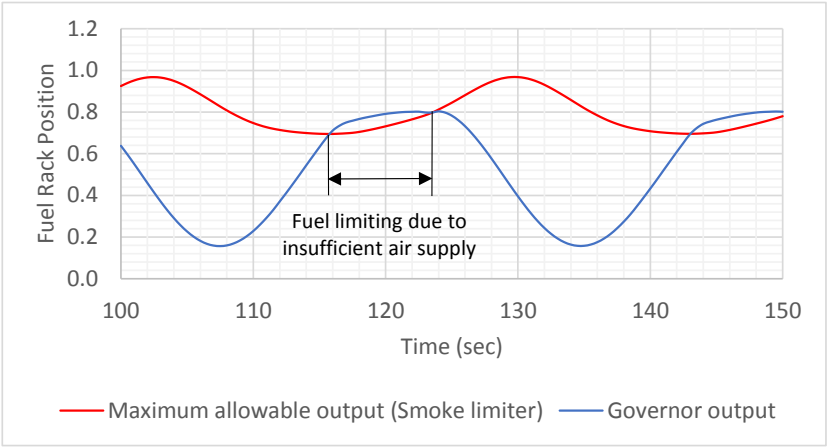

Figure 4.15 Time series of fuel rack position command and the maximum allowable value from the smoke limiter [30].

4.2.3.5 Simulations in irregular waves

All the simulations in paper 2 and paper 3 were performed in the presence of regular waves. However, irregular waves should be considered to simulate realistic conditions. One might also think that the engine control system may react differently in the presence of irregular waves, thus affecting the engine performance. Therefore, the tool of engine-propeller coupled simulations was extended to include irregular waves. Torque and shaft speed obtained in the irregular wave have been plotted in Figure 4.16 and Figure 4.17 respectively. Peaks in the shaft speed are due to propeller emergence causing a corresponding drop in the torque signal. Even in the presence of irregular waves, engine performance did not vary significantly (less than 1%). However, such time domain simulation can be useful for the assessment of the safety of engine

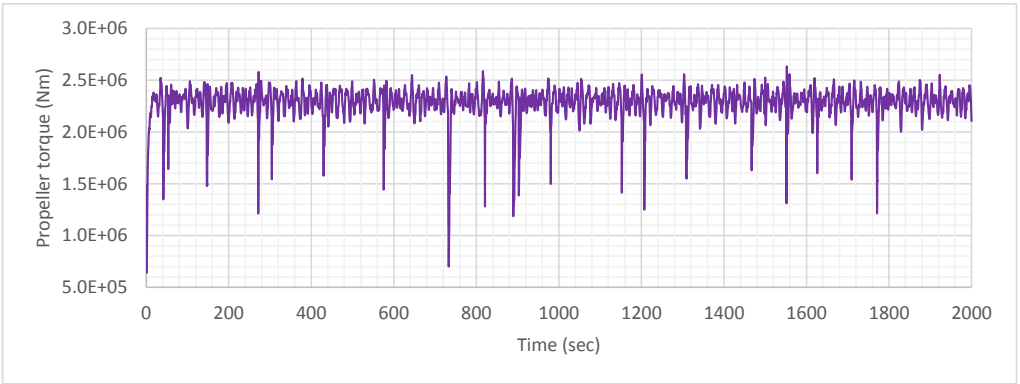

Figure 4.16 Torque variation at the propeller end of shaft in irregular wave of significant wave amplitude 5m and significant wavelength corresponding to $\lambda/L = 1.6$.

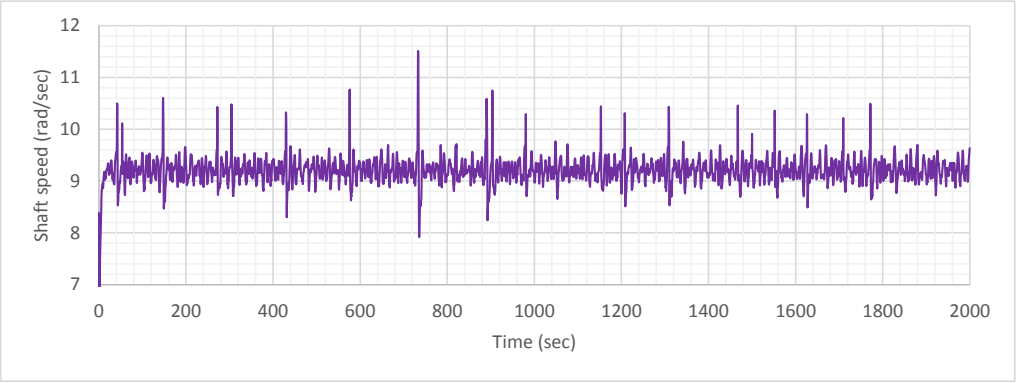

Figure 4.17 Shaft speed variation in irregular wave of significant wave amplitude 5m and significant wavelength corresponding to λ/L = 1.6.

in different weather conditions as well as for evaluating the performance of various control systems in realistic conditions.

4.2.3.6 Simulations with flexible shaft

Earlier, engine-propeller interactions have been studied using an inertial shaft model. Thus, a flexible shaft model along with crankshaft kinematics was implemented in the system to investigate if shaft flexibility affects engine-propeller interactions. Simulations were performed in the presence of waves to compare the results of power, torque and RPM fluctuations using inertial and flexible shaft models. Comparison of shaft speed and propeller torque using inertial and flexible shaft model can be seen in Figure 4.18 and Figure 4.19. Including a flexible shaft instead of an inertial one did not change engine or propeller performance, as shaft frequencies getting affected due to flexibility are much higher than the frequencies that affect engine or propeller performance in waves. High frequency fluctuations in torque and propeller speed seen in the simulation with flexible shaft are due to the effect of individual cylinder firings. In the current simulation model, having flexible shaft is of limited use as different phenomena occurring in waves are of much lower frequency than those affecting the shaft dynamics. However, the model might be updated to include relevant effects like forces and moments of blade pass frequency in different conditions to study shaft vibrations in various conditions.

Simulations of the starting maneuver can be performed for cases where it is required to pass barred speed range (range of RPM close to natural frequency of shafting system) as quickly as possible to reduce the load cycles. Due to EEDI regulations, new engines might not have enough additional power available to be able to accelerate the ship as quickly as required. Coupled simulations can help in identifying such issues in advance.

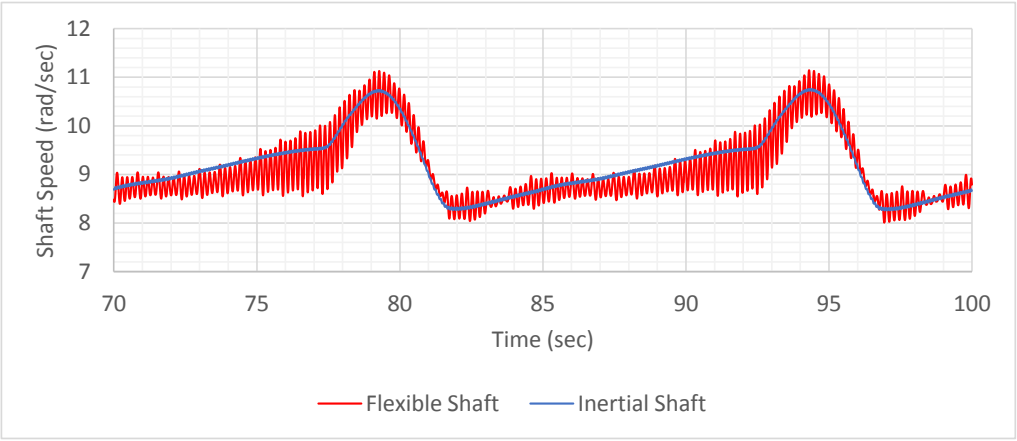

Figure 4.18 Shaft speed using flexible shaft and inertial shaft model in λ/L = 1.6.

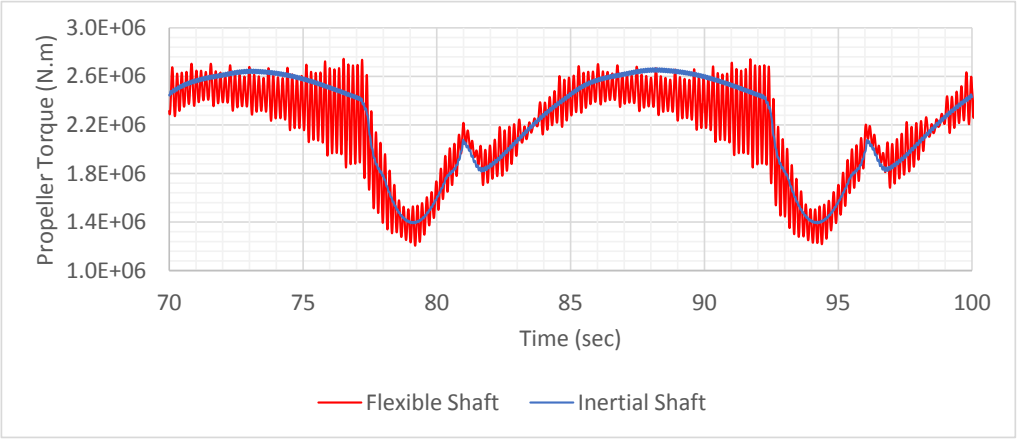

Figure 4.19 Propeller torque using flexible shaft and inertial shaft model in λ/L = 1.6.

4.3 Cavitation and Pressure Pulses

4.3.1 Paper 4: Effect of waves on cavitation and pressure pulses

As seen in paper 1, the amount of cavitation did not change much in the presence of waves despite notable wake variation. However, an increase in wake gradient was observed, which was the reason to investigate the level of pressure pulses in the presence of waves; the analysis included in paper 4 using KVLCC2 as a case vessel.

While designing the propeller, efficiency is maximized while keeping the pressure pulses under a certain limit. Lowering the level of pressure pulses comes at the expense of efficiency. Therefore, accurately knowing the level of pressure pulses in realistic operating condition is necessary to maximize the propeller efficiency while making sure that the pressure pulses are under a certain limit. As propellers are adapted for calm water wake; it is necessary to investigate how they perform in the presence of waves where wake varies considerably.

Although cavitation did not vary notably, pressure pulses increased significantly in the presence of waves, especially when the wavelength is close to the ship length. In most of the cases, pressure pulses in the presence of waves were higher than in calm water wake (Figure 4.20). This observation is important given the current practice of designing the propeller using calm water wake as an input in the absence of any wake data in waves.

The analysis of propeller blade section revealed significant variation in section lift coefficient and cavitation number in the presence of waves as compared to that in calm water. At certain time intervals, there is a possibility of having pressure side cavitation, which is much more dangerous than suction side cavitation in terms of erosiveness and pressure pulses. Hence, propeller blades experience many different conditions in waves than that in calm water (Figure 4.21).

Effects of various factors affecting cavitation and pressure pulses were studied to find out the relative importance of ship motions, wake change, RPM variation, and speed loss so that important factors can be considered in the design stage of a propeller. It was observed that wake variation has by far the largest impact on propeller performance (Figure 4.22). Pressure pulses increased substantially when the wavelength was close to the ship length.

This analysis serves a couple of purposes. First, it analyses the possible performance drop in the presence of waves e.g. pressure pulses may increase causing undesired vibrations in the structure along with an increase in noise levels. Second, knowing the wake distribution in worst intended operating condition can help us maximize the propeller efficiency while still avoiding the unwanted effects of cavitation and pressure pulses.

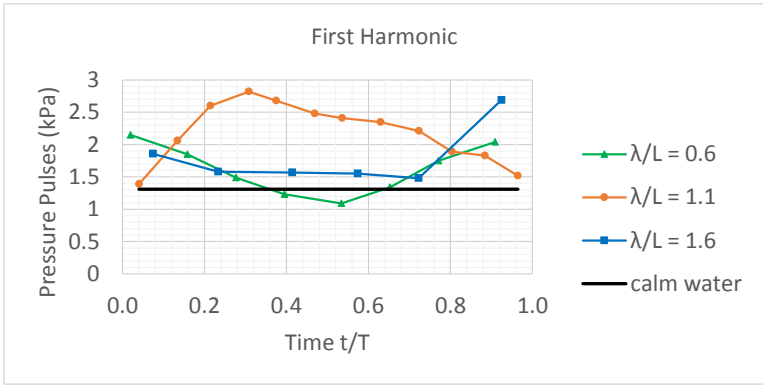

Figure 4.20 First harmonic of pressure pulses in waves considering wake change, ship motions and wave dynamic pressure.

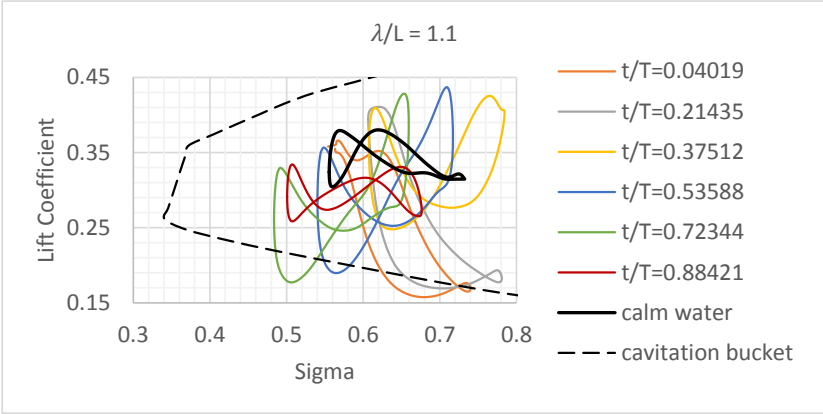

Figure 4.21 Variation in lift coefficient of blade section at 0.7R at different times as wave passes in λ/L = 1.1 considering wake change, ship motions and dynamic wave pressure.

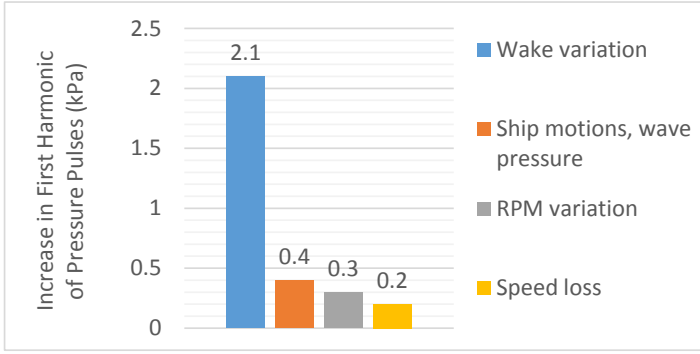

Figure 4.22 Comparison of maximum increase in the first harmonic of pressure pulses due to different factors in the presence of waves.

4.3.2 Supporting work

4.3.2.1 Grid dependence

Propeller analysis using MPuF-3A in paper 4 has been performed using the fine grid on the key blade while coarse grid was applied on all other blades. The analysis was carried out to check if cavitation volume changes if the fine grid is used on all the blades. Cavity volume variation using the fine grid on all the blades has been compared with the one obtained using fine grid only on the key blade in calm water wake. The difference in the cavity volume is minor as seen in Figure 4.23. Moreover, the work is about comparing the cavitation volume variation in different wakes rather than exactly predicting the cavitation volume.

4.3.2.2 Pressure pulses with increased load

In some cases, maximum cavitation volume decreased along with the pressure pulses after increasing the propeller load i.e. after considering the speed loss. Cavitation volumes in one such case have been plotted in Figure 4.24 with and without speed loss. In the case of speed loss or increased loading, the cavity is present for a larger range of blade angles but maximum cavitation volume is lower. However, the decrease in maximum cavitation volume is small.

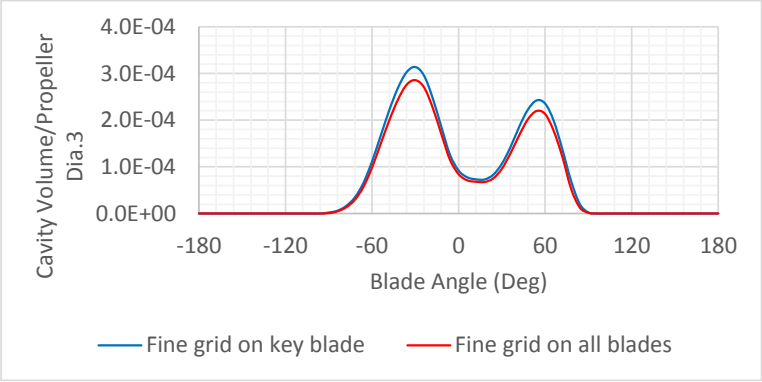

Figure 4.23 Grid dependence of cavity volume variation.

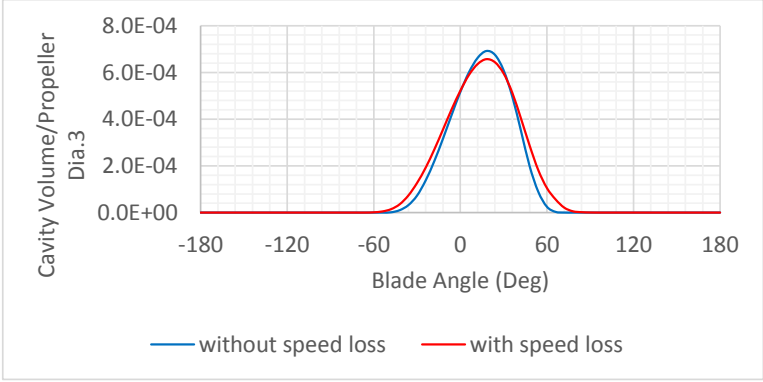

Figure 4.24 Cavitation volume variation with and without speed loss in case when maximum cavitation volume and pressure pulses decrease in the presence of speed loss (λ/L=1.1, t/T= 0.30813).

4.3.2.3 Mean change in thrust and torque in waves

In paper 4, the analysis has been performed considering ship motions as well as speed loss. An increase in wake velocities due to pitching motion will lead to lower K_T whereas speed loss will tend to increase it. (Here both thrust and torque coefficients refer to K_T and K_Q averaged over one wave encounter period.)

Thrust and torque coefficients were calculated in the presence of speed loss along with wake variation. The comparison of average K_T and K_Q in calm water, in the presence of wake change (at design speed of the ship), and in the case of wake change along with speed loss has been presented in Table 1.

Table 1 Variation of average K_T and K_Q due to wake change and speed loss.

	K_T			$10K_Q$		
λ/L	wake change	wake change + speed loss	calm water	wake change	wake change + speed loss	calm water
0.6	0.217	0.227		0.235	0.244	
1.1	0.200	0.213	0.219	0.221	0.232	0.238
1.6	0.206	0.219		0.226	0.237	

As observed in Table 1, the combined effect of wake change and speed loss can lead to either higher or lower thrust and torque coefficients as compared to calm water K_T and K_Q, depending upon the wave condition. In the case of $\lambda/L = 0.6$, the effect of speed loss seems to dominate as K_T is higher than in calm water. However, in the wavelength $\lambda/L = 1.1$, the effect of wake change is dominant as K_T is lower despite the speed loss. In the case of $\lambda/L = 1.6$ both the factors seem to cancel each other since K_T and K_Q are very close to their calm water value.

While comparing the effect of speed loss and wake change it is important to notice that speed loss has been calculated in irregular waves whereas wake change has been obtained in the presence of regular waves. Therefore, one would expect that the effect of wake change would be more pronounced in these calculations, leading to lower thrust and torque coefficients as compared to those in free running model tests. It could be the reason why thrust and torque coefficients are higher in free running model tests. Also, wake variation might be different at lower ship speed. However due to unavailability of wake data at lower ship speed, wake variation at design speed has been used also in the case of speed loss, which might not be accurate.

4.3.2.4 Effect of wake change on tip loading

Pressure pulses due to wake change in the presence of waves have been analyzed in paper 4. However, in addition to cavity volume variation, cavitating tip vortex can be a major source of noise typically occurring at frequencies higher than blade pass frequency. Currently, there are no reliable methods available to predict tip vortex noise. It is known that tip loading has an influence on the strength of the tip vortex [31] therefore, to avoid noise and vibrations, the tip is often unloaded at the expense of efficiency. In the presence of wake variation, tip loading should also be checked to analyze the probability of higher tip loading, which may cause

increased noise in the ship. Percentage change in blade tip circulation (at an instance when the blade is at 12 O'clock position) in waves as compared to calm water wake has been presented in Figure 4.25. The tip loading is lower than in calm wake for most time instances in the presence of three different waves. Which means the risk of noise due to cavitating tip vortex decreases in the presence of waves at least in this case.

4.3.2.5 Effect of wake change on hub loading

As the circulation changes along the blade, hub circulation should also be checked. Increased hub loading can cause the hub vortex to cavitate, which can cause erosion on the rudder that is placed downstream. Therefore, to observe the effect of wake variation, the average hub loading was compared with that in calm water. Unlike in the case of tip loading where the circulation at a single blade location has been compared, it would be appropriate to compare the average circulation of the hub. Hub-vortex cavitation depends on the intensity of the hub vortex formed due to individual vortices coming from the root of each blade. It can be observed from Figure 4.26 that the hub circulation in the presence of waves is higher than that in calm water wake for most of the time intervals in each wavelength. Especially in $\lambda/L = 0.6$ the average hub loading is greater than calm water hub loading for all the time intervals. Figure 4.26 indicates that there is a higher probability of hub cavitation in the presence of waves than in calm water.

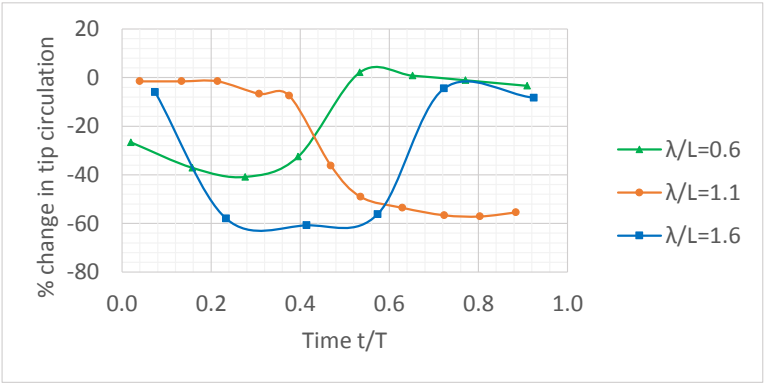

Figure 4.25 Percentage change in tip circulation in waves as compared to calm water wake.

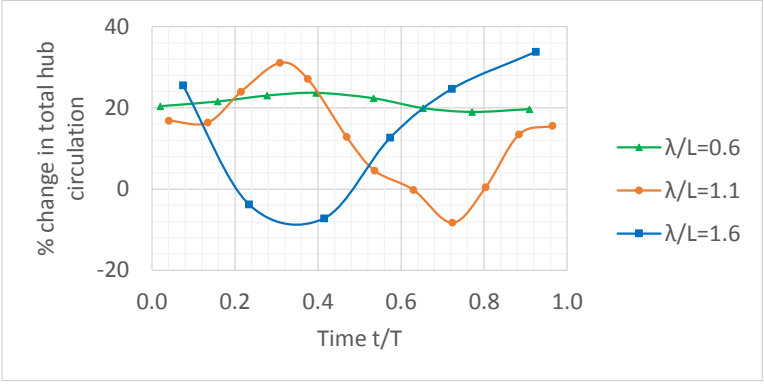

Figure 4.26 Percentage change in average hub circulation in waves as compared to calm water wake.

4.3.3 Paper 5: Effect of waves on cavitation and pressure pulses of a tanker with twin podded propulsion

In paper 4, an increase in pressure pulses was remarkable in the presence of waves. The ship hull studied, KVLCC2, is a single-screw ship with a full hull form and therefore a strong wake. The effect of waves on the wake and therefore on propeller performance depends on the geometry and other features of the ship. It has been attempted to reveal the reasons for the performance changes, but still it is clearly a need to study more cases to check the importance of waves on propeller performance, and whether the theories put forward based on the first case study will still hold. It can be expected that the effect of waves should be less important in the case of twin-screw ships or even more so in twin azipull arrangement, since there is less wake at the position of the propellers for such ships than for full-bodied single screw ships. Hence, in paper 5, an 8000 dwt tanker equipped with twin azipull propulsion was studied to obtain wake in waves, followed by cavitation and pressure pulses calculation. This ship is a concept design for a chemical tanker, designed by Rolls-Royce Marine and used in several research projects and studies, but never built. The full-scale vessel was simulated in the presence of three head waves using CFD. Contrary to the expectations, notable changes in wake were observed as in Figure 4.27.

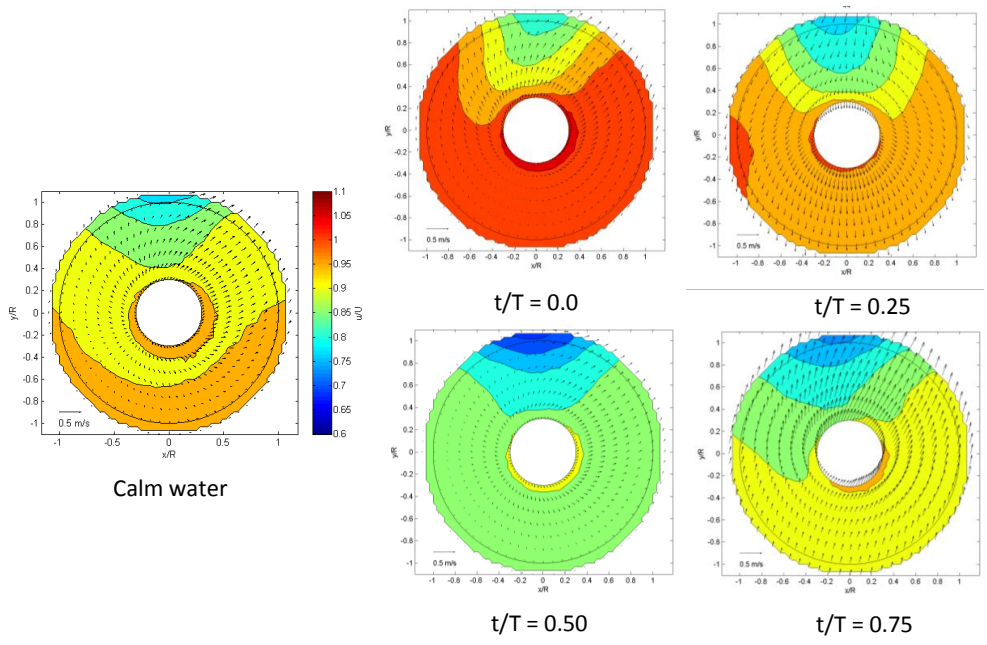

Figure 4.27 Wake in calm water and in the presence of wave having wavelength ratio λ/L = 1.6.

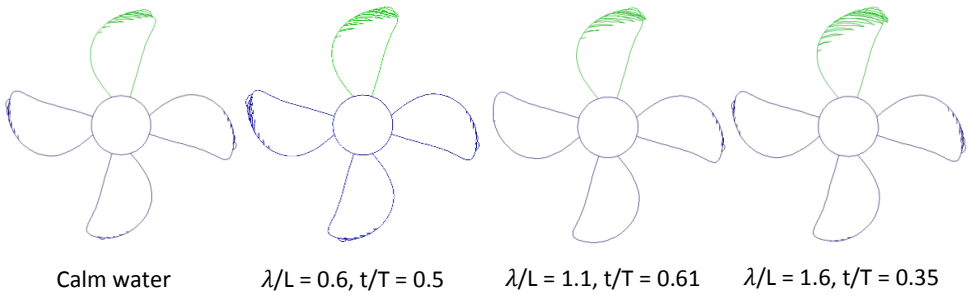

Figure 4.28 Maximum cavitation in each wave condition only considering the wake change.

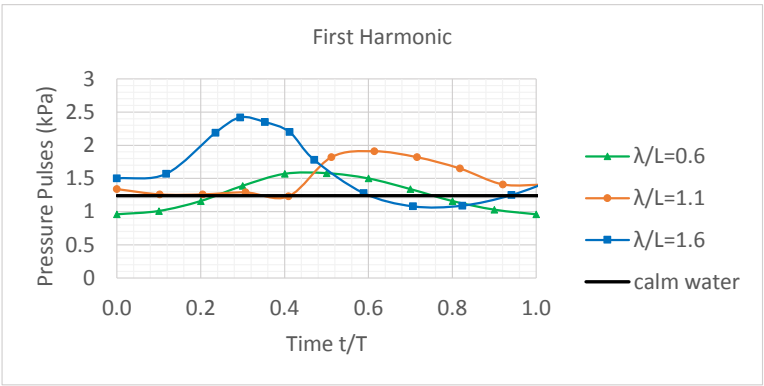

Figure 4.29 First harmonic amplitude of pressure pulses in waves only considering wake variation.

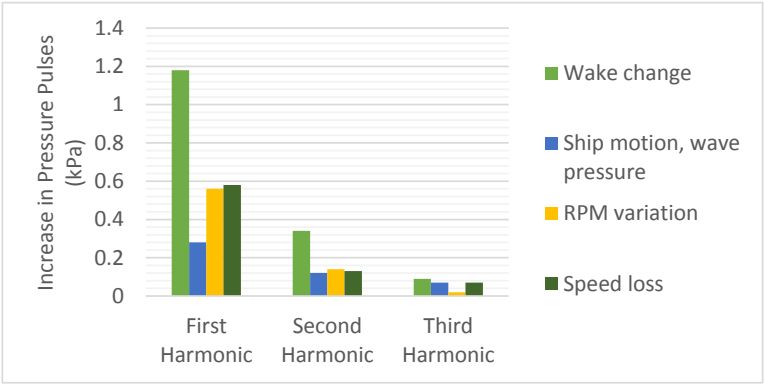

Figure 4.30 Comparison of maximum increase in pressure pulses due to different factors in the presence of waves.

The propeller was analyzed in different wakes considering the effects of ship motion, dynamic wave pressure, RPM fluctuation and added resistance. Both cavitation and pressure pulses increased remarkably in the presence of waves, primarily due to wake variation as seen in Figure 4.28 and Figure 4.29.

The maximum increase in the first three harmonic amplitudes of pressure pulses due to different factors affecting the propeller has been compared in Figure 4.30. The effect of wake variation is greater than the other factors, as in the case of KVLCC2. Therefore, in spite of having small influence of hull on the wake distribution, wake varies considerably in the presence of waves, causing an increase in cavitation as well as pressure pulses. Hence, considering wake variation is of importance for the propeller design even in the case of a ship with twin azipull propellers.

5. Conclusions and Future work

The major contribution of this work is to develop and demonstrate a relatively simple method to study engine-propeller interactions in the presence of waves. The tendency of pressure pulses to increase in the presence of waves is one of the main conclusions of the work. Comparative study of the effect of different factors on cavitation and pressure pulses provides an essential information to propeller designers to further optimize propellers for efficient operation in waves. Detailed contributions and conclusions are presented in following sections.

5.1 Original Contributions

The work presented in the thesis is a step towards optimizing the propulsion system of ships in realistic operating conditions. The ways in which propulsion systems gets affected in waves have been studied along with the identification of which all propulsion performance indexes get affected. Original contributions of this thesis can be listed as follows:

- Coupled model of engine, propeller, and vessel with wake estimation in waves has been built, which provides the capability to analyze any component of propulsion system like control system, shaft, etc. with realistic inputs from the engine as well as propeller side.
- The model is capable of simulating a ship in the presence of regular or irregular waves of different wavelengths and waveheights coming from different directions.
- Effects of waves on the engine, propeller, and vessel performance in terms of change in engine efficiency, engine power, propulsion efficiency and vessel speed have been investigated.
- The importance of engine-propeller coupling and wake estimation in waves in the prediction of vessel performance has been analyzed.
- Engine performance has been studied in the presence of waves considering the effects of wake variation, propeller emergence, and free surface effects.
- Propeller performance has been analyzed in the presence of waves considering effects of wake variation, ship motions, speed loss and rpm variation to identify the relevant factors to be considered while designing propellers for operation in waves.
- The effect of waves on propeller efficiency, cavitation, pressure pulses, hub loading and tip loading has been studied and compared with the performance in calm water to identify the extent to which different performance parameters get affected in the presence of waves.
- The validity of calculating wake in waves using potential flow calculation for propeller analysis in waves has been studied.

5.2 Conclusions

Findings of the analysis performed to examine the engine-propeller dynamics using the case vessel KVLCC2 are:

- Wake variation, especially mean wake change in waves due to pitching motion of ship influences the performance of a vessel.
- Mean change in wake is significant at low ship speed; it affects the quasi-propulsive efficiency. Therefore, modeling the wake variation and propulsion losses in waves can significantly improve speed and power prediction in the presence of waves.
- Engine-Propeller dynamics has a minor impact on the propulsion performance except in cases where the engine is operating close to MCR.
- Engine performance regarding fuel efficiency gets affected in waves only when mean load is low but load fluctuations are high.

The effect of waves on propeller performance was analyzed using two case vessels; KVLCC2, which is single screw ship, and an 8000 dwt chemical tanker equipped with twin Azipull propulsion. General conclusions from this study can be stated as follows:

- Pressure pulses created by a cavitating propeller increase substantially in the presence of waves.
- Wake variation is the major factor affecting cavitation induced pressure pulses in waves in case of both case ships. Hence, it is recommended to consider the wake variation at least in one regular wave of length close to the ship length, due to practical difficulties related to determining the wake variations.
- In the case of KVLCC2, the amount of cavitation did not change much in spite of noteworthy wake variation in waves; whereas cavitation increased considerably in the case of the chemical tanker.
- In both cases, the propeller efficiency was dependent on average wake rather than wake distribution.
- Calculation of wake variation in waves using potential flow method is not sufficiently accurate to be used for assessing propeller performance in terms of cavitation and pressure pulses.
- Effect of waves on propeller performance is largest when the wavelength is close to ship length.

5.3 Limitations and Future Work

Engine-propeller interactions have been studied using one case vessel that is KVLCC2. Therefore, the conclusions obtained from this study might not apply to other configurations of hull, propeller, and engine. Although this study provides an idea about potential factors affecting the propulsion in waves along with likely impact, more such studies are necessary to draw any generalized conclusions regarding the importance of engine-propeller interactions in waves. Also, the type of engine, and settings of the engine controller is believed to be important, as well as engine system – for instance diesel-electric power plant. This emphasizes the need for further studies of engine-propeller interaction in waves.

The coupled model of engine and propeller should be compared with full-scale data to see if all the important effects are captured in the model. Currently, each model in the simulation has been validated, however, the behavior of coupled system needs to be confirmed.

In the study, wake variation in waves has been estimated, but thrust deduction has been assumed constant. From the literature, it is known that thrust deduction also varies in the presence of waves, yet there are no available methods to predict the variation, outside of model experiments and complete CFD simulations. Once the change in thrust deduction is taken into consideration, change in propulsive efficiency in the presence of waves can be predicted more accurately. Thus, an analysis method to simulate or calculate thrust deduction in the presence of waves is required.

While analyzing the propeller performance regarding cavitation and pressure pulses, propellers have been analyzed only in case of regular head waves of fixed waveheight due to limited availability of wake data. The propeller should also be analyzed in irregular waves as well as in waves coming from different directions. Effects of wake variation are supposed to be less pronounced in the case of irregular waves, as ship motions and added resistance are often higher in regular waves as compared to that in irregular waves. Head waves are often thought to be the most severe condition; however, as far as wake variation is concerned, following waves might also have a noteworthy impact as these waves can directly affect the propeller without being shielded by the hull.

Pressure pulses vary significantly in the presence of waves. Integration of pressure pulses on the hull creates a vertical force on the stern region, which affects the hull vibrations. However, pressure pulses need a medium of water to influence the hull. Due to relative stern motion in waves, the wetted part of the stern may be reduced, leading to limited part of hull getting affected by pressure pulses thus reducing total force on the stern. Therefore, the analysis should be performed to take into account the stern submergence along with the level of increase in pressure pulses.

References

[1] Wu P.C. A CFD Study on Added Resistance, Motions and Phase Averaged Wake Fields of Full Form Ship Model in Head Waves [Doctoral Dissertation]: Osaka University; July 2013.

[2] Kim H. Phase-Averaged SPIV Wake Field Measuremet for KVLCC2 Propeller Plane in Waves [Doctoral Dissertation]: Osaka University Japan; July 2014.

[3] Moor D.I., Murdey D.C. Motions and Propulsion of Single Screw Models in Head Seas, Part II. The Royal Institution of Naval Architects. 1970; Vol 112(2).

[4] Nakamura S., Naito S. Propulsive performance of a container ship in waves. J. Soc. Naval Archit. Jpn. 1975; Vol 158.

[5] Guo B.J., Steen S., Deng G.B. Seakeeping prediction of KVLCC2 in head waves with RANS. Applied Ocean Research. 2012; Vol 35: 56-67. http://dx.doi.org/10.1016/j.apor.2011.12.003

[6] Albers A.B., Gent W.v. Unsteady wake velocities due to waves and motions measured on a ship model in head waves. 15th Symposium on Naval Hydrodynamics, 1985.

[7] Chevalier Y., Kim Y.H. Propeller Operating in a Seaway. PRADS'95, Seoul, Korea, 1995.

[8] Jessup S.D., Wang H.-C. Propeller Cavitation Prediction for a Ship in a Seaway. DTIC Document; 1996.

[9] ABS. Guidance notes on ship vibration. Houston, USA; April 2006 (Updated January 2015).

[10] VERITEC. Vibration control in ships. Høvik, Norway: A.S. Veritec Marine Technology Consultants, Noise and Vibration Group; 1985.

[11] Lee C.S. Propeller in waves. The 2nd international symposium on practical design in shipbuilding, Tokyo & Seoul, 1983.

[12] Amini H. Azimuth propulsors in off-design conditions [Doctoral thesis]: Norges teknisk-naturvitenskapelige universitet (NTNU); 2011.

[13] Kyrtatos N.P. Engine operation in adverse conditions - The ACME project. 2nd international symposium CIMAC, Athens, 1997.

[14] Kayano J., Yabuki H., Sasaki N., Hiwatashi R. A Study on the Propulsion Performance in the Actual Sea by means of Full-scale Experiments. TransNav, International Journal on Marine

Navigation and Safety of Sea Transportation. 2013; Vol 7(4): 521-526. http://dx.doi.org/10.12716/1001.07.04.07

[15] Kyrtatos N., Theodossopoulos P., Theotokatos G., Xiros N. Simulation of the overall ship propulsion plant for performance prediction and control. MarPower '99, IMarE, Newcastle-upon-Tyne, UK, 1999.

[16] Livanos G.A., Simotas G.N., Dimopoulos G.G., Kyrtatos N.P. Simulation of Marine Diesel Engine Propulsion System Dynamics During Extreme Maneuvering. ASME 2006 Internal Combustion Engine Division Spring Technical Conference, 2006.

[17] Theotokatos G., Tzelepis V. A computational study on the performance and emission parameters mapping of a ship propulsion system. Proceedings of the Institution of Mechanical Engineers, Part M: Journal of Engineering for the Maritime Environment. 2013; Vol 227(2): 83-97. http://dx.doi.org/10.1177/1475090212457894

[18] Campora U., Figari M. Numerical simulation of ship propulsion transients and full-scale validation. Proceedings of the Institution of Mechanical Engineers, Part M: Journal of Engineering for the Maritime Environment. 2003; Vol 217(1): 41-52. http://dx.doi.org/10.1243/147509003321623130

[19] el Moctar O., Lantermann U., Mucha P., Höpken J., Schellin T.E. RANS-Based Simulated Ship Maneuvering Accounting for Hull-Propulsor-Engine Interaction. Ship Technology Research. 2014; Vol 61(3): 142-161. http://dx.doi.org/10.1179/str.2014.61.3.003

[20] Papanikolaou A., Zaraphonitis G., Bitner-Gregersen E., Shigunov V., El Moctar O., Guedes Soares C., et al. Energy efficient safe ship operation (SHOPERA). Proceedings 12th International Marine Design Conference IMDC2015, Tokyo, Japan, 2015.

[21] Carlton J.S. Marine propellers and propulsion (Third Edition). Oxford: Butterworth-Heinemann; 2012.

[22] Holden K.O., Fagerjord O., Frostad R. Early design-stage approach to reducing hull surface forces due to propeller cavitation. SNAME Transactions. November 1980; Vol 88: 403-442.

[23] Skaar K., Raestad A. The relative importance of ship vibration excitation forces. Symposium on Propeller Induced Ship Vibration, Trans. RINA, 1979.

[24] He L., Tian Y., Kinnas S.A. MPUF-3A (Version 3.1) User's Manual and Documentation 11-1. Ocean Engineering, University of Texas at Austin; 2011.

[25] Sun H., Kinnas S.A. HULLFPP, Hull Field Point Potential, User's Manual and Documentation. University of Texas, Austin; 2007.

[26] Ueno M., Tsukada Y., Tanizawa K. Estimation and prediction of effective inflow velocity to propeller in waves. J Mar Sci Technol. 2013; Vol 18(3): 339-348. http://dx.doi.org/10.1007/s00773-013-0211-8

[27] Faltinsen O.M., Minsaas K.J., Liapis N., Skjordal S.O. Prediction of resistance and propulsion of a ship in a seaway. 13th Symposium on Naval Hydrodynamics, 1980.

[28] Yum K.K., Lefebvre N., Pedersen E. An experimental investigation of the effects of cyclic transient loads on a turbocharged diesel engine. Applied Energy. 2016; Vol 185(1): 472–481. http://dx.doi.org/10.1016/j.apenergy.2016.10.138

[29] Flowtech. SHIPFLOW 6.1, Users Manual. 2015.

[30] Yum K.K., Taskar B., Pedersen E., Steen S. Simulation of a two-stroke diesel engine for propulsion in waves. International Journal of Naval Architecture and Ocean Engineering. 2016; http://dx.doi.org/10.1016/j.ijnaoe.2016.08.004

[31] Raestad A.E. Tip vortex index-an engineering approach to propeller noise prediction. The Naval Architect, July/August 1996.

Paper 1

Analysis of propulsion performance of KVLCC2 in waves

Bhushan Taskar, Sverre Steen

Proceedings of Fourth International Symposium on Marine Propulsors (SMP'15), Austin, Texas, USA, 2015.

Fourth International Symposium on Marine Propulsors
smp'15, Austin, Texas, USA, June 2015

Analysis of Propulsion Performance of KVLCC2 in Waves

Bhushan Taskar[1], Sverre Steen[2]

[1, 2] Department of Marine Technology, NTNU, Trondheim, Norway

ABSTRACT

In this paper, we have analyzed the propulsion performance of KVLCC2 in presence of waves. Different factors affecting the propulsion performance have been studied. Analysis of the extent of change in wake quality and its effect on the cavitation of propeller has been presented. Effect of wake change alone was separately calculated to analyze its importance in the design process, as wake data in waves is usually not available. It was observed that wake change itself does not significantly affect the amount of cavitation hence; cavitation margin should be considered only to handle increased load and relative stern motion.

Keywords

Cavitation Analysis in Seaway, Propeller in Waves, Performance in Off-Design Conditions.

1 INTRODUCTION

Currently, propellers are designed using wake, thrust deduction and relative rotative efficiency obtained in calm water conditions. These factors vary when ship is subjected to waves (Moor and Murdey 1970). Wake distribution also changes due to waves and ship motion (Nakamura and Naito 1975). Similar results were obtained in the RANS simulation carried out by Guo, Steen et al. (2012) where the nominal wake field was obtained in the presence of waves. In this simulation, axial wake velocities increased up to 35% of ship speed in some regions. Such changes in the wake distribution of a ship travelling in waves were experimentally confirmed by Wu (2013) using KVLCC2 ship model. PIV measurements of wake field found strong variation in presence of waves.

In view of this recently obtained data, which demonstrates significant effect of waves on wake, a possible drop in the performance of the propeller should be calculated. Full-scale experiments performed by Kayano, Yabuki et al. (2013) found a discrepancy between the calculated and obtained performance of the ship. This can be due to inability of prediction methods to take into account the effect of waves on the propulsion performance. Currently, off-design conditions are covered by simple sea margin, which may result in overdesign or failure in off design conditions. Therefore, previously considered assumptions and margins should be revisited and updated by detailed knowledge of propeller performance in waves.

Along with the efficiency of the propeller, cavitation and vibration characteristics should be studied in presence of waves as they depend on the wake distribution (Odabasi and Fitzsimmons (1978) and Huse (1974)). Moreover, a change in wake distribution changes the angle of attack and the cavitation number of the propeller blades as shown by Albers and Gent (1985). Chevalier and Kim (1995), Jessup and Wang (1996) studied the cavitation of a propeller operating in waves by calculating wake velocities using potential flow calculations. Drop in the cavitation inception speed of a vessel was observed in waves.

The cavitation characteristics of propellers designed using calm water wake data must be studied in order to validate currently used cavitation margins, so that future propellers can be designed for low cavitation and noise along with acceptable performance even in rough weather.

In this paper, we have evaluated the performance of the KVLCC2 propeller operating in waves. Time varying wake data in three different wavelengths provided by Sadat-Hosseini, Wu et al. (2013) have been used. The effect of waves on changes in the angle of attack and the cavitation number of propeller blade sections has been studied. The effect of wake change and relative stern motion has been separately observed to decide the order of importance of each effect. The effect of this time varying wake on vibration and noise characteristics of the propeller has been calculated using the BSRA wake criteria given by Odabasi and Fitzsimmons (1978). Other possible factors causing changes in propulsion performance in waves have been noted.

2 METHODS AND VALIDATION

2.1 Wake Data in Presence of Waves

Experiments were performed by Sadat-Hosseini, Wu et al. (2013) to obtain wake data in three different wavelengths in head sea condition at design speed. A model of KVLCC2 was used for this purpose with model scale of 1:100. Ship particulars are given in Table 1 (SIMMAN 2008). In these

experiments, PIV (Particle Image Velocimetry) was used to obtain time varying nominal wake field in the propeller plane. CFD simulations were also performed and results were validated using existing data from PIV experiments. Since the CFD data are smoother and less noisy, we have used them in our calculations. These results were available for waves $\lambda/L = 0.6$, 1.1 and 1.6 at 8, 12 and 6 time intervals respectively in one wave period. Waveheight of these waves correspond to the full-scale waveheight of 3m.

Table 1 Ship Particulars

Length beween perpendiculars (m)	320.0
Length at water line (m)	325.5
Breadth at water line (m)	58.0
Depth (m)	30.0
Draft (m)	20.8
Displacement (m^3)	312622
Block coefficient (C_B)	0.8098
Design Speed (m/s)	7.97

Table 2 Propeller Geometry

Diameter (D) (m)	9.86
No of blades	4
Hub diameter (m)	1.53
Rotational speed (RPM)	76
A_e / A_0	0.431
$(P/D)_{mean}$	0.690
Skew (°)	21.15
Rake (°)	0

2.2 Wake Quality Assessment

In the preliminary investigation of the wake data in waves, the quality of wake was assessed and compared with the quality of the calm water wake using the BSRA wake criteria proposed by Odabasi and Fitzsimmons (1978). These criteria are based on a large collection of wake distribution data and noise and vibration characteristics of full-scale ships. Five conditions are mentioned for assessing the wake. Although satisfying these conditions does not guarantee good vibration and noise characteristics, it is recommended to be extra careful when the conditions are not met. For our purpose, these simple criteria are useful to assess the extent to which waves can affect vibration and noise characteristics without using any particular propeller geometry.

2.3 Wake Contraction Method

For further investigation of the performance of the propeller operating in waves, scaling of wake data from model scale to full scale was required. According to ITTC (2011), the wake scaling procedure given by Sasajima, Tanaka et al. (1966) is most commonly used and gives reasonable results. In this method, only viscous wake is scaled and a correction is applied to the potential component. However, in the absence of potential wake data, we have contracted the whole wake field towards the center plane by the ratio of viscous resistance coefficient between model and full scale. Hence, the difference between potential wake component of model and ship has been neglected.

Potential wake is almost constant in a horizontal section in the propeller plane as seen from the typical ship scale wake presented in ITTC (2011). In such cases, the same full-scale total wake would be obtained by scaling the total wake or just the frictional component of the model-scale wake. The only error would be due to the neglected correction in the potential wake.

2.4 Software Validation Using Existing Data

After the initial wake assessment, a detailed study of propeller operating in presence of waves was performed. Existing KVLCC2 propeller design was analyzed in time varying wake. Details about propeller geometry can be seen in Table 2 (more details can be obtained from SIMMAN (2008)). The open source program Openprop based on vortex lattice lifting line theory (Epps 2010) has been used for this purpose.

Openprop requires blade section details, corresponding frictional drag coefficient, advance coefficient, axial and tangential wake velocities and at each radial location for the analysis. Blade section details can be found in SIMMAN (2008). *Javafoil* was used for the calculation of frictional drag at each radial section for the given Reynolds number. It uses panel method to calculate velocity profile and pressure distribution over the foil section. Using these pressure and velocity distributions, boundary layer calculations are performed where drag is calculated using momentum loss in the boundary layer (Hepperle).

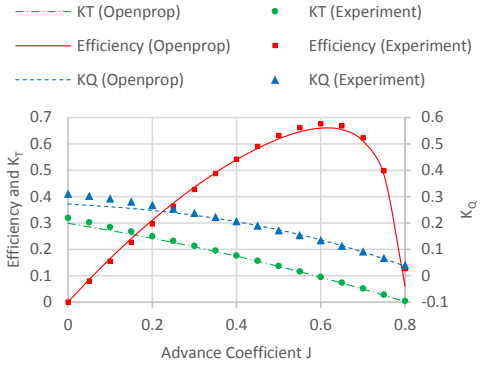

Figure 1 Comparison of Openprop and open water data of KVLCC2 propeller

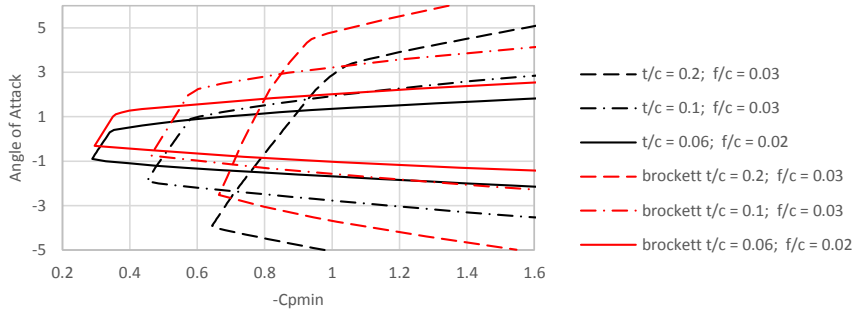

Figure 2 Comparison of cavitation bucket diagrams obtained from Openprop with those calculated by Brockett (1966)

Openprop is based on steady lifting line theory. As we know, a propeller operating even in calm water condition faces time varying inflow due to spatial variation of wake. Such cases should ideally be analyzed with unsteady calculations. Gaggero and Brizzolara (2009) have shown that a quasi-steady approach also gives good results compared to fully unsteady calculations. In their research, the quasi-steady approach was seen to correctly predict the change in thrust, torque and efficiency between propeller and its modified version. Hence, we have used quasi-steady approach for our analysis. Openprop analyzes propeller in a steady flow with only radial wake variation, however, in reality there is angular as well as radial variation of wake. Hence, performance of the propeller with four blades facing different radial wake distribution was assumed to be the average performance of four hypothetical propellers, each facing the radial wake distribution faced by each blade.

Performance of Openprop with frictional drag obtained from *Javafoil* was validated by comparing open water characteristics with the experimental data. Thrust, torque and efficiency in open water condition obtained using this approach match well with the experimental data as can be seen from Figure 1.

Openprop has also been used to predict the cavitation on the propeller blades. In order to calculate the cavitation, pressure distribution over the foil has been calculated using linear foil theory; possible effects of viscosity have been neglected. Areas where pressure falls below the vapor pressure is assumed to cavitate. The cavitation bucket can be obtained by observing the angle of attack and cavitation number at which cavitation starts. Cavitation buckets were plotted for foils with three different combinations of camber and thickness. These plots were compared with those obtained by Brockett (1966) where minimum pressure envelopes were calculated for steady two dimensional flow with an empirical correction for the viscosity. There is discrepancy in the exact values of the angle of attack where cavitation inception is predicted. However, Openprop correctly predicts the cavitation inception trends as seen in Figure 2. Even though more complicated and accurate theories like lifting surface theory and cavitating foil theory are available to predict exact cavitation pattern, change in efficiency, thrust and torque of a cavitating propeller; we have used this simple theory since we are interested in comparing the performance of a propeller in waves with that in calm water, rather than very accurately predicting the performance in cavitating condition. Thus, correct prediction of trends would serve the purpose.

While calculating the cavitation pattern, depth variation of the propeller due to ship motion was also taken into account. Relative stern motion was calculated using the motion response of the ship. All the analysis was performed at constant rpm. Hence, variation of rpm due to time varying torque was neglected in the analysis, which may cause some inaccuracies.

3 ANALYSIS

3.1 Wake Assessment in Presence of Waves

Vibration and noise characteristics of a propeller depend on the wake field in which it operates. Odabasi and Fitzsimmons (1978) have listed certain criteria to be fulfilled by the wake distribution for low noise and vibration. Time varying wake in waves will now be compared with the calm water wake field considering four out of five BSRA wake criteria.

Criterion 1 –

The maximum wake measured inside the angular interval $\theta_B = 10 + 360/Z$ degrees and in the range $0.4 - 1.15R$ around the top dead center position of the propeller disc should satisfy the following:

$$Wmax < 0.75 \; or \; Wmax < C_B$$

whichever is smaller. Where Z is the number of blades. $Wmax$ has been obtained at given locations at different times in one wave period to compare with the value observed in calm water. Values greater than that in calm water can increase vibration and noise.

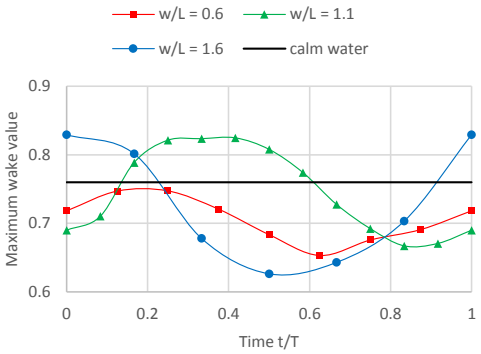

Figure 3 Comparison of wake peak observed in waves and in calm water

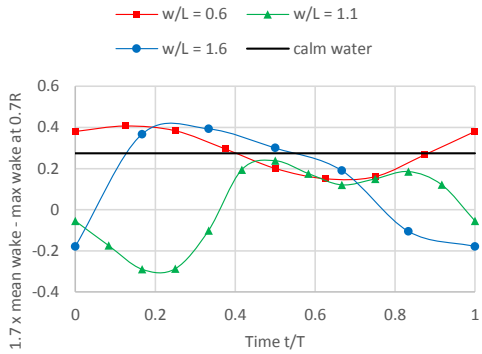

Figure 4 Comparison of wake with respect to criterion 2

Variation of $Wmax$ in different waves can be seen in Figure 3. When the wave is shorter than the ship, the maximum value of wake is always smaller than in calm water. In the longest wavelength, only few values are greater than that in calm water. While, when wavelength is close to ship length, $Wmax$ in wave is higher than that in calm water for almost 50% of the time as seen from Figure 3. Hence, this condition is not greatly affected due to waves except in case of wavelength close to ship length.

Criterion 2 –

The maximum acceptable wake peak should satisfy the following relationship with respect to the mean wake at $0.7R$:

$$Wmax < 1.7\bar{W}_{0.7}$$

Therefore, $(1.7\bar{W}_{0.7} - Wmax)$ was plotted in different wavelengths, at different times in time varying wake and compared with the calm water condition (Figure 4). Value of this variable should be positive for the criterion to be satisfied.

Figure 4 shows that this condition would be most stringent if it is to be satisfied in wavelength $\lambda/L = 1.1$. Since, all the values of $(1.7\bar{W}_{0.7} - Wmax)$ are lower than that in calm water and many of them are negative. Also in the wavelength $\lambda/L = 1.6$, values lower than that in calm water are observed for almost 50% of the time period. Hence, in case of designs where this condition is just satisfied in calm water, its violation is highly probable in presence of waves. This gives us an idea about the margin to be considered while satisfying this condition in realistic sea when only calm water wake data is available.

Criterion 3 –

Wake non-uniformity criterion is important to avoid unsteady cavitation and high levels of pressures on the hull. In this criterion, tip cavitation number is plotted against average non-dimensional wake gradient. Tip cavitation number is defined as-

$$\sigma_n = \frac{\left(9.903 - \frac{D}{2} - Z_p + T_A\right)}{0.051(\pi n D)^2}$$

while average non-dimensional wake gradient is defined as $(\Delta w/(1-\overline{w}))$, where D is the propeller diameter (m). Z_p is the distance between the propeller shaft axis and the base line (m). T_A is the ship's draught at the aft-perpendicular (m). n is the propeller rotational speed (rev/s). Δw is the wake variation. Plotted point should lie above the dividing line of Figure 5 to satisfy the criterion.

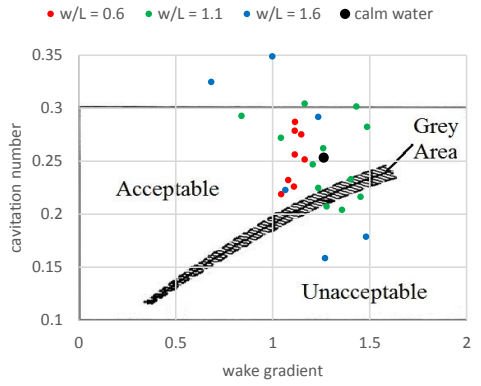

Figure 5 Wake non-uniformity criterion

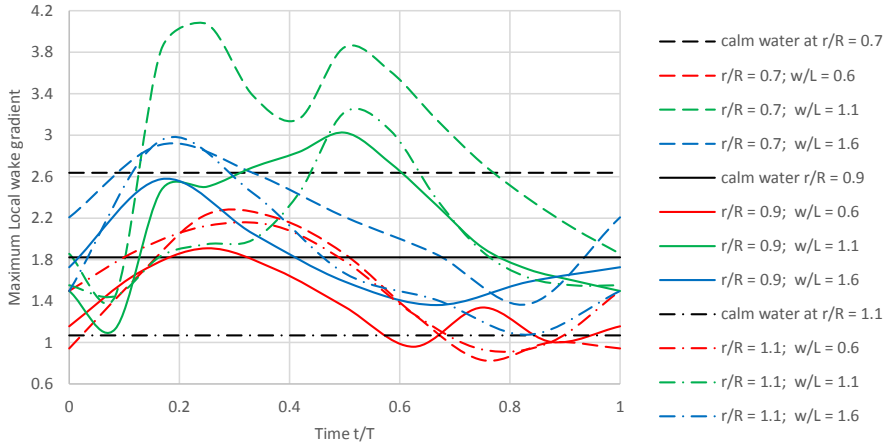

Figure 6 Maximum wake gradient at different time intervals in three different wavelengths

Figure 5 shows the plot for this criterion in three different head waves. Variation in cavitation number is due to change in the submergence of the propeller due to ship motion while change in the horizontal axis variable (wake gradient) is due to wake variations in waves. Wake gradient is becoming favorable (i.e. less) in more cases than in those it is getting worse than the calm water value. Some values are present in the unacceptable region, which may cause intermittent cavitation and vibration while ship is travelling in waves. Figure 5 also provides the information about the extent to which waves can worsen the cavitation and vibration characteristics of the propeller. Therefore, appropriate cavitation margin can be considered for the calm water design to have acceptable cavitation and vibration performance in waves.

Criterion 4 –

For the propellers susceptible to the cavitation, that is near the grey area of Figure 5, the local wake gradient per unit axial velocity for radii inside the angular interval θ_B in the range of $0.7 - 1.15R$ should be less than unity; that is,

$$\frac{1}{\left(\frac{r}{R}\right)}\left|\frac{\left(\frac{dw}{d\theta}\right)}{(1-w)}\right| < 1.0$$

where θ is in radians.

This criterion limits the wake gradient in order to reduce volume variations of the cavity. It is required only when the relation between wake gradient and cavitation number lies in the grey area in Figure 5. However, here we are more interested in comparing quality of wake in waves with calm water wake. Hence, local wake gradient for unit axial

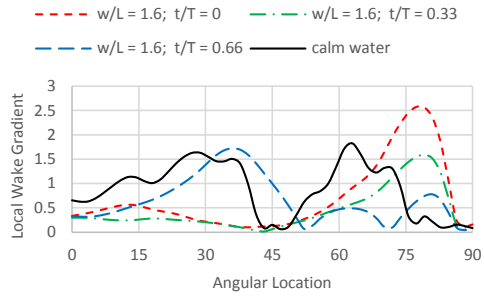

Figure 7 Wake gradient at w/L=1.6 at different time intervals as a function of angular position

velocity was calculated (Figure 7) and maximum value was obtained in the angular interval θ_B in the range 0.7R to 1.15R. This maximum value obtained at different time intervals of wave period is plotted in Figure 6.

As seen in Figure 6, from 0.7R to R, in wave $\lambda/L = 0.6$ values of wake gradient hardly exceed corresponding calm water value. While in wavelengths $\lambda/L = 1.1$ and 1.6 local wake gradient is higher than calm water value for approximately 66% and 33% of the time respectively. At r = 1.1R almost all the wake distributions in waves show higher local gradients. Amount of exceedance, whenever it occurs is considerable. Moreover, in this case, all the values including those in calm water exceed the criterion limit, i.e. all values are greater than one. Therefore, points lying in grey or unacceptable region in Figure 5 are the cause of concern. Since, unstable cavitation in large wake gradient can cause significant amount of noise due to the cavity volume

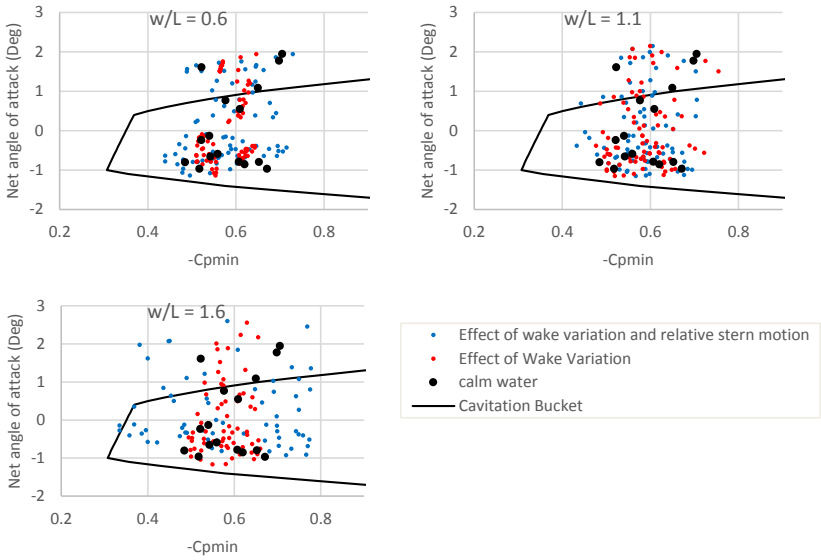

Figure 8 Cavitation number and angle of attack faced by propeller blade section at 0.7R in calm water and in waves

variation. Radial section r/R = 1.1 is analyzed since there is chance of wake at that location coming in way of propeller due to propeller action (contraction of stream tube).

3.2 Propeller Analysis Using Openprop

After analyzing the wake quality, propeller geometry of KVLCC2 ship was examined in time varying wake using Openprop. As noted earlier, significant change in the wake, observed in presence of waves is expected to affect the operation of wake-adapted propellers. Although wake assessment gives some idea about possible cavitation, examining the propeller geometry can reveal additional details like changes in the type and the extent of cavitation, thrust and torque fluctuations. Therefore, performance of the propeller in waves was compared with that in calm water.

3.2.1 Effect of Waves on Cavitation

Propeller cavitation is affected by the following factors in the presence of waves:

1. Relative stern motion causing change in the cavitation number
2. Change in wake field leading to alteration of inflow velocities and blade angle of attack
3. Added resistance causing increased propeller loading

Out of these three, relative stern motion and added resistance of ship can be estimated at the design stage, while considering the effect of wake change is tough. Wake in waves can be obtained either experimentally or computationally. Experimentally finding time varying wake is not a common practice, it would require specialized instruments like PIV. Moreover, multiple runs would be required to find wake in different wavelengths. Computationally finding wake variation in waves is also expensive. Therefore, it is important to know the extent to which the wake change alone influences the propeller performance, especially due to significant changes in the wake field observed in presence of waves.

Therefore, propeller design was analyzed in time varying wake using the method based on the lifting line theory. These calculations were also used to predict the extent of cavitation on the propeller blade along with thrust and torque fluctuations in different conditions.

Cavitation Number and Blade Angle of Attack –

While designing the propeller, the knowledge of variation in the angle of attack and cavitation number is important to choose correct blade thickness. However, certain cavitation margin has to be assumed for possible off design conditions including the ship operation in rough sea, as wake in waves is rarely available. Therefore, since wake data in waves is available in this case, the correctness of cavitation margin has been analyzed further. This would help propeller designers to estimate the change in the extent of cavitation in presence of waves as compared to the calm water condition.

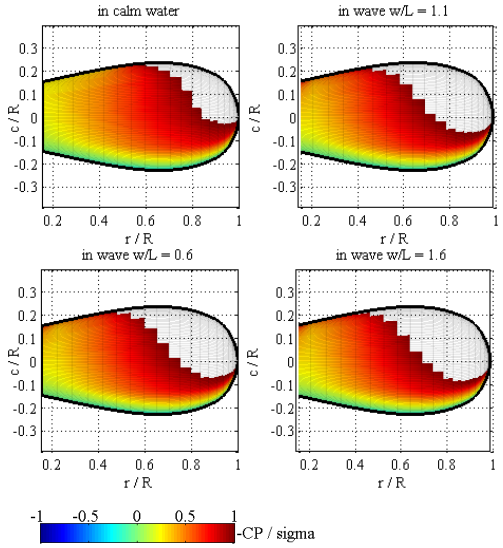

Figure 9 Propeller cavitation in different conditions

Cavitation characteristics of the propeller were examined in presence of waves. Cavitation numbers and angle of attacks faced by the blade section at 0.7R were plotted along with the cavitation bucket of the blade section. Plotted points for the calm water condition correspond to sixteen different angular positions of the blade as it rotates in the calm water wake. While points in waves correspond to eight different angular positions of the blade at ten different time intervals in one wave period. This can be seen in Figure 8.

In Figure 8, influence of wake change and relative stern motion was analyzed while effect of added resistance was not considered. Out of these two, relative stern motion only affects the range of –Cpmin and not angle of attack; since it affects only cavitation number. While, wake change can affect both the variables. Spread in the values of –Cpmin is predominantly due to relative stern motion. In all 3 cases, the effect of wake variation does not decrease the minimum value of –Cpmin seen in calm water. Maximum of half a degree increase in angle of attack can be seen due to wake variation only in wavelength w/L = 1.6. In other two waves, no significant change in maximum or minimum angle of attack is observed. Similar trends were observed at other blade sections as well.

Cavitation Due to Wake Variation –

Due to wake variation alone, there is no increase in the range of cavitation numbers while angle of attack increases slightly in some cases as compared to the calm water condition. Influence of this slight increase in the angle of attack (only due to wake variation) on the extent of cavitation can be seen in Figure 9 where maximum amount of cavitation in each condition has been plotted. No significant change in cavitation is seen due to the effect of wake variation. This observation is in line with the earlier result of cavitation bucket diagram. Since spread of operating points is similar to the one obtained in calm water wake, similarity in the extent and pattern of cavitation is expected.

These results obtained using quasi-steady approach were validated using fully unsteady simulations with cavity volume calculations. The unsteady panel method software AKPA, developed by MARINTEK and University of St. Petersburg, was used to simulate the propeller in calm water

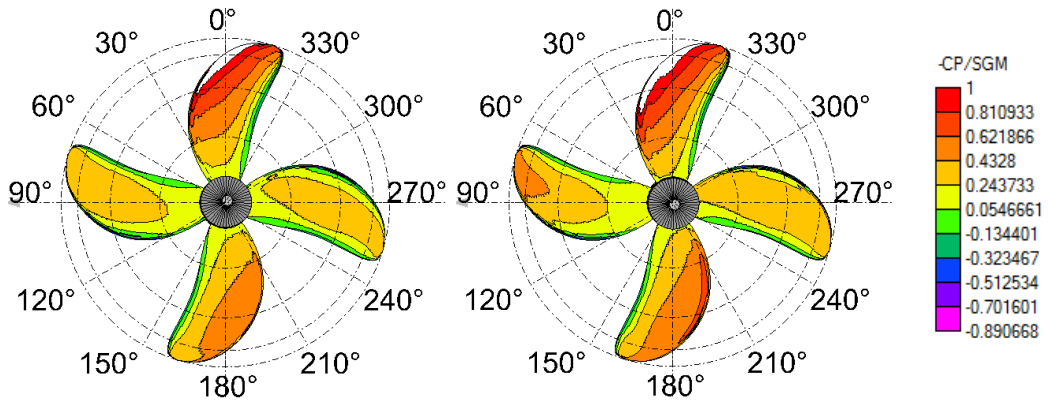

In calm water

In wave $\lambda/L = 1.6$

Figure 10 Unsteady simulation results of propeller in calm water and in wave

wake and in case of $\lambda/L = 1.6$ where maximum increase in cavitation volume was observed in Figure 9. Effect of wake change alone was considered in order to compare the results with those in Figure 9. For the simulation in presence of wave, wake at the time instance showing maximum cavitation in Openprop simulation was chosen. Time period of the propeller being much smaller than that of wake variation, wake field was assumed constant in this unsteady simulation. Cavitation pattern obtained from this analysis can be seen in Figure 10.

Unsteady panel method (Figure 10) show significantly less cavity volume as compared to Openprop (Figure 9). However, maximum cavitation seen in presence of waves hardly differs from the cavitation in calm water, as can be observed in Figure 10.

Effect of Waves on Cavitation –

Therefore, the effect of wake change, excluding other factors, on the cavitation is minor in spite of significant changes observed in the wake field. This can be due to the large induced velocities as compared to the wake velocities, and that even though the change of wake pattern due to waves is quite significant, the critical features, like maximum wake and wake gradient don't worsen much. The effect of such wake variation could be more pronounced in case of a lightly loaded propeller. It is important to note that this analysis has been performed using wake data in regular waves of fixed waveheight. Therefore, influence of waves can increase in case of higher waves. However, effects are expected to be less severe in irregular waves with significant waveheight equal to the height of the regular wave.

Increased load caused by added resistance increases the angle of attack of blade sections making them susceptible to backside sheet cavitation. In this case, since propeller is already cavitating in calm water wake, increased load will increase the extent of this cavitation. However, as noted earlier, this effect can be easily taken into account while designing the propeller, since the increased propeller load can be calculated from the added resistance.

3.2.2 Thrust and torque fluctuations in waves

Along with the changes in cavitation and vibration characteristics, wake variation also causes thrust and torque to fluctuate. The amount of these fluctuations should be examined to see if they affect the operation of the engine. Fluctuations of K_Q at constant propeller rpm obtained using Openprop can be seen in Figure 11 for three different wavelengths. Maximum fluctuation is evident when wavelength is equal to the ship length. Change in mean value of K_Q as compared to the calm water value is due to the increase in average inflow to the propeller caused by the pitching motion of ship.

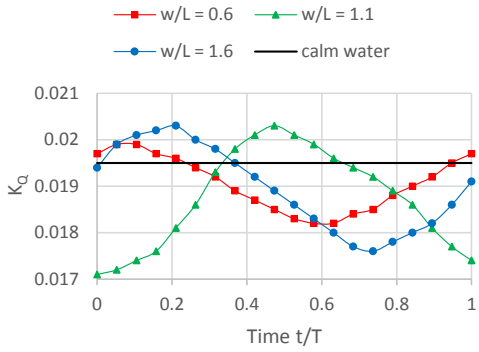

Figure 11 Variation of K_Q in waves

Fluctuations in K_Q have been calculated assuming constant propeller rpm while in reality rpm is a function of torque and engine behavior.

These variations in torque can cause transients in engine operations, and might influence engine performance negatively. Here it is important to observe the magnitude of torque fluctuations. Furthermore, engine simulation should be carried out with this torque input in order to calculate effect of torque fluctuation on engine operations, and its efficiency and emissions. The changes in the propeller speed due to engine response can be taken into account in the propeller analysis, in order to "close the loop".

4 CONCLUSION

We now have an information about an extent to which the criteria required for good noise and vibration characteristics get affected due to waves. Hence, in future designs appropriate margins can be considered for the similar type of vessels. However, such analysis should be performed for the variety of ships for multiple propeller loadings in order to generalize the results.

As per the analysis, it seems, presence of waves does not significantly affect cavitation in spite of large changes observed in the wake field. Thus, a margin for cavitation would mainly be required for increased loading, relative stern motion and not much for the wake change due to waves. Therefore, in practice the required margin can be estimated using added resistance and relative stern motions.

Vibration and noise characteristics have been analyzed using the BSRA wake criteria. However, more advanced techniques should be used to quantify the pressure pulses in different wakes. Pressure pulses may increase since higher wake gradients were observed in presence of waves.

Present analysis being in regular waves gives conservative estimate of the effect of waves on the propeller performance. We expect the effects to be less severe in case of irregular

waves. It should also be mentioned that current wake field in waves is obtained at model scale corresponding to the actual waveheight of 3m for a 340m long ship. Hence, there is a possibility of larger performance changes in presence of higher waves. Thus, it would be of interest to perform a similar investigation, but for a significantly smaller ship.

Significant fluctuations observed in propeller torque in waves should be analyzed further to calculate its effect on the engine operation. Coupled response of engine and propeller should be obtained to examine the effect of waves on whole propulsion system.

ACKNOWLEDGMENTS

Authors would like to thank Professor Frederick Stern from the University of Iowa for providing the wake data in waves used to analyze propeller in different conditions. We also thank Professor Bjørnar Pettersen for helping us obtain the wake data. This work is funded by the project 'Low Energy and Emission Design of Ships' (LEEDS, NFR 216432/O70) where the Research Council of Norway is the main sponsor.

REFERENCES

SIMMAN (2008). "SIMMAN 2008." from http://www.simman2008.dk/KVLCC/KVLCC2/kvlcc2_geometry.html.

Albers, A. B. and W. v. Gent (1985). Unsteady wake velocities due to waves and motions measured on a ship model in head waves. 15th symposium on naval hydrodynamics.

Brockett, T. (1966). Minimum pressure envelopes for modified naca-66 sections wih naca a = 0.8 camber and buships type I and type II sections, David Taylor Model Basin.

Chevalier, Y. and Y. H. Kim (1995). Propeller Operating in a Seaway. PRADS'95. Seoul, Korea.

Epps, B. (2010). OpenProp v2.4 Theory Document.

Gaggero, S. and S. Brizzolara (2009). Parametric Optimization Of fast Marine Propellers via CFD Calculations. 10th International Conference on Fast Sea Transportation. Athens, Greece.

Guo, B. J., S. Steen and G. B. Deng (2012). "Seakeeping prediction of KVLCC2 in head waves with RANS." Applied Ocean Research 35(0): 56-67.

Hepperle, M. "JavaFoil." from http://www.MH-AeroTools.de/.

Huse, E. (1974). Effect of afterbody forms and afterbody fins on the wake distribution of single-screw ships, Ship Research Inst. of Norway.

ITTC (2011). Specialist committee on scaling of wake field. Final report and recommendations to the 26th ITTC, ITTC. Volume 2.

Jessup, S. D. and H.-C. Wang (1996). Propeller Cavitation Prediction for a Ship in a Seaway, DTIC Document.

Kayano, J., H. Yabuki, N. Sasaki and R. Hiwatashi (2013). "A Study on the Propulsion Performance in the Actual Sea by means of Full-scale Experiments." TransNav, the International Journal on Marine Navigation and Safety of Sea Transportation 7(4): 521-526.

Moor, D. I. and D. C. Murdey (1970). "Motions and Propulsion of Single Screw Models in Head Seas, Part II." The Royal Institution of Naval Architects Vol. 112(No. 2).

Nakamura, S. and S. Naito (1975). "Propulsive performance of a container ship in waves." J. Kansai Soc. N. A. Japan No. 158.

Odabasi, A. Y. and P. A. Fitzsimmons (1978). "Alternative Methods for Wake Quality Assessment." International Shipbuilding Progress 25: 8 p.

Sadat-Hosseini, H., P.-C. Wu, P. M. Carrica, H. Kim, Y. Toda and F. Stern (2013). "CFD verification and validation of added resistance and motions of KVLCC2 with fixed and free surge in short and long head waves." Ocean Engineering 59(0): 240-273.

Sasajima, H., I. Tanaka and T. Suzuki (1966). "Wake Distribution of Full Ships." Journal of Zosen Kiokai 1966(120): 1-9.

Wu, P. C. (2013). A CFD Study on Added Resistance, Motions and phase averaged wake fields of full form ship model in head waves, Osaka University.

DISCUSSION

Question from Tom van Terwisga

Did you check the cavitation effect for the ship in waves considering an unsteady method and did you look at the corresponding unsteady pressure variations?

Author's Reply

Along with lifting line method, cavitation analysis was also performed using unsteady panel method with cavity volume calculations using the software AKPA as mentioned in the paper. However, wake was assumed quasi steady i.e. calculations were performed for wake distribution at different time intervals. Wake variation was assumed constant in time in each calculation. We believe that quasi-steady wake assumption is reasonable since the frequency of wake variation is much smaller than the frequency of propeller rotation.

The effect of change in cavitation number due to relative stern motion has been taken into account using hydrostatic approximation. Hence, the effect of dynamic pressure due to wave has been ignored. However, we agree that it would have been interesting to include the effect of unsteady pressure variations on the propeller performance.

Question from Johan Bosschers

Can you say something about the influence of the change in transverse velocities on the results? Is the influence of ship motions included?

Author's Reply

In some cases, transverse velocities show significant change. We believe, change in transverse can affect the tip vortex inception, which has not been studied in this paper. Transverse velocities can affect the cavitation due to change in the blade angle of attack. However, total induced velocities being much larger compared to the transverse velocities, any recognizable effect due to transverse velocities alone was not observed in the analysis.

Ship motions influences the propeller in two ways. Part of wake variation is due to ship motion and cavitation number changes due to change in propeller immersion. Influence of wake variation on propeller operation has been studied in detail in this paper as wake data in waves was obtained for the ship free to heave and pitch. The effect of variation in propeller immersion has been compared with the effect of wake variation in Figure 8.

Question from Moustafa Abdel Maksoud

Did you consider the effect of added resistance on the amount of cavitation on the propeller surface? Do you think that the following wave condition is more critical than the head waves one?

Author's Reply

In this paper, added resistance has not been considered, since wake data was available for the design speed of ship and since considering the added resistance would change the ship speed as well as motion response, leading to significant changes in wake. Even if the speed could be kept the same by increasing the shaft power to compensate for the added resistance, this change in propeller operating point means that we would not be able to single-out the effect of the wake change. However, the effect of added resistance is planned to be included in future studies.

Following wave condition can be more critical as waves would be directly affecting the propeller. However, authors are not aware of any measurement data or computations of wake in following waves. Limited availability of wake data is in general a limitation for analyzing propeller in waves.

Question from Mehmet Atlar

Interesting paper. The authors may also consider the BSRA criteria of Odabasi and Fitzimmons in terms of propeller-excited vibrations (PEV) since these two authors provided diagram (i.e. criteria) for cavitation and PEV assessment in their work (i.e. similar to the diagram in Figure 5 of the paper) that would be interesting to compare with the performance in waves.

Author's Reply

The paper mentions the Odabasi criterion. We believe, this is same as the BSRA criteria you mention. We have used the opportunity to update the paper so that it now also refers to this as the BSRA criterion.

Paper 2

Dynamics of a marine propulsion system with a diesel engine and a propeller subject to waves

Bhushan Taskar, Kevin Koosup Yum, Eilif Pedersen,
Sverre Steen

Proceedings of 34th International Conference on Ocean, Offshore and Arctic (OMAE2015), St. John's, Newfoundland, Canada, 2015.

http://dx.doi.org/10.1115/OMAE2015-41854

Is not included due to copyright

Can be accessed at

http://dx.doi.org/10.1115/OMAE2015-41854

Paper 3

The effect of waves on engine-propeller dynamics and propulsion performance of ships

Bhushan Taskar, Kevin Koosup Yum, Sverre Steen,
Eilif Pedersen

Ocean Engineering, 2016, Vol 122, pp 262-77

http://dx.doi.org/10.1016/j.oceaneng.2016.06.034

Ocean Engineering 122 (2016) 262–277

Contents lists available at ScienceDirect

Ocean Engineering

journal homepage: www.elsevier.com/locate/oceaneng

The effect of waves on engine-propeller dynamics and propulsion performance of ships

Bhushan Taskar*, Kevin Koosup Yum, Sverre Steen, Eilif Pedersen

Department of Marine Technology, Norwegian University of Science and Technology (NTNU), Trondheim, Norway

ARTICLE INFO

Article history:
Received 26 November 2015
Received in revised form
15 June 2016
Accepted 21 June 2016

Keywords:
Propulsion in waves
Engine propeller dynamics
Propulsion performance
Propulsion losses in waves
Marine propellers
Engine control in waves

ABSTRACT

This paper investigates the effect of waves on the propulsion system of a ship. In order to study the propulsion in different wave conditions, a procedure for wake estimation in waves has been implemented. A clear drop in the propulsion performance was observed in waves when engine propeller dynamics, wake variation and thrust and torque losses were taken into account. This can explain the drop in vessel performance often experienced in presence of waves in addition to the effect of added resistance. Therefore, performance prediction of ships in rough weather can be improved if the effects of waves on the propulsion system are considered. Specific problems causing drop in performance have also been identified. System response in case of extreme events like propeller emergence has been simulated for analyzing the performance and safety of the propulsion system. The framework of engine-propeller coupling demonstrated in this paper can also be used to analyze different components of propulsion system (e.g. propeller shaft, control system) in higher detail with realistic inputs. This paper is a step towards optimizing the propulsion of ships for realistic operating conditions rather than calm water condition for energy efficient and economic ships.

1. Introduction

Traditionally, ships have been optimized for calm water operation, because this is the intended condition during the contractual sea trials, and probably also because one has not had the knowledge and tools to optimize ships properly for operations in waves. Ships have of course been designed to be safe in all operational conditions they are supposed to be used in, but not to be optimally efficient in the typical operation condition, which for most ships is not calm water. Optimization for operation in waves is increasingly viable, and so it is expected that more energy-efficient and economical ships can be designed if seakeeping and powering in waves is taken into account in the design optimization.

Currently, propulsion plants are optimized for calm water operation. While off-design conditions like rough weather are taken care of by adding simple sea margin to the required power. Sea margin is typically 15–25% of the power required in calm water condition. However, to optimize the installed engine size, sea margin should be accurately calculated based on the performance of ship in worst intended operating condition, so that minimum possible engine power can be used while still ensuring safety and performance of vessel. Various factors affecting the ship performance in waves can be seen in Fig. 1.

The effects of waves on the propulsion system are yet to be clearly understood. It has been observed that the system of engine and propeller react to the time varying flow field encountered in waves, and it would be useful to simulate this effect, to take into account the effect of waves on the engine propeller system already on the design stage. In case of propeller emergence, when the propeller is coming partly out of the water, the propeller torque drops significantly, and depending on how the engine is controlled, propeller racing might occur. This is one of the primary indicators for voluntary speed reduction. Therefore, to predict attainable speed in waves and engine dynamic response, prediction of propeller emergence is important.

In waves, changes in flow field alters propulsion factors as compared to calm water condition. Nakamura and Naito (1975) have demonstrated the effect of waves and ship motions on thrust deduction and wake fraction of a ship. Wake is also affected by pitching motion of a ship, causing increase in average wake (Faltinsen et al., 1980) along with wake fluctuations (Ueno et al., 2013). Significant changes in wake field were observed in presence of waves and ship motions in the RANS simulations carried out by Guo et al. (2012), where the nominal wake field was obtained in waves. Similar results were obtained by Sadat-Hosseini et al. (2013) where wake was obtained in presence of waves using particle image velocimetry (PIV).

Abbreviations: MCR, Maximum continuous rating; BSFC, Brake specific fuel consumption; EVC, Exhaust valve close

* Corresponding author.
E-mail address: bhushan.taskar@ntnu.no (B. Taskar).

http://dx.doi.org/10.1016/j.oceaneng.2016.06.034
0029-8018/

Nomenclature

h	Depth of the propeller shaft
R	Propeller radius
β	Thrust diminution factor
w_P	Effective wake fraction
U	Ship speed
A	Wave amplitude (m)
λ	Wavelength
L	Ship length
ω_e	Wave encounter circular frequency
ξ_a	Surge amplitude with phase delay of ζ_ξ
ζ_ξ	Phase delay
ω	Wave circular frequency
h_a	Wave amplitude
k	Wave number
$(x_P,0, z_P)$	Propeller co-ordinates
t	Time
X	Wave encounter angle (0 for following sea; 180 for head sea)
α	Coefficient representing effect of wave amplitude decrease at the stern
$V_{fluctuating}$	Wake velocity considering fluctuations due to waves
V_{mean}	New wake velocity considering the effect of pitching motion
V_{total}	Total wake velocity considering mean increase as well as wake fluctuations
x	Longitudinal distance of the propeller from the center of gravity of the ship
$\Delta\bar{p}$	Pressure gradient below the bottom of the ship due to pitching motion
η_5	Pitch amplitude
m	Mass of ship
m'	Surge added mass of ship
$\dot{x}$	Surge speed of ship
$\ddot{x}$	Surge acceleration of ship
T'	Thrust produced by the propeller
t'	Thrust deduction fraction
ρ	Density of seawater
S	Wetted surface area of the ship
C_T	Total resistance coefficient of the ship
R_1	Added resistance of the ship in waves
J_{Shaft}	Mass moment of inertia of the propeller shaft
ω_{Shaft}	Propeller shaft speed
a_1	Friction coefficient for the main engine
a_2	Friction coefficient of the propulsion shaft
Q_{Eng}	Engine torque
Q_{Load}	Propeller load torque
η_m	Mechanical efficiency of engine crank system
p	Pressure
T	Temperature
F	Fuel-air equivalent ratio
M	Mass of gas
$\dot{M}$	Mass flow of gas or rate of change of mass in a control volume
M_b	Mass of burned fuel in gas
$\dot{M}_b$	Mass flow or rate of change of mass of burned fuel in gas
E	Energy in a volume
$\dot{E}$	Energy flow or rate of change in energy in a control volume
V	Volume
$\dot{V}$	Rate of change of volume

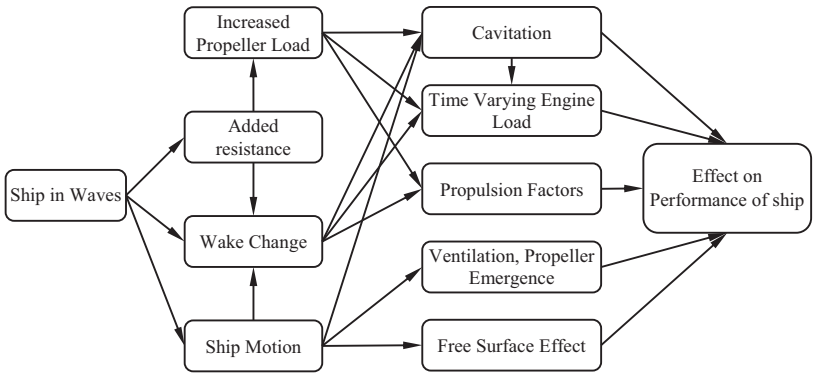

Fig. 1. The effects of waves on ship propulsion.

Changes in flow field explained previously cause fluctuations in propeller thrust and torque as observed by Nakamura and Naito (1975), Lee (1983) and Amini (2011). Taskar and Steen (2015) have identified a need to study the effect of large torque variations observed in presence of waves on engine performance. Moreover, waves cause surge motions and periodic change in propeller submergence due to heave and pitch. Such changes in propeller submergence, surge motion and occasional propeller emergence give rise to fluctuating loads on the engine. This may affect engine performance as well as propeller performance due to shaft speed variations. Therefore, engine and propeller should be studied together as a system to correctly simulate interaction between them. Also, ship and propeller dynamics should be taken into account while optimizing the control strategy of machinery (Kyrtatos, 1997). Investigations by Taskar et al. (2015), have shown that unsteady propeller inflow can cause significant increase in power and fuel consumption in order to keep the ship speed constant.

Variable loads on the propeller in presence of waves can cause mechanical failures (Amini, 2011). Therefore, it is necessary to estimate the magnitude of such loads. Tanizawa et al. (2013) have developed a methodology to include realistic engine response in the self-propulsion tests to emulate real condition and get accurate estimates of fuel consumption in waves at different pitch settings in case of controllable pitch propellers. It also serves the

Table 1
Ship particulars.

Length beween perpendiculars (m)	320.0
Length at water line (m)	325.5
Breadth at water line (m)	58.0
Depth (m)	30.0
Draft (m)	20.8
Displacement (m^3)	312,622
Block Coefficient (C_B)	0.8098
Design Speed (m/s)	7.97

Table 2
Propeller geometry.

Diameter (D) (m)	9.86
No of blades	4
Hub diameter (m)	1.53
Rotational speed (RPM)	95
$A_e/\ A_0$	0.431
$(P/D)_{mean}$	0.47
Skew (°)	21.15
Rake (°)	0

purpose of obtaining realistic dynamic response of the ship's propulsion system. Queutey et al. (2014) have studied the effect of waves on the flow around a ship with pod, considering the effect of waves on cavitation and ventilation with the help of model tests and experiments. The effect of environmental conditions like wind and waves on the propulsion performance has been studied by Kayano et al. (2013) using full scale experiments. They observed that DHP (Delivered Horse Power) measured in the full-scale experiments in presence of wind and waves was higher than the estimated value and propulsive efficiency lower than the estimated value. Therefore, need of predicting power curve more precisely considering the effect of wind and waves was proposed in order to improve the energy saving of ship operations.

For the study of coupled dynamics of vessel-propulsion-diesel engine system, Kyrtatos et al. (1999) conducted a simulation of propeller – diesel engine dynamics and applied a PI governor. The engine model used was built based on the filling and emptying approach and phenomenological submodels for combustion and scavenging. They demonstrated the model's reliability to test the governor in different transient load. Livanos et al. (2006) and Theotokatos and Tzelepis (2013) studied coupled dynamics for a vessel-propulsion-diesel engine system. The first tested the case with a controllable pitch propeller under maneuvering operation with primary interest on the engine system response like shaft speed, turbocharger speed and power development under transient load. The engine model used was a mean value model, derived from their phenomenological model called MoTher. The latter authors did a similar study with more focus on emission from the engine. Campora and Figari (2003) used a phenomenological engine model with two-zone description in the cylinder for the coupled simulation. Their simulation result was validated by full-scale measurement. In all studies mentioned, the propeller is modeled as either a basic propeller model, obtained from an open water performance test, or as a time series of experimentally measured torques. Therefore, influence of waves on the propulsion system is excluded or statically taken into account.

In this paper, we have investigated effects of waves on the propulsion system. Waves from different directions causing unsteady interaction between engine and propeller have been studied. Events like propeller emergence have been simulated to observe the combined behavior of engine, response of control system and its effect on the vessel operation. The total efficiency of the propulsion system has been investigated in presence of waves to check if a drop in propulsive efficiency should be taken into account for power and speed predictions in waves. This paper also explores the validity of computing unsteady propeller loads using the assumption of constant propeller speed.

For this investigation, a coupled model of engine and propeller has been implemented in MATLAB-Simulink along with a method to estimate wake in waves. Multiple wave conditions have been simulated with different wavelengths, wave heights and wave directions to observe their impact on the propulsion. This study demonstrates the importance of using a coupled engine propeller system for accurate estimation of ship performance. It can be further used to optimize installed power while ensuring safety of vessel in all weather conditions, rather than just adding a simple sea margin. This study will also clarify the effects of propeller emergence on the engine performance.

2. Geometries and wake data

Wake field is one of the important inputs required for the propeller design and performance estimation. Therefore, to study the effect of waves on propeller performance, it is essential to know the wake field in waves. However, wake data in waves are rarely available since in most of the cases the wake field is obtained only in calm water condition. It is also both complicated and time-consuming to acquire such data. Sadat-Hosseini et al. (2013) performed model tests on the KVLCC2 hull to obtain wake fields in three different waves. Therefore, KVLCC2 was used as a case vessel for this study. Hull geometric details are found in Table 1. Sadat-Hosseini et al. (2013) have carried out experiments in head sea conditions using PIV measurements. Nominal wake observations were performed for wavelength to ship length ratios of 0.6, 1.1 and 1.6 at 8, 12 and 6 time instants respectively for each wave period. Their study also reports CFD simulations validated with the PIV measurements. For our analysis, we have used the CFD data because it is smoother and less noisy compared to the PIV measurements. However, CFD data and PIV measurements are available only for head sea condition.

The propeller design was altered in order to match the existing engine model. Pitch of the propeller blades was uniformly changed to be able to deliver maximum engine power. Geometric details of this design can be seen in Table 2. There is no engine specified for KVLCC2 by her designers. In this study, an existing engine model was used with fine-tuned parameters and validated against data from the manufacturer of the engine used in this paper. Selection of engine was limited by the availability of the data to validate the simulation model. Since the power of the available engine model was insufficient to propel the hull at design speed, simulations were run at a lower vessel speed, chosen such that the engine runs at 85% MCR (Maximum Continuous Rating). The design speed of KVLCC2 is 15.5 knots, while the simulations were performed for a speed of 14.7 knots.

2.1. Wake contraction procedure

Wake distribution was available in model scale only, and needed to be contracted to obtain ship scale wake. According to the ITTC (2011), the wake scaling procedure given by Sasajima et al. (1966) is most commonly used and gives reasonable results. In this method, frictional wake is obtained by separating the potential wake from the total wake field. Frictional wake is then scaled and added to the potential wake to obtain ship scale wake. However, in absence of potential wake data we have contracted the total wake field by the ratio of viscous resistance coefficient between model and full scale. Hence, the difference between potential wake component of model and ship has been neglected.

Potential wake is almost constant in the propeller plane as seen from the typical ship scale wake presented in ITTC (2011). In such cases, the same full-scale total wake would be obtained by scaling the total wake or just the frictional component of the model-scale wake. The only error would be due to the neglected correction in the potential wake. This procedure has been applied to each snapshot of the wake field at different times as if it were calm water wake distribution. Model and full-scale wakes can be seen in Fig. 2.

2.2. Ship motion and added resistance calculations

Ship motion RAOs were calculated using linear strip theory, utilizing potential theory and pressure integration, implemented in the ShipX Veres software. Surge, pitch and relative stern motion RAOs have been calculated. Pitch RAO is required to calculate mean increase in propeller inflow using Faltinsen's method (described later). RAO for relative stern motion has been used to compute variation in thrust and torque due to the variation in propeller submergence in different wave conditions. Surge motion RAO is necessary to compute wake fluctuations in waves using Ueno's method (described later). These RAOs can be seen in Figs. 3–7.

Surge and pitch RAOs have been compared with the experimental investigations performed by Wu (2013). Experimental data was available only in head waves. This comparison can be seen in Fig. 3 and Fig. 5. Surge motion is slightly over estimated as compared to experimental values.

Using the motion response of the vessel, added resistance coefficients have been calculated using the method by Loukakis and Sclavounos (1978) (which is an extension of the classical Gerritsma and Beukelman's method) implemented in ShipX Veres. Calculated added resistance coefficients can be seen in Fig. 8 along with the experimental values by (Wu, 2013). Using these added resistance coefficients, added resistance was then computed in irregular waves for different peak frequencies and wave directions using the Pierson Moskowitz wave spectrum.

3. Marine diesel engine details

The engine model selected for the simulation is Wartsila 8RT-flex68D. There is no engine specified for KVLCC2, and this one was selected partly based on availability of the model. The engine particulars can be seen in Table 3. The detailed information of the engine can be found from the project guide for the specific engine. Also the engine performance in terms of fuel consumption, power, mass flow, pressure and temperature are available from the manufacturer's website (WÄRTSILÄ, 2014). These performance data are used in order to validate the engine system model.

4. Simulation model

Engine and propeller models have been coupled using an inertial shaft model. Time dependent wake and shaft speed are inputs to the propeller model, which computes thrust and torque. Thrust is used by the vessel model to update the ship speed based on ship resistance and inertia. Torque is used by the shaft model to compute new shaft speed depending on shaft inertia and net torque applied to the shaft. Shaft speed is fed to the engine model to obtain torque produced at that speed and fuel injection commanded by the controller. An engine controller is used to control the fuel injection to the engine to keep engine speed constant and

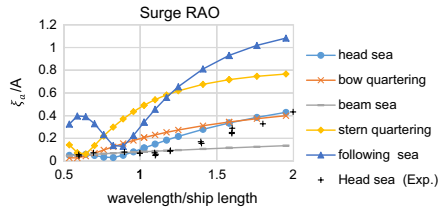

Fig. 3. Surge RAO of KVLCC2 hull in different wave conditions with experimental validation.

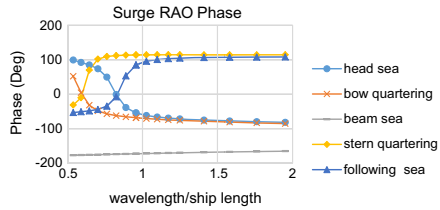

Fig. 4. Phase of surge RAO of KVLCC2 hull in different wave conditions.

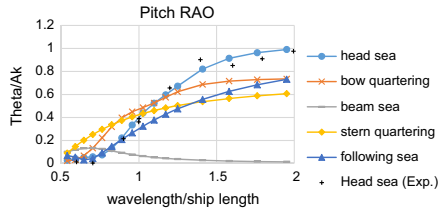

Fig. 5. Pitch RAO of KVLCC2 hull in different wave conditions with experimental validation.

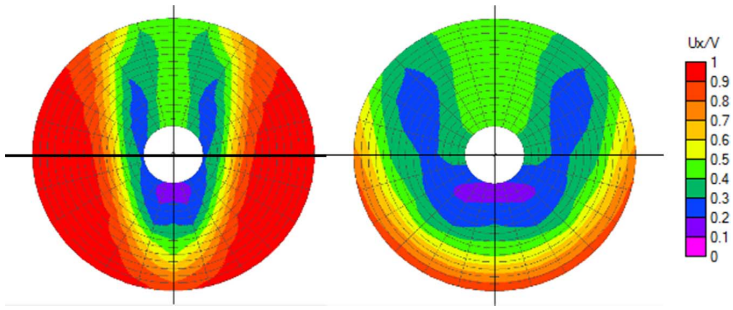

Fig. 2. Full scale contracted wake velocities (Left) and model scale wake velocities (Right).

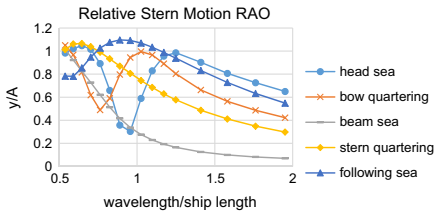

Fig. 6. relative stern motion RAO of KVLCC2 hull in different wave conditions.

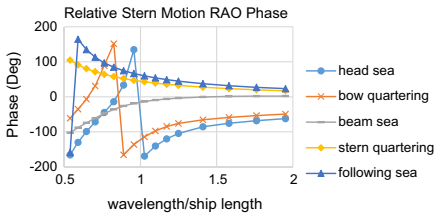

Fig. 7. Phase of relative stern motion RAO in different wave conditions.

Table 3
Engine particulars.

Model	Wartsila 8RT-flex68D
Bore (mm)	680
Rated MCR (kW)	25,040
Speed at rated power (RPM)	95
Stroke (mm)	2720
Mean effective pressure (bar)	20
Number of cylinders	8
Turbocharger	2 x ABB A175-L35

to avoid any over speeding. The overall model can be seen in Fig. 9. Details of the modeling blocks are given further down.

The simulation model has been implemented in Matlab Simulink™ for overall integration of the submodels. A variable step solver (ODE45) has been used in order to capture transient dynamics of the overall system.

4.1. Propeller model

For the propeller analysis, the open-source program Openprop based on vortex lattice lifting line theory (Epps, 2010) has been used. It requires blade section details, frictional drag coefficient and wake velocities at each radial section. Frictional drag coefficients were obtained using *Javafoil* (Hepperle), which uses a panel method to calculate velocity profile and pressure distribution over the foil section. Using these velocity and pressure distributions, boundary layer calculations are performed. Drag is calculated using momentum loss in the boundary layer.

In order to validate the Openprop results, open water curves obtained from Openprop were compared with the experimental open water data of original KVLCC2 propeller design. Good comparison between Openprop results and experimental results can be seen in Fig. 10. Full-scale open water curves were obtained for the new propeller design for the calculation of thrust and torque at given propeller speed and ship speed, which means open water curves were used for the calculation of thrust and torque based on ship speed, propeller RPM and wake. Relative rotative efficiency has been assumed equal to one in all the cases.

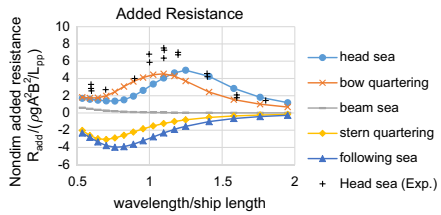

Fig. 8. Added resistance in irregular waves of different peak wavelengths for KVLCC2 hull in different wave conditions.

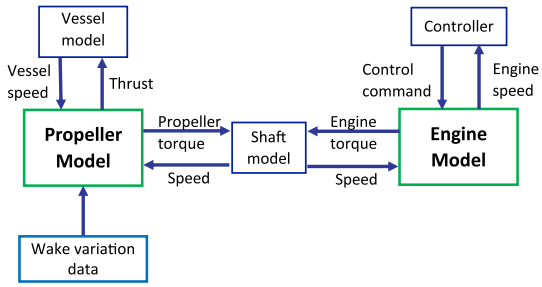

Fig. 9. Overall model used for engine-propeller coupled simulations.

In order to consider the effect of waves on the propulsion of the ship, thrust and torque losses due to propeller emergence, free surface effect and Wagner effect have been modeled. Thrust loss in case of propeller emergence has been assumed proportional to the out of water area of the propeller disc as suggested by Faltinsen et al. (1980). In case of propeller emergence, propeller blades take some time to develop the lift once they re-enter the water and thereby reducing average thrust and torque. This effect has been considered in terms of average thrust and torque loss as suggested by Minsaas et al. (1983). In addition, thrust and torque is lost when the propeller operates close to free surface generating waves on the free surface due to propeller action. These effects have been formulated using thrust diminution factor given by Minsaas et al. (1983) as follows:

$$\beta=\begin{cases}1-0.675\left[1-0.769\left(\frac{h}{R}\right)\right]^{1.258} & \frac{h}{R}<1.3\\ 1, & \frac{h}{R}\geq 1.3\end{cases} \quad (1)$$

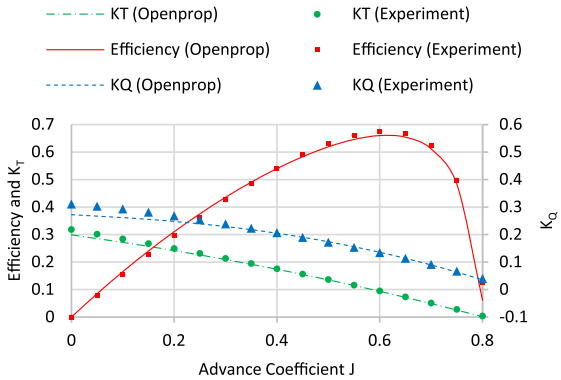

Fig. 10. Comparison of Openprop and open water data of KVLCC2 propeller.

β is multiplied with the propeller thrust to obtain diminished thrust due to the effect of proximity to free surface.

The effects have been considered in quasi-steady sense as propeller depth varies much slower than its rate of rotation. Thrust and torque are considered varying in wave frequency, and higher harmonics have been ignored. These higher harmonics are mostly filtered away by the inertia of the shaft and propeller, and it is found that they do not affect the engine operation.

4.2. Procedure to estimate propeller inflow velocity

As mentioned earlier, one of the obstacles in the analysis of engine-propeller interaction in different weather conditions is the limited availability of wake data. Thus in order to simulate a variety of cases it is necessary to estimate wake in different wave-conditions.

Nakamura and Naito (1975) have shown that in presence of waves and ship motions, wake velocities fluctuate. Moreover, the mean of these fluctuations is different from the calm water wake. Hence, in presence of waves, mean wake changes along with the fluctuations. Ueno et al. (2013) have demonstrated that fluctuating wake velocities are caused by the wave induced particle motion and surge motion of the ship. Therefore, they state that wake velocities can be calculated as follows-

$$V_{fluctuating}=\left(1-w_P\right)\left\{U-\omega_e\xi_a\sin\left(\omega_e t-\zeta_\xi\right)\right\}+\alpha\omega h_a\exp\left(-kz_P\right)\cos X\cos\left(\omega_e t-kx_P\cos X\right) \quad (2)$$

where

$$\alpha=\begin{cases}0.2\left(\dfrac{\lambda}{L|\cos X|}\right)+0.5, & for\ \dfrac{\lambda}{L|\cos X|}\le 2.5\\ 1, & for\ \dfrac{\lambda}{L|\cos X|}>2.5\end{cases} \quad (3)$$

The coefficient α is different from 1.0 in case of head and bow-quartering waves since the waves reaching the propeller are modified due to the presence of the hull in front of it (Ueno et al., 2013). However, in case of following and stern quartering waves this coefficient is not required as the waves are directly felt by the propeller without significant disturbance from the hull. This means that we assume that the effect of reflected waves is negligible when it comes to wave induced fluctuations felt by the propeller.

Faltinsen et al. (1980) have proposed that the increase in mean propeller inflow (wake) due to the pitching motion of ship observed by Nakamura and Naito (1975) is caused by potential flow effects. Wake velocities due to the pitching motion of the ship can be calculated assuming the bottom of the ship to be a flat plate. Wake velocities can then be obtained as follows:

$$V_{mean}=\sqrt{\left(1-\frac{\Delta\bar{p}}{0.5\rho U^2}\right)}U \quad (4)$$

where

$$\Delta\bar{p}\sim-\frac{\rho}{4}\omega_e^2|\eta_5|^2x^2 \quad (5)$$

Comparison between mean increase in propeller inflow calculated by this method and that observed in the CFD has been presented in Table 4. Although there is a difference in the exact values between the calculation and experiment, trends are correctly predicted by the calculation.

Therefore, time varying total wake velocity in waves considering mean increase as well as fluctuations can be calculated as:

Table 4
Comparison of increase in mean propeller inflow using formula and experiments.

$\frac{\lambda}{L}$	A	% Increase in mean wake velocities	
		(Calculation)	(Experiment)
0.6	3	0.03	0
1.1	3	2.70	5.0
1.6	3	2.66	2.2

$$V_{total}=\left(\left(1-w_P\right)\left\{U-\omega_e\xi_a\sin\left(\omega_e t-\zeta_\xi\right)\right\}+\alpha\omega h_a\exp\left(-kz_P\right)\cos X\cos\left(\omega_e t-kx_P\cos X\right)\right)\sqrt{\left(1-\frac{\Delta\bar{p}}{0.5\rho U^2}\right)} \quad (6)$$

Time varying wake velocities computed by Eq. (6) were then compared with the wake velocities obtained from the wake data in waves. Comparison can be seen in Fig. 11. Due to good match between predicted and observed wake variation in waves, this formulation was used to obtain wake variations in different wave conditions. This made it possible to simulate engine propeller dynamics in presence of waves of various wavelengths, wave-heights and wave directions, without being restricted to the conditions of the model test by Sadat-Hosseini et al. (2013).

Although these simple methods might not be accurate in all the conditions, they can certainly be used to access the possible effect of waves on the propulsion in waves before going for more accurate but time consuming analysis.

4.3. Vessel model

The following vessel model has been implemented to include vessel dynamics in the simulations:

$$\left(m+m'\right)\ddot{x}=\left(1-t'\right)T'-\left(0.5\rho SC_T\dot{x}^2+R_1\right) \quad (7)$$

Although thrust deduction varies in presence of waves (Moor and Murdey, 1970), it has been considered to be constant and equal to its calm water value, due to the lack of knowledge about how thrust deduction vary in presence of waves for this particular ship. R_1 and T' are the only time dependent inputs that are updated each time step. The added resistance coefficient was modeled as a function of ship speed. In each wave condition, the added resistance coefficient was computed for different ship speeds from 9.5 knots to 15.5 knots and it was curve-fitted with second order polynomial of ship speed. One such curve fitting in case of irregular head waves with peak frequency equal to that of wave $\lambda/L=1.1$ can be seen in Fig. 12.

Simulations have been performed to analyze the interaction of regular waves with the propulsion unit. However, added resistance has been calculated in irregular waves of significant waveheight equal to the waveheight of the regular wave and peak frequency same as the frequency of the regular wave. This is done to keep the analysis simple and yet keep ship resistance and engine load realistic. Therefore, simulation conditions are similar to the ship traveling in irregular waves and encountering a wave train of regular waves.

4.4. Propulsion shaft model

The shaft is assumed to be rigid and the quadratic friction model is used. Mass moment of inertia is assumed to be twice as much as that of the engine (J_{Shaft}=323,000 kg m^2). The dynamic equation for the shaft is given as:

$$J_{Shaft}\dot{\omega}_{Shaft}=\eta_m\left(\omega_{Shaft}\right).Q_{Eng}-Q_{Load} \quad (8)$$

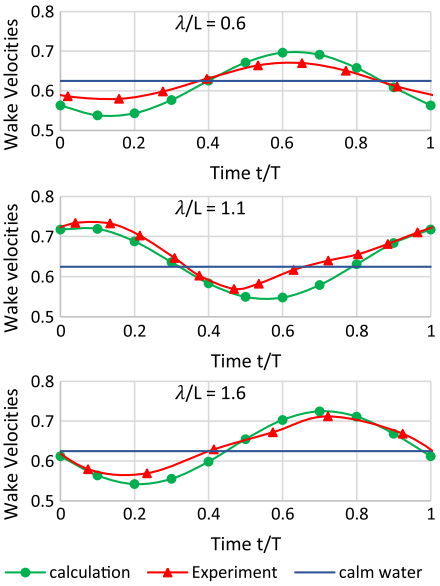

Fig. 11. wake variation procedure vs. experimental wake.

where η_m is a mechanical efficiency of the engine crank system and the propulsion shaft, given as an empirical function:

$$\eta_m = 1 - a_2\omega_{Shaft} + \frac{a_1}{1-a_2}(a_2\omega_{Shaft} - \omega_{Shaft}^2) \quad (9)$$

4.5. Marine diesel engine model

The purpose of the engine system model in this paper is: (1) to provide dynamic shaft torque and (2) to predict the cycle efficiency of the engine under transient conditions. The transient load from the propeller changes both torque and speed, causing highly nonlinear behavior of the system. Therefore, the engine system model should include the physical process of the essential components of the engine system, namely turbocharger, air coolers, air/exhaust receiver volumes and engine cylinder blocks in order to predict nonlinear and transient aspects of engine operation. The physical interface of the system is through the mechanical shaft where rotational speed is input to the engine model and torque is output. In addition, the engine model takes inputs from the engine controller, which are fuel rack position, valve timing, and injection timing.

The engine system model is based on the filling and emptying method, which is most commonly used for engine system modeling (Rakopoulos and Giakoumis, 2006). Filling and emptying method is a lumped parameter modeling approach where the system is divided into a finite number of uniform thermodynamic control volumes. Such a model is capable of simulating pressure and temperature in the component and flow between the components. Since we will observe system performance in terms of torque response as well as efficiency, more detailed methods like gas dynamic model (Takizawa et al., 1982) or multi-zone model (Hiroyasu et al., 1983) are not required. In addition, the engine contains large receiver volumes before and after the cylinder, which smooths pressure fluctuations entering the engine cylinder and turbine. This further justifies the use of a filling and emptying model.

In a filling and emptying method, all components are grouped

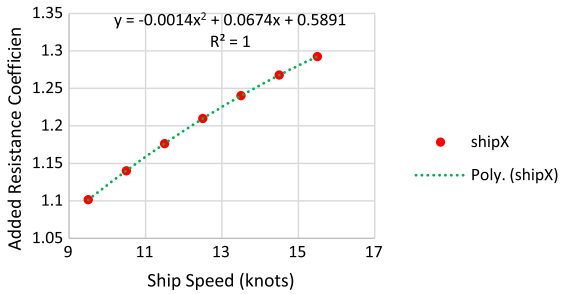

Fig. 12. Dependence of added resistance coefficient on vessel speed.

into two categories: control volume and flow restriction. In a control volume, mass and energy are accumulated depending on the net flows and the thermodynamic properties are determined in the volume. It is assumed that such properties are uniform in the volume. On the other hand, flow restriction allows mass and energy to flow between two control volumes or between a control volume and environment. It is assumed that there is no mass and energy accumulated in restrictions. Any physical flow restriction like valves, ports, and orifices are grouped in this category. In addition, a cooler or turbomachinery can be grouped in this as a simplified model.

Three common groups of system variables are used inside the thermodynamic part of the engine model and their interfaces, namely thermodynamic states, mass and energy flows. As the main part of an engine system is a thermodynamic process of gas mixture, thermodynamic states used in this work are pressure, temperature and the composition of the gas, for which we use fuel-air equivalent ratio, whereas mass flow of gas, enthalpy flow or rate of change in internal energy and mass flow of burned-fuel are flow variables. In case of varying volume, the rate of change of volume should also be included in the flow variables.

The input to a flow restriction element is a set of thermodynamic states (p, T, F) of adjacent control volumes and the output is a set of mass and energy flows (M, $\dot{E}$, $\dot{M}_b$) determined depending on the specific process of the component. For example, isentropic compressible flow equation through a restriction (Heywood, 1988) is used for valve, orifice or port whereas a performance map is used for a compressor and a turbine. On the other hand, a control volume has the input of a set of flows from connected flow restrictions and output of the thermodynamic states. The first law of thermodynamics and mass conservation is used to calculate the net rate of change in mass and energy in the control volume. Those net rate of changes are integrated to find the mass and energy of the volume (M, E, V, M_b). Then, we used Zacharias' correlation (Zacharias, 1967) for thermodynamic properties of the combustion gas and the ideal gas law to algebraically obtain the thermodynamic states (p, T, F). In addition, if the control volume is connected to a mechanical component, it will have an additional input of rate of volume change and a pressure output on this interface.

The system model is assembled from the model libraries of components developed by the authors. Then, the block diagram of the overall system looks like in Fig. 13.

The simulation model has sub-models to describe the specific physical processes in the internal combustion engine. For the combustion in the cylinder, a Wiebe function is used with fixed parameters to describe the rate of heat release. An ignition delay model is also included, which correlates the delay to pressure and temperature of the cylinder. For the gas exchange process, a scavenging model suggested by Sher (1990) is adapted to a single-

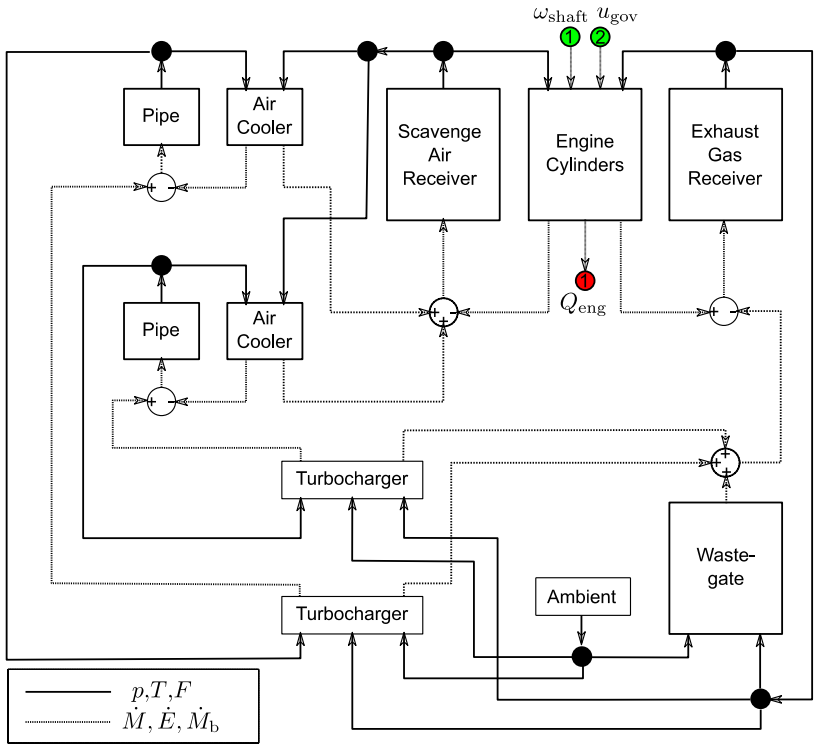

Fig. 13. Block diagram of the engine system model.

zone model. For the turbochargers, a quasi-steady approach was used where flow and efficiency are obtained from the performance map provided by the manufacturer. For the heat transfer, the model by Woschni (1967) was used to predict the heat transfer coefficient whereas radiation was neglected. Heat transfer from the radiation was not separately computed but included in the overall heat transfer model. For the heat exchanger model, effectivity-the NTU model was used (Incropera et al., 2007).

The engine system model was then validated against the steady state performance data provided by the engine manufacturer. The engine system model for validation is connected with a shaft model described in the paper. A simple propeller model is also used as a quadratic curve between torque and speed. The propeller curve was derived from the power and engine speed relation given in the engine performance data. From numerous simulations, we found that brake specific fuel consumption (BSFC) is well-correlated with maximum cylinder pressure. Since the combustion profile described by the Wiebe function is fixed, we could regulate the maximum cylinder pressure by changing exhaust valve close (EVC) timing and injection timing. Early exhaust valve closing will make apparent compression ratio high and vice versa. Also retarded fuel injection may enable keeping high compression ratio without exceeding permissible maximum cylinder pressure. In this work, a controller was devised to set a reference maximum cylinder pressure from comparison of measured BSFC and the reference value. While the firing pressure, which is the pressure differential between maximum cylinder pressure and compression, was kept constant by regulating fuel injection timing, the compression pressure was controlled to the reference value by regulating exhaust valve timing.

From the simulations at difference loads, the EVC timing and fuel injection timing were obtained to achieve the reference BSFC. In addition, other performance data were compared to the reference data and they generally show good fit as shown in the Fig. 14.

For the transient simulation model, the EVC timing and fuel injection timings are parametrized into a table with reference engine speed and the actual values are interpolated at given engine speed. For the governor, a PI controller is used to regulate the shaft speed to a reference value. The measured shaft speed is low-pass filtered in order to filter any noise and cylinder-to-cylinder variation. The controller is also tuned so that the system has reasonably fast response while avoiding oscillation. While tuning the control parameters, a sensitivity analysis was performed in order to see the influence of the variation in the uncertain parameters. As a result, it was found that the mass moment of inertia of the shaft, among other parameters such as proportional gain of the controller and turbocharger inertia, has a negligible influence on the time constant of the engine speed response to the step change in speed command. This result justifies using rough estimation of inertia of the propulsion system.

However, the turbocharger shaft inertia has significant influence in case of a large step change in speed command because of the smoke limiter. This additional controller limits the fuel rack position depending on the charge air available in the cylinder. The amount of charge air available is predicted from the scavenge air receiver pressure and the volumetric efficiency of gas exchange process. As the rate of pressure development for load increase is delayed due to inertia of the turbocharger and filling the receiver volume, the fuel rack position from the governor saturates by this limit. This phenomenon is commonly referred as “turbo-lag”. Combination of both PI type governor and smoke limiter ensures

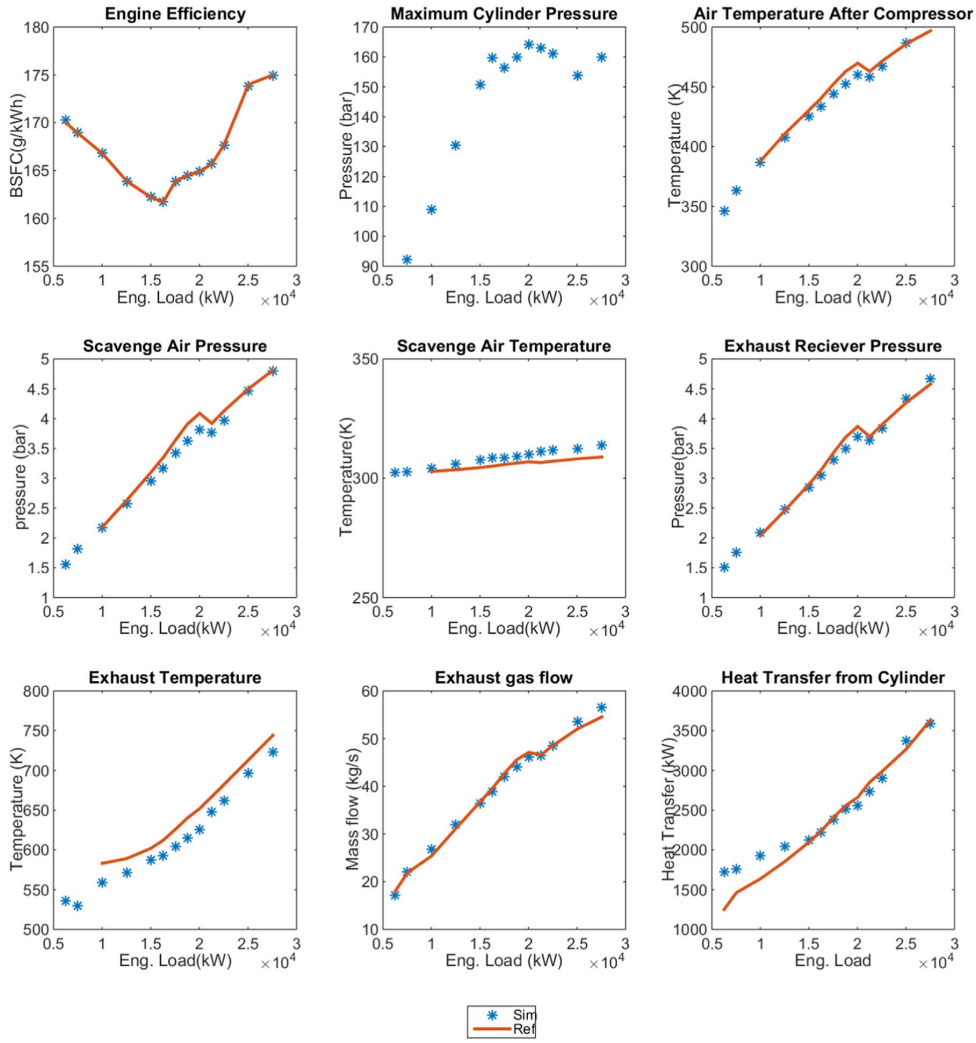

Fig. 14. Diesel engine steady state simulation.

reasonable response of the engine especially in case of abrupt change in load.

5. Engine-propeller coupled simulations and results

Two sets of simulations were performed. Firstly, added resistance was excluded from the simulations in order to observe the effect of unsteady flow alone on the propulsion performance. Excluding the added resistance makes different cases directly comparable. Effect of waves on engine efficiency and propeller efficiency was separately studied along with their combined impact on vessel performance. Secondly, simulations were performed including the added resistance to simulate the situations that are more practical. Importance of wake change, engine-propeller interaction and thrust and torque losses in waves on power and velocity prediction of vessel was analyzed.

5.1. Simulations without added resistance

5.1.1. Engine-propeller dynamics in waves

Power, speed and torque variations in presence of head sea can be seen in Figs. 15–17. Power variations in wave $\lambda/L=1.1$ are larger as compared to those in $\lambda/L=0.6$. This can be explained by the fact that larger waves reach the propeller without much decrease in amplitude as compared to smaller waves. In case of $\lambda/L=1.6$, distinct sharp peaks in shaft speed are caused by propeller emergence, causing sharp drops in torque seen in Fig. 17.

High frequency fluctuations in torque and shaft speed (appearing as thick lines in the graphs) in Figs. 16 and 17 are due to the firings of individual cylinders. These can be clearly seen in the instantaneous engine power plot in Fig. 18.

5.1.2. Engine propeller coupled model vs. constant propeller speed assumption

Propeller speed is often assumed constant in the investigation of variation in the propeller forces and propeller performance to

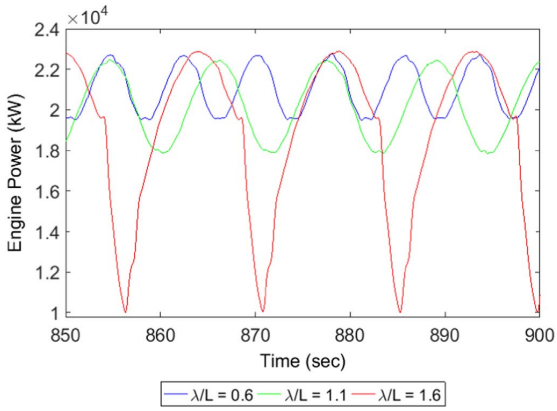

Fig. 15. Low frequency engine power fluctuations in presence of three different head waves of 5 m wave amplitude.

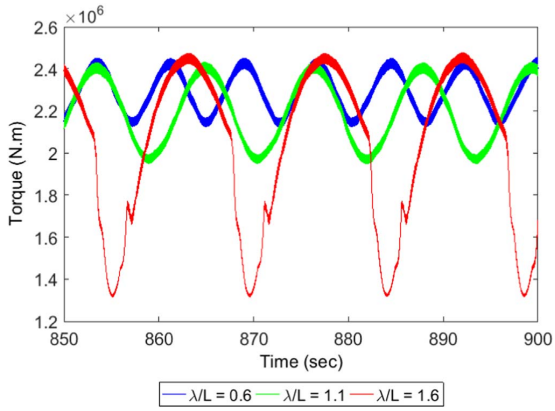

Fig. 17. Propeller torque fluctuations in presence of three different head waves of 5 m wave amplitude.

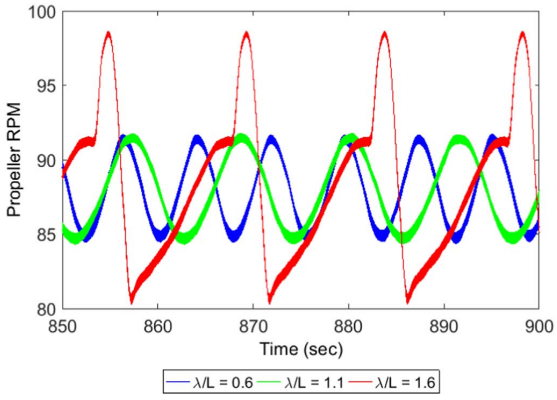

Fig. 16. Engine speed fluctuations in presence of three different head waves of 5 m wave amplitude.

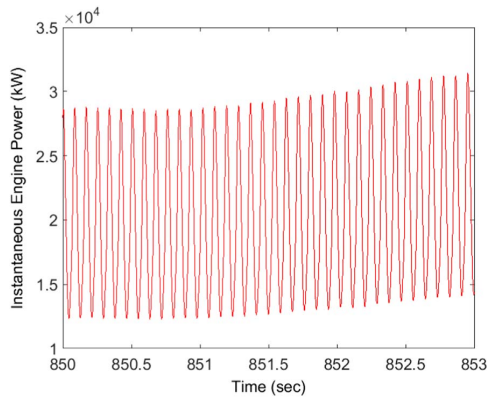

Fig. 18. High frequency power variation due to individual cylinder firing.

avoid the complexity of engine-propeller coupling. To check the validity of this assumption, simulations were run without the engine model assuming constant propeller speed. Torque and power variations obtained using fixed speed in head wave were then compared with those obtained using the coupled model. For the fixed speed calculations, engine power is computed simply as torque times propeller speed.

Comparison of power and torque variations with and without engine model can be seen in Figs. 19 and 20 in the event of propeller emergence. Variation in torque and power is higher in case of constant speed assumption whereas, when engine model is included, torque and power variation reduces due to the combined effect of the diesel engine response and control system. The phase difference seen in the figures is incidental, not due to real differences in the two models.

Similar comparisons can be seen in other wavelengths ($\lambda/L=0.6$ and $\lambda/L=1.1$) in Figs. 21–24 without propeller emergence. In all the cases, power and torque fluctuations are lower in case of the simulations with a diesel engine model. However, the ratio of power and torque fluctuations with and without a diesel engine model is different in each case due to different response of the system to different load frequencies.

It is, however, important to note that torque and power variations are qualitatively similar with and without a diesel engine model. Hence, if relevant effects like wake variation, ship motion and propeller depth variation are included, then the simulations without a diesel engine model will give conservative estimates of variation in propeller forces, torque and power. However, for accurate estimates of system response the coupled engine propeller model should be used.

5.1.3. Engine-propeller dynamics in the event of propeller emergence

As we know, over-speeding is detrimental for the diesel engine. Thus, for safety purpose, the fuel supply to the diesel engine might be shut off in an event of over-speeding, eventually tripping the unit. The control system is designed such that even in rough weather the engine operates within the range of safe operating speed. However, events like propeller emergence can cause sharp increase in speed. The amount of speed overshoot before the control system kicks in to limit the fuel injection is important to investigate. For this investigation, coupled engine-propeller simulations are required as propeller torque variation at different propeller immersions, ship motions and engine reaction play important roles in such an event. This will also tell us if the propeller-engine system with the given control-strategy is safe in the event of propeller emergence. If the system is found to limit the over-speeding, it would allow us to keep the engine running at high power even in relatively harsh weather without the danger of causing damage to the engine.

The event of propeller emergence observed in wave $\lambda/L=1.6$

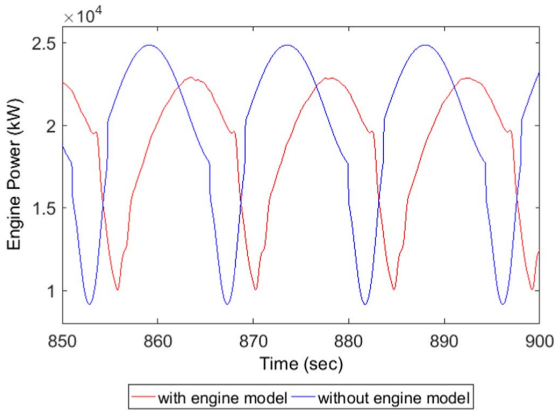

Fig. 19. Low frequency engine power variation with engine model and with constant speed assumption in wavelength $\lambda/L=1.6$ and 5 m wave amplitude.

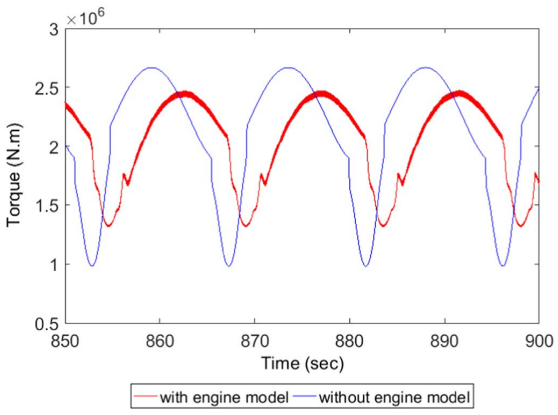

Fig. 20. Torque variation with engine model and with constant speed assumption in wavelength $\lambda/L=1.6$ and 5 m wave amplitude.

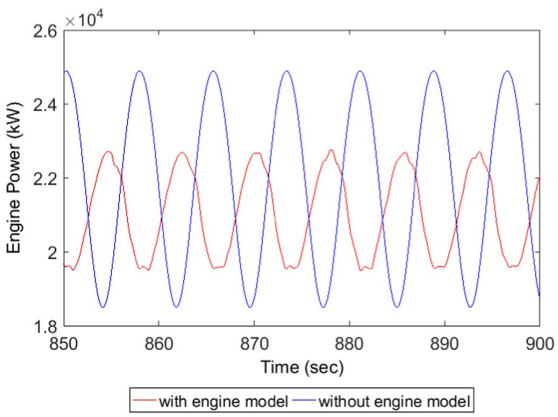

Fig. 21. Low frequency engine power variation with engine model and with constant speed assumption in wavelength $\lambda/L=0.6$ and 5 m wave amplitude.

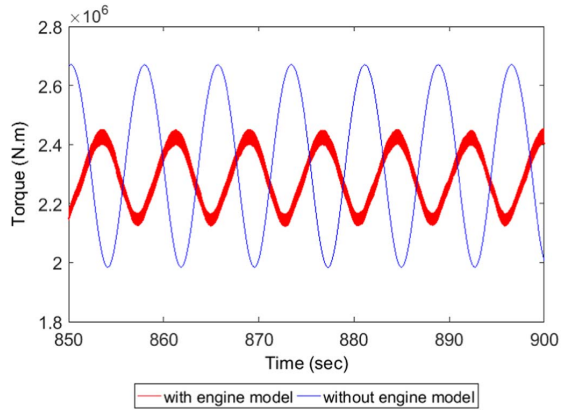

Fig. 22. Torque variation with engine model and with constant speed assumption in wavelength $\lambda/L=0.6$ and 5 m wave amplitude.

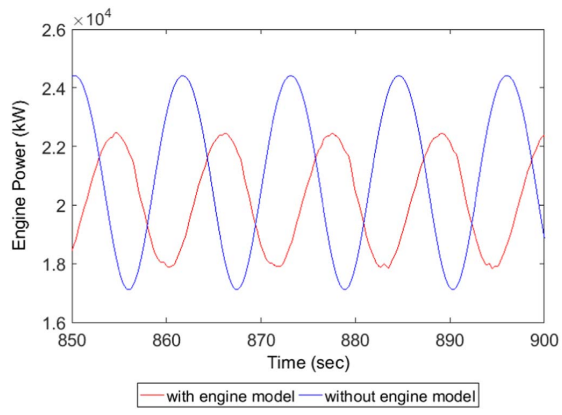

Fig. 23. Low frequency engine power variation with engine model and with constant speed assumption in wavelength $\lambda/L=1.1$ and 5 m wave amplitude.

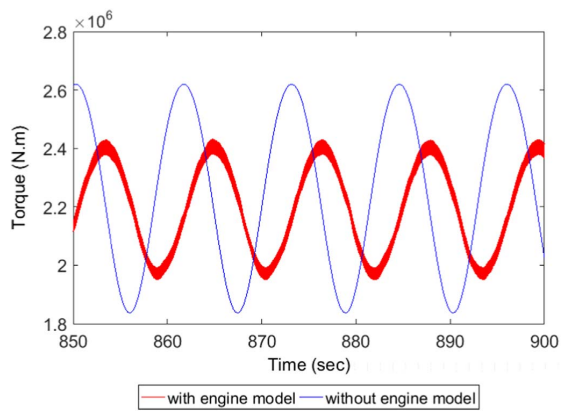

Fig. 24. Torque variation with engine model and with constant speed assumption in wavelength $\lambda/L=1.1$ and 5 m wave amplitude.

with 5 m wave amplitude has been studied in detail. Simulation in the same wavelength with 6 m wave amplitude has been carried out to study larger propeller emergence where, as much as half of the propeller disc comes out of water (i.e. propeller submergence ≈ 0). Variation of torque, engine power, propeller speed and propeller submergence has been plotted in both the cases as

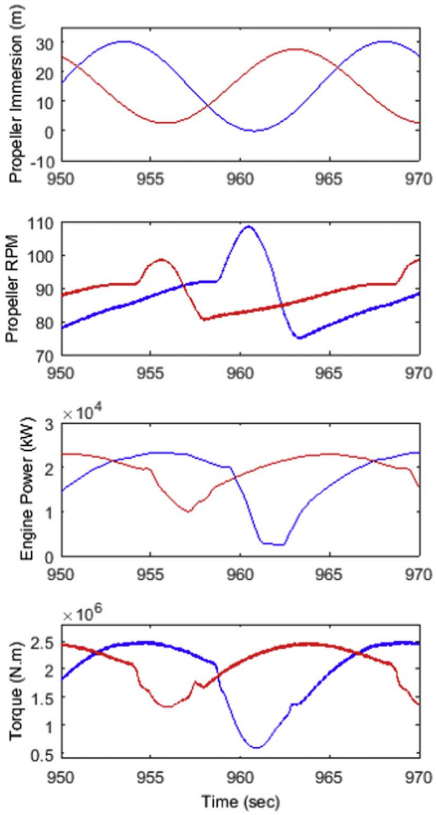

Fig. 25. Propeller emergence in wavelength $\lambda/L=1.6$ in wave amplitudes 5 m (red) and 6 m (blue). (Please refer the web version of this article for colored figure.)

seen in Fig. 25.

Torque drops sharply as soon as propeller starts coming out of water and propeller speed starts to increase. Minima in torque and maxima in speed occurs when the propeller submergence is minimum (i.e. maximum part of propeller is out of water) as expected. At this point, power continues to fall, reaching its minimum when the propeller is fully submerged again. These trends can be observed in both the cases of propeller emergence.

Assuming that up to 10% over speeding of the engine is safe; the control system successfully limits the engine speed in 5 m wave amplitude. Whereas in 6 m wave amplitude, it fails to limit the propeller speed. Hence, in 6 m waves, engine power has to be brought down in order to avoid engine shutoff in rough weather but in 5 m waves, it is safe to keep the engine running at design speed.

We can conclude that such coupled simulations are capable of assessing the safety of the propulsion system and the performance of control system in different weather conditions beforehand. Therefore, such a framework can be effectively used to develop an efficient as well as safe engine control system.

5.1.4. *Effect of waves on the overall propulsion system due to engine propeller dynamics*

Currently, for speed loss and sea margin calculations only added resistance and change of propulsion point due to change in ship speed is taken into account as per ITTC (2008). Wake is assumed constant and propulsion system is assumed to perform like a steady state even in a dynamic flow field. Therefore, influence of time varying flow field on the performance of engine propeller system has been investigated.

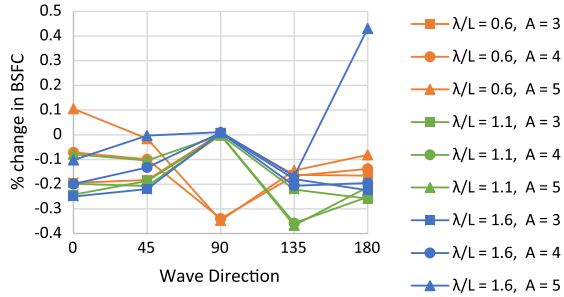

Fig. 26. Increase in engine BSFC due to time varying propeller torque in different waves.

The efficiency of the propulsion system can be divided into two parts, the efficiency at which fuel is converted into power i.e. efficiency of engine and the efficiency at which the engine power is used to propel the ship i.e. propulsive efficiency. Effect of waves on both the efficiencies has been investigated in waves encountered from different directions with three different wavelengths each with three different wave amplitudes. Here it is necessary to remember that added resistance was not included in these sets of simulations. These results have been presented considering the simulation in calm water condition to be the benchmark case. Wave direction has been considered to be the angle between the direction of propagation of wave and the heading of the ship. (0 degree is following sea; 180 degrees is head sea).

5.1.4.1. Change in engine efficiency. Variation in BSFC in different conditions as a result of load fluctuations due to waves can be observed in Fig. 26. In all the cases, change in BSFC is relatively small. As mentioned in the control part of the diesel engine, the cycle efficiency of the engine highly depends on the timing of the exhaust valve or, in other word, apparent compression ratio. Since the speed is controlled at a single reference value and the speed variations are relatively low, we could not observe meaningful deviation of the average cycle efficiency.

5.1.4.2. Change in propulsive efficiency. All the simulated conditions show different power as well as ship speed at constant propeller speed setting, making it difficult to directly compare required engine power in different cases. Since there is no added resistance in this set of simulations, it would be meaningful to compare the ratio of power and the cube of the ship speed (the ratio that can be assumed constant in calm water). This ratio can give us an indication of propulsive efficiency. Increase in the ratio means that higher power is required compared to calm water operation to propel the ship at same speed. Percentage increase in the ratio of power and the cube of ship speed in presence of waves can be seen in Fig. 27. Change is significant in case of head and bow quartering sea for $\lambda/L=1.1$ and 1.6. Whereas, $\lambda/L=0.6$ shows comparatively small change in any wave direction. This power loss is due to the combined effect of drop in propeller efficiency and change in hull efficiency as wake fraction changes in waves.

Change in propeller and hull efficiency has been studied separately to study how much each of these factors contributes to increase in P/V^3. Variation in propeller efficiency in different wave conditions can be seen in Fig. 28.

Change in the propeller efficiency can be attributed to two factors. One, due to variation in propeller speed because of time varying propeller inflow and engine dynamics; second, due to

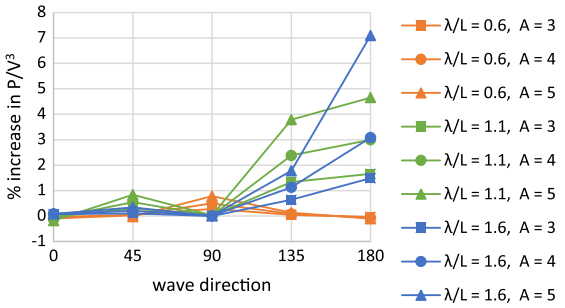

Fig. 27. Change in the performance of propulsion system (engine+propeller) due to unsteady wake and propeller engine interaction.

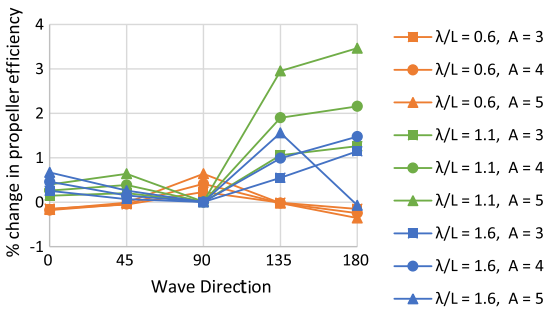

Fig. 28. Change in propeller efficiency in different wave conditions due to time varying flow field.

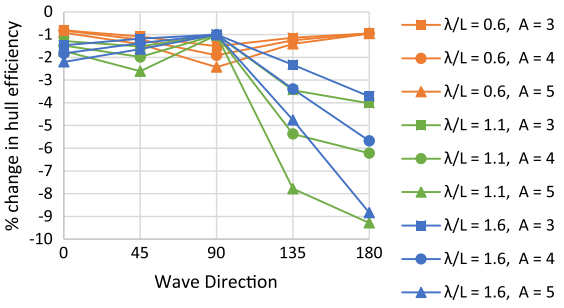

Fig. 29. Change in hull efficiency due to time varying wake in waves.

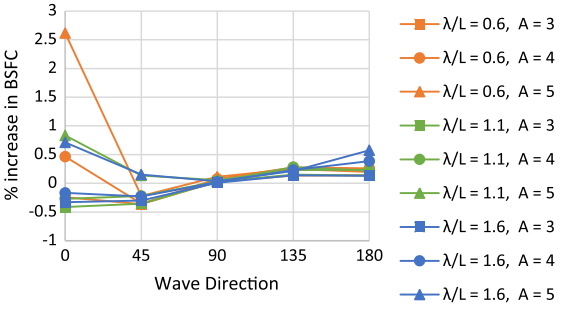

Fig. 30. Increase in BSFC of engine due to combined effect of fluctuating load and change in power load due to added resistance in different wave conditions as compared to BSFC in calm water condition.

change in operating point of propeller because of mean change in wake velocities as a result of pitching motion of the ship. Increase in wake velocities increase the advance coefficient, leading to higher efficiency but lower thrust as compared to calm water condition. This can lead to drop in ship speed, which would reduce the advance coefficient, since propeller speed is kept constant. Effectively it was observed that final advance coefficient in waves was higher than the calm water condition in most of the cases.

Propeller efficiency increases in head waves and bow quartering waves for $\lambda/L=1.1$ and 1.6. In these cases, the effect of increase in advance coefficient seems to dominate. Whereas, in head wave $\lambda/L=0.6$, small drop in advance coefficient together with dynamic shaft speed variation causes drop in efficiency. A similar trend is seen in following and stern quartering sea but the amount of increase in efficiency is much lower. These cases have relatively higher wake variation since wave induced particle velocities directly affect the propeller unlike in case of head waves, where the hull in front of the propeller reduces this effect.

Another part of the propulsive efficiency is the hull efficiency. The change in hull efficiency has been plotted in Fig. 29. It can be observed that the drop in hull efficiency is more significant than the drop in propeller efficiency. It is a dominating factor causing change in the ratio of P/V^3. Moreover, since we have neglected change in thrust deduction due to waves, it can be concluded that accurate estimation of wake variation is essential for the performance estimation of the ship. However, engine dynamics has minor influence on change in propulsive efficiency in case of simulations without added resistance.

5.2. Simulations with added resistance

Realistic cases were simulated by including the added resistance in the simulations to determine propulsion performance in waves. However, in these simulations, the performance of the ship is affected by added resistance as well as change in engine and propulsive efficiency, and it is difficult to separate the effects of the two.

5.2.1. Effect of waves on the engine performance

From comparison of Fig. 30 with Fig. 26, it can be seen that changes in BSFC are only slightly higher than those in case of simulations without added resistance. Therefore, even after including the added resistance, variation in BSFC is small in most of the wave conditions.

5.2.2. Importance of engine-propeller coupled model in performance prediction in waves

Since it is difficult to separate the effects of added resistance from those of unsteady engine propeller dynamics and wake variation, the another set of simulations was run without the engine model. However, effects of wake variation, ship motion, thrust and torque losses were considered. The propeller speed was kept constant. Therefore, the difference between the simulation results with and without the engine model is purely due to engine propeller dynamics. The simulation results have been compared in terms of quasi-propulsive efficiency and the ship speed achieved.

Difference between the quasi-propulsive efficiency with and without engine model can be observed in Fig. 31. Changes in quasi-propulsive efficiencies are minor except in case of head and bow quartering waves of 5 m wave amplitude where efficiencies are lower in case of simulations with engine model. In these cases, engine is operating close to 100% MCR where control system tries to constrain the engine power by limiting the fuel injection. This effect being absent in the simulations without engine model, leads to the differences in the performance prediction. This difference in the efficiencies causes difference between the ship speeds

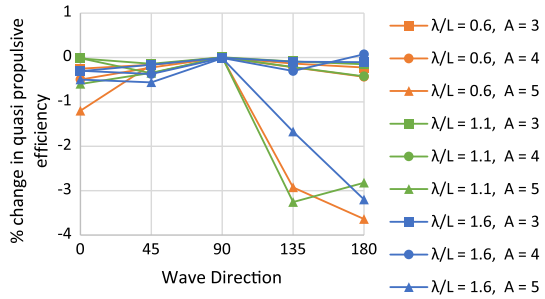

Fig. 31. Percentage change in quasi-propulsive efficiency due to the use of engine model as compared to that without engine model (including wake change, thrust and torque loss calculations).

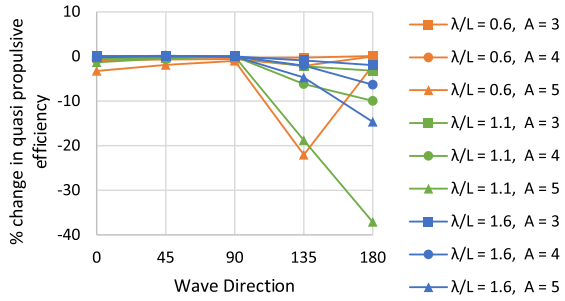

Fig. 33. Percentage change in quasi-propulsive efficiency due to the use of engine model as compared to that without engine model without considering wake change and changes in thrust and torque.

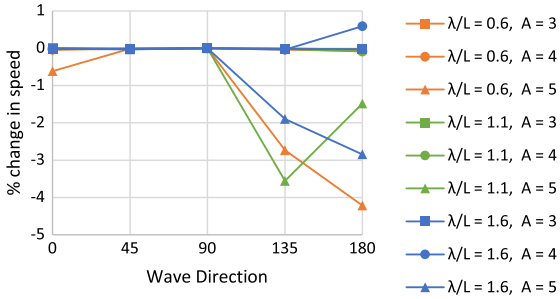

Fig. 32. Change in the prediction of final ship speed including engine model as compared to that without engine model but including wake change, thrust and torque loss calculations.

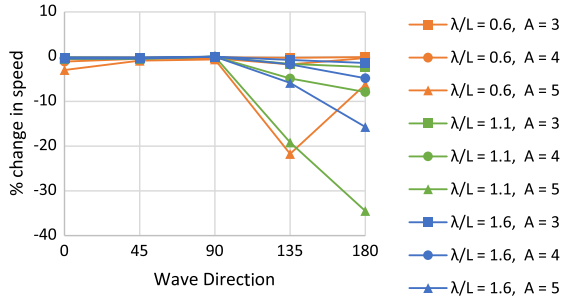

Fig. 34. Change in the prediction of final ship speed including engine model as compared to that without engine model without considering wake change and changes in thrust and torque.

predicted by two simulations as seen in Fig. 32.

Simulations were also run without the engine model, without considering wake variations and change in thrust and torque in order to analyze the importance of considering wake change and propulsion losses. These simulations without the engine model resemble the traditional calculations performed to analyze ship in waves, where effect of waves is taken into account only in terms of added resistance and change of propulsion point. In most of the cases, vessel speed predictions are even higher than the simulations without the engine model including wake variation and thrust, torque losses. Therefore, as compared to these cases, simulations with an engine model predict much lower ship speeds as seen in Fig. 34. Significant difference can also be observed in quasi-propulsive efficiency in Fig. 33.

Therefore, it was observed that engine modeling plays an important role while predicting ship performance in rough sea where the engine has to operate close to 100% MCR. Whereas, modeling of wake change, thrust and torque losses are important to correctly predict the ship performance in head and bow quartering waves.

5.2.3. The effect of power fluctuation on vessel performance

Engine load variation in presence of waves, including the added resistance has been plotted in Fig. 35. In the simulations, propeller emergence was found to occur in head waves of 5 m amplitude in cases $\lambda/L=1.1$ and 1.6. Due to the propeller emergence, the control system reduces the engine power to control the engine speed as seen in Fig. 35. Therefore, in such cases full engine power cannot be utilized causing further drop in speed. Therefore, in Fig. 36 the engine load reduces in 5 m wave amplitude as compared to 4 m wave amplitude for these two cases ($\lambda/L=1.1$ and 1.6). This also means that speed prediction in such condition without considering ship motions will predict higher speed. Moreover, having higher engine power will not increase the ship speed in these two cases. Hence, effects like propeller emergence and engine propeller dynamics play an important role in performance prediction of vessel.

6. Conclusions

In this study, an effective method for modeling wake in waves has been demonstrated which enables us to study different aspects of the propulsion system in time varying wake in waves of different wavelength, waveheight and wave direction. It has been shown that engine propeller response i.e. power fluctuations, propeller speed fluctuations and torque fluctuations can be obtained through coupled simulations by using realistic engine and propeller models. Therefore, the framework of coupled system described in this study can be used to investigate engine load variations, propeller loads in waves, shaft vibration and engine control system. This model is capable of analyzing the performance as well as safety of a control system used for controlling the engine.

Significant changes in the propulsion performance have been observed in presence of waves as compared to steady state operation. Therefore, when estimating the sea margin, drop in propulsion efficiency due to the effect of waves should be taken into account. Engine modeling, wake variation in waves and, thrust and torque losses due to variable propeller submergence are crucial in

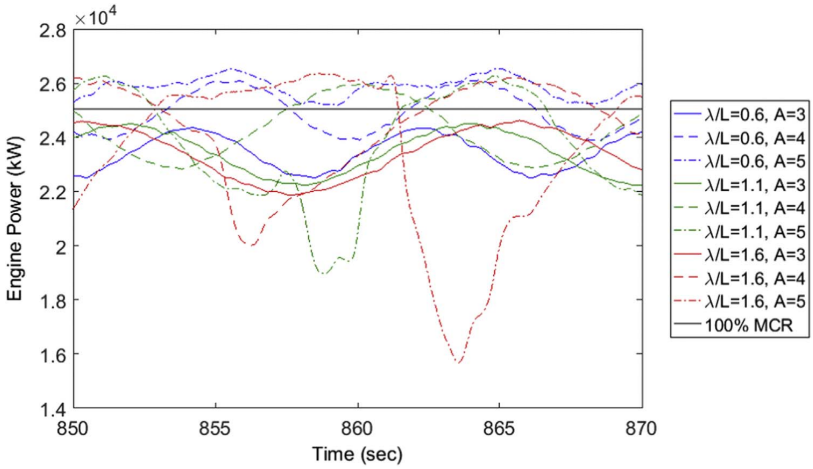

Fig. 35. Power variation in waves including added resistance in head waves.

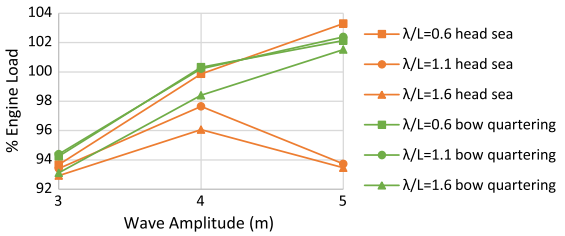

Fig. 36. Engine load in presence of head sea and bow quartering waves including the effect of added resistance.

predicting vessel performance in terms of propulsion efficiency. Wave direction is found to have strong influence on the performance drop, with bow quartering and head sea conditions affecting propulsion performance the most.

Wake variation and engine response will change for different type and sizes of vessels. Hence more vessels should be analyzed in order to draw any generalized conclusions. In this study, an inertial shaft model has been considered. A flexible shaft model can also be implemented in the same framework to study torsional vibrations with realistic engine response and propeller loading. Currently, the analysis has been performed in regular waves. However, in future, simulations can be carried out for irregular wave condition to observe the effect of irregular waves on the overall performance of ship.

Acknowledgments

Authors would like to thank Professor Frederick Stern from the University of Iowa for providing the wake data in waves.

This work is funded by the projects 'Design to Verification of Control Systems for Safe and Energy Efficient Vessels with Hybrid Power Plants' (D2V, NFR: 210670/070), and 'Low Energy and Emission Design of Ships' (LEEDS, NFR 216432/O70) where the Research Council of Norway is the main sponsor of both projects. This work is also supported by the Research Council of Norway through the Centers of Excellence funding scheme, project number 223254 – AMOS.

References

Amini, H., 2011. Azimuth Propulsors in Off-design Conditions. Norges teknisk-naturvitenskapelige universitet, Trondheim.

Campora, U., Figari, M., 2003. Numerical simulation of ship propulsion transients and full-scale validation. Proc. Inst. Mech. Eng. M: J. Eng. Marit. Environ. 217 (1), 41–52.

Epps, B., 2010. OpenProp v2.4 Theory Document.

Faltinsen, O.M., Minsaas, K.J., Liapis, N., Skjordal, S.O., 1980. Prediction of resistance and propulsion of a ship in a seaway. In: Proceedings of the 13th Symposium on Naval Hydrodynamics.

Guo, B.J., Steen, S., Deng, G.B., 2012. Seakeeping prediction of KVLCC2 in head waves with RANS. Appl. Ocean Res. 35 (0), 56–67.

Hepperle, M. JavaFoil. ⟨http://www.MH-AeroTools.de/⟩.

Heywood, J.B., 1988. Internal Combustion Engine Fundamentals. McGraw Hill, New York.

Hiroyasu, H., Kadota, T., Arai, M., 1983. Development and use of a spray combustion modeling to predict diesel engine efficiency and pollutant emissions: Part 1 combustion modeling. Bull. JSME 26 (214), 569–575.

Incropera, F.P., DeWitt, D.P., Bergman, T.L., Lavine, A.S., 2007. Fundamentals of Heat and Mass Transfer. John Wiley & Sons, New York.

ITTC, 2008. ITTC – recommended procedures and guidelines. Testing and Extrapolation Methods, Propulsion, Performance, Predicting Powering Margins.

ITTC, 2011. Specialist committee on scaling of wake field. Final Report and Recommendations to the 26th ITTC, ITTC, Vol. 2.

Kayano, J., Yabuki, H., Sasaki, N., Hiwatashi, R., 2013. A study on the propulsion performance in the actual sea by means of full-scale experiments. Trans. Nav. Int. J. Mar. Navig. Saf. Sea Transp. 7 (4), 521–526.

Kyrtatos, N., Theodossopoulos, P., Theotokatos, G., Xiros, N., 1999. Simulation of the overall ship propulsion plant for performance prediction and control. Trans.-Inst. Mar. Eng.-Ser. C 111, 103–114.

Kyrtatos, N.P., 1997. Engine operation in adverse conditions – the ACME Project. In: Proceedings of the 2nd International Symposium CIMAC. Athens.

Lee, C.S., 1983. Propeller in waves. In: Proceedings of the 2nd International Symposium on Practical Design in Shipbuilding. Tokyo & Seoul.

Livanos, G.A., Simotas, G.N., Dimopoulos, G.G., Kyrtatos, N.P., 2006. Simulation of marine diesel engine propulsion system dynamics during extreme maneuvering. In: Proceedings of the ASME 2006 Internal Combustion Engine Division Spring Technical Conference, American Society of Mechanical Engineers.

Loukakis, T.A., Sclavounos, P.D., 1978. Some extensions of the classical approach to strip theory of ship motions, including the calculation of mean added forces and moments. J. Ship Res. 22 (1), 1–19.

Minsaas, K., Faltinsen, O.M., Persson, B., 1983. On the importance of added resistance, propeller immersion and propeller ventilarion for large ships in a seaway In: Proceedings of the 2nd international symposium on practical design in shipbuilding. Tokyo & Seoul.

Moor, D.I., Murdey, D.C., 1970. Motions and propulsion of single screw models in head seas, Part II. R. Inst. Nav. Archit. 112 (2).

Nakamura, S., Naito, S., 1975. Propulsive performance of a container ship in waves. J. Kansai Soc. Nav. Archit. Jpn. (158)

Queutey, P., Wackers, J., Leroyer, A., Deng, G., Guilmineau, E., Hagesteijn, G., Brouwer, J., 2014. Dynamic Behaviour of the Loads of Podded Propellers in Waves: Experimental and Numerical Simulations. OMAE2014 San Francisco – ASME, California, USA.

Rakopoulos, C.D., Giakoumis, E., 2006. Review of thermodynamic diesel engine

simulations under transient operating conditions. SAE Paper (2006-01):0884.
Sadat-Hosseini, H., Wu, P.-C., Carrica, P.M., Kim, H., Toda, Y., Stern, F., 2013. CFD verification and validation of added resistance and motions of KVLCC2 with fixed and free surge in short and long head waves. Ocean Eng. 59 (0), 240–273.
Sasajima, H., Tanaka, I., Suzuki, T., 1966. Wake distribution of full ships. J. Zosen Kiokai (120), 1–9.
Sher, E., 1990. Scavenging the two-stroke engine. Progress. Energy Combust. Sci. 16 (2), 95–124.
Takizawa, M., Uno, T., Oue, T., Yura, T., 1982. A study of gas exchange process simulation of an automotive multi-cylinder internal combustion engine. SAE Techechnical Paper.
Tanizawa, K., Kitagawa, Y., Takimoto, T., Tsukada, Y., 2013. Development of an experimental methodology for self-propulsion test with a marine diesel engine simulator. Int. J. Offshore Polar Eng. 23 (3), 197–204.
Taskar, B., Steen, S., 2015. Analysis of propulsion performance of KVLCC2 in waves. In: Proceedings of the Fourth International Symposium on Marine Propulsors. Austin, Texas, USA.
Taskar, B., Yum, K.K., Pedersen, E., Steen, S., 2015. Dynamics of a marine propulsion system with a diesel engine and a propeller subject to waves. In: Proceedings of the 34th International Conference on Ocean, Offshore and Arctic (OMAE2015). St. John's, Newfoundland, Canada.
Theotokatos, G., Tzelepis, V., 2013. A computational study on the performance and emission parameters mapping of a ship propulsion system. Proc. Inst. Mech. Eng. M: J. Eng. Marit. Environ. 1475090213498715
Ueno, M., Tsukada, Y., Tanizawa, K., 2013. Estimation and prediction of effective inflow velocity to propeller in waves. J. Mar. Sci. Technol. 18 (3), 339–348.
WÄRTSILÄ, 2014. netGTD Wärtsilä 2-stroke Marine Diesel Engines. Retrieved 12/12, 2014, from: ⟨http://www.wartsila.com/en/products/netGTD⟩.
Woschni, G., 1967. A universally applicable equation for the instantaneous heat transfer coefficient in the internal combustion engine. SAE Technical Paper.
Wu, P.C., 2013. A CFD Study on Added Resistance, Motions and Phase Averaged Wake Fields of Full form Ship Model in Head Waves. Osaka University, Osaka.
Zacharias, F., 1967. Analytical representation of the thermodynamic properties of combustion gases. SAE Technical Paper, 670930.

Paper 4

Effect of waves on cavitation and pressure pulses

Bhushan Taskar, Sverre Steen, Rickard E. Bensow,
Björn Schröder

Applied Ocean Research, 2016, Vol 60, pp 61-74

http://dx.doi.org/10.1016/j.apor.2016.08.009

Applied Ocean Research 60 (2016) 61–74

Contents lists available at ScienceDirect

Applied Ocean Research

journal homepage: www.elsevier.com/locate/apor

Effect of waves on cavitation and pressure pulses

Bhushan Taskar[a,*], Sverre Steen[a], Rickard E. Bensow[b], Björn Schröder[c]

[a] Department of Marine Technology, Norwegian University of Science and Technology (NTNU), Trondheim, Norway
[b] Chalmers University of Technology, Sweden
[c] Rolls-Royce Hydrodynamic Research Centre, Rolls-Royce AB, Kristinehamn, Sweden

ARTICLE INFO

Article history:
Received 16 April 2016
Received in revised form 24 August 2016
Accepted 28 August 2016
Available online 13 September 2016

Keywords:
Propulsion in waves
Cavitation
Pressure pulses
Marine propeller
Propeller performance in waves
Propeller design

ABSTRACT

In view of environmental concerns, there is increasing demand to optimize the ships for the actual operating condition rather than for calm water. Now, in order to apply this for propeller design, a first step would be to study the effects of waves on propeller operation. Therefore, the aim of this paper is to identify and quantify the effect of various factors affecting the propeller in waves. The performance of KVLCC2 propeller in the presence of three different waves has been compared with calm water performance. Changes in performance in terms of cavitation, pressure pulses, and efficiency have been studied. Significant increase in pressure pulses has been observed due to wake change in waves even though cavitation did not show any significant change. An analysis using cavitation bucket diagram in different wave conditions indicates that a propeller optimized for calm water wake may perform much worse in the presence of waves. Therefore, having wake variation at least in critical wave conditions (where the wavelength is close to ship length) in addition to calm water wake could be very useful to ensure that the propeller performs equally well in the presence of waves.

1. Introduction

Traditionally, propellers have been optimized for calm water conditions partly because one has not had the knowledge and tools to optimize propellers for operations in waves. However, with increasing environmental concerns and emission regulations, there is growing demand for the propulsion being optimized for the actual operating conditions, which typically include waves.

Currently, propellers are designed using wake, thrust deduction and relative rotative efficiency obtained in calm water conditions. Moor and Murdey [1] have shown through model tests of multiple ship hulls in calm water and in waves that wake, thrust deduction and propeller efficiency change in the presence of waves. Circumferentially averaged wake also changes due to waves and ship motions as demonstrated by Nakamura and Naito [2]. They also found that wake velocities increase in waves, and it is primarily caused due to pitching motion of the ship. Similar results confirming significant wake variation in waves were obtained in the RANS simulation carried out by Guo et al. [3] where the nominal wake field was obtained in the presence of waves. In these simulations, the axial wake velocities increased with up to 35% of ship speed in some regions. Such changes in the wake distribution of a ship traveling in waves were experimentally confirmed by Hayashi [4] using a model of the KVLCC2 ship. Strong variation of wake was observed in the presence of waves through the PIV (Particle Induced Velocimetry) measurements.

Change in wake distribution changes the angle of attack and the cavitation number of the propeller blades as shown by Albers and Gent [5]. Chevalier and Kim [6], Jessup and Wang [7] studied the cavitation of a propeller operating in waves by calculating wake velocities using potential flow calculations and observed a drop in the cavitation inception speed of the vessel in waves.

Due to increasing demand for efficiency, it is no longer possible to design the propellers without cavitation. Cavitation can lead to erosion on the propeller blades. Moreover, the pressure pulses can cause vibration in the ship structure thus affecting passenger comfort and in severe cases damage the structural integrity of the hull. In merchant ships, about 10% of propeller-induced vibration velocities are caused by bearing forces, whereas approximately 90% are due to pressure fluctuations, or hull surface forces [8]. Survey of 47 ships with vibration problem has shown that around 80% of the cases could be traced back to pressure pulses as a source of vibration problems. Based on reported cracks in the aft peak of 20 ships, strong correlation between fatigue damages in the afterbody and

* Corresponding author.
E-mail address: bhushan.taskar@ntnu.no (B. Taskar).

http://dx.doi.org/10.1016/j.apor.2016.08.009
0141-1187/

Table 1
Propeller Geometry.

Diameter (D) (m)	9.86
No of blades	4
Hub diameter (m)	1.53
Rotational speed (RPM)	76
A_e/A_0	0.431
$(P/D)_{mean}$	0.690
Skew (°)	21.15
Rake (°)	0

Table 2
Ship Particulars.

Length between perpendiculars (m)	320.0
Length at water line (m)	325.5
Breadth at water line (m)	58.0
Depth (m)	30.0
Draft (m)	20.8
Displacement (m^3)	312,622
Block coefficient (C_B)	0.8098
Design Speed (knots)	15.5

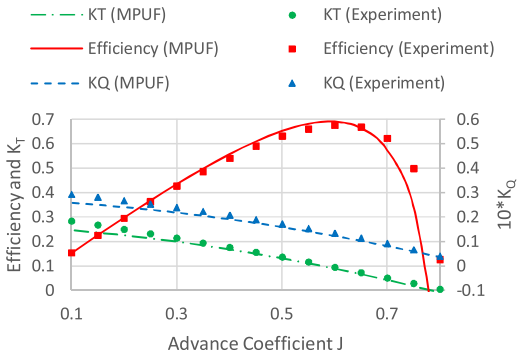

Fig. 1. Comparison of open water data of KVLCC2 using MPUF-3A and model tests.

the amplitude of pressure pulses at blade harmonic frequency was observed [9]. Therefore, it is necessary to avoid cavitation erosion and high pressure pulses even when the cavitation is present. It is achieved by adapting the propeller design to calm water wake as cavitation and pressure pulses depend on the wake distribution [10,11]. However, given the significant wake variation, it is essential to investigate the performance of propeller in the presence of waves. Moreover, lowering the pressure pulses comes at the expense of efficiency. Therefore, accurate estimation of pressure pulses in realistic operating condition can help us maximize the efficiency while still avoiding the unwanted consequences.

In this paper, we have analyzed the performance of the KVLCC2 propeller operating in waves. Time-varying wake data in three different head waves provided by Sadat-Hosseini et al. [12] have been used. Effect of various factors affecting propeller performance in waves like wake change, ship motions, wave dynamic pressure, added resistance and RPM fluctuation has been studied separately to decide the order of importance of each factor. Cavitation and pressure pulses have been calculated in different wave conditions and compared with that in calm water wake. An analysis of propeller blade sections using a cavitation bucket diagram was performed to explore the possibility of improving propeller design to ensure optimized performance not just in calm water but also in the presence of waves.

2. Methods and validation

2.1. Propeller analysis tools

The KVLCC2 propeller has been analyzed using the vortex lattice method implemented in MPUF-3A [13]. Details about the propeller geometry are given in Table 1 [14]. The fine grid has been used on the key blade while coarse grid has been used on other blades. Open water curves obtained using MPUF-3A for the KVLCC2 propeller are compared with experimentally obtained open-water data [14] in Fig. 1. When the propeller was analyzed in waves, the variation in inflow caused by waves and ship motions is taken into account in a quasi-steady manner, meaning that for each time instant, the flow field entering the propeller disk is treated as time-invariant. The propeller is then analyzed at each time instance in time-invariant wake using unsteady calculations. This approach is justified by the fact that the wave encounter frequency is much lower than the propeller rotation frequency.

For the analysis of propeller blade section in calm water and in waves, the lift coefficient has been obtained for the propeller blade section at 0.7R from MPUF-3A calculations. Cavitation bucket has been calculated by giving the blade section shape at 0.7R as an input to Xfoil [15]. While cavitation number (Sigma) is calculated as follows-

$$\text{Sigma} = \frac{P_0 + \rho g h - P_v}{0.5\rho[V_a^2 + (0.7\pi n D)^2]}$$

where P_0 is atmospheric pressure, ρ is the density of water, g is acceleration due to gravity, h is the instantaneous submergence of the blade section at 0.7R, P_v is the vapour pressure of water, V_a is average propeller inflow velocity, n is propeller rps and D is diameter of the propeller. It should be kept in mind that since both h and V_a varies in waves, the cavitation number varies with time.

2.2. Wake data in the presence of waves

Experiments were performed by Sadat-Hosseini et al. [12] to obtain wake data in three different wavelengths in head sea condition at design speed. A model of KVLCC2 was used for this purpose with the model scale of 1:100. Ship particulars are given in Table 2 [14]. In these experiments, PIV (Particle Image Velocimetry) was used to obtain time-varying nominal wake field in the propeller plane. CFD simulations were also performed and results were validated using the data from the PIV measurements. Since the CFD data are smoother and less noisy, we have used them in our calculations. These results were available for waves λ/L = 0.6, 1.1 and 1.6 at 8, 12 and 6 time intervals respectively in one wave encounter period. Wakes at different time intervals have been denoted by t/T, which is a fraction of time 't' in one wave encounter period 'T'. Note that 'T' is different in each wave case. At t/T = 0 the wave crest is located at the forward perpendicular of the ship. Waveheight of these waves corresponds to a full-scale wave amplitude of 3m. Wake fields in calm water and at four instances in λ/L = 1.1 can be seen in Fig. 2.

Due to the higher friction coefficient of the model scale ship, the wake field calculated in model scale should be contracted (scaled) for analyzing the propulsion performance in full scale. However, it is not uncommon that propellers are evaluated in model scale wake as far as pressure pulses are concerned. It is partly because the model scale hull is used in the tests carried out in the cavitation tunnel for the measurement of pressure pulses, which means that the propeller is analyzed in model scale wake to prove that the pressure pulses in full scale are within the contractual requirements. The general experience is that analyzing the propeller in model scale wake gives a conservative estimate of cavitation and pressure pulses.

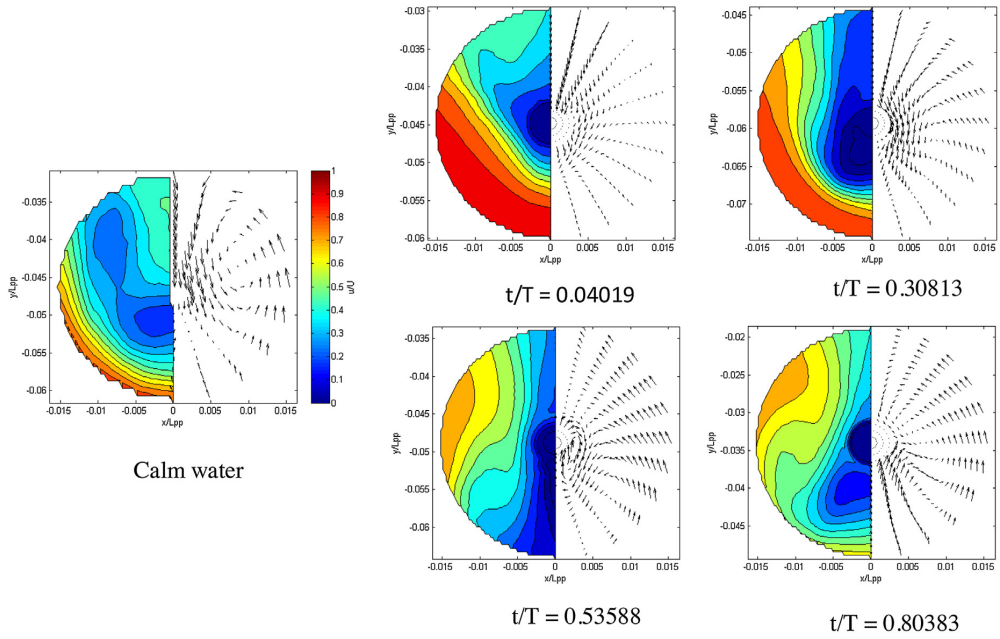

Fig. 2. Wake in calm water compared to the wake in the presence of wave having wavelength ratio λ/L = 1.1.

The analysis in model scale wake also avoids the complexity and uncertainty of the wake scaling procedure. Moreover, for this study, it is more important to compare the propeller cavitation and pressure pulses in calm water with that in waves than predicting the exact amount of cavitation and pressure pulses in full scale. We think that the use of model scale wake is sufficient for the qualitative study of the effect of waves on propeller performance.

Time-varying potential wake in the presence of waves has been calculated using Shipflow Motions [16]. Simulations were performed at design speed in three different wavelengths (λ/L = 0.6, 1.1, 1.6), free to heave and pitch. Wake variation obtained using the potential flow calculation has been compared with the wake data obtained from CFD to investigate the appropriateness of computing the wake variation in waves using potential flow theory. The motivation for this being the excessive computational expense of seakeeping calculations with CFD.

2.3. Calculation of ship motions and added resistance

Ship motion RAOs (Response amplitude operators) were calculated using linear strip theory, utilizing potential theory and pressure integration, implemented in the ShipX Veres software. Using the motion response of the vessel, added resistance coefficients have been calculated using the method by Loukakis and Sclavounos [17] (which is an extension of the classical Gerritsma and Beukelman's method) also implemented in ShipX Veres. Heave RAO, pitch RAO and added resistance calculations have been compared with the experimental investigations performed by Wu [18]. These comparisons can be seen in Fig. 3. Added resistance was then computed in irregular waves for different peak frequencies using the Pierson–Moskowitz wave spectrum. Speed loss for a particular wave condition (e.g. λ/L = 1.1, wave amplitude = 3 m) has been calculated in irregular waves having a peak frequency equal to the regular wave frequency and significant waveheight equal to the height of the regular wave. The reason behind using irregular waves for the computation of speed loss is to avoid getting unreasonably low ship speeds as a results of added resistance in regular waves which is often much larger than the added resistance in corresponding irregular waves.

2.4. Calculation of propeller RPM fluctuation

In order to calculate the RPM fluctuation, a coupled engine-propeller model of Taskar et al. [19,20] has been utilized. The study analyzes the engine-propeller interaction in the presence of waves considering a fluctuating wake field, propeller emergence, and free surface effects. Simulations in regular head waves of 3 m wave amplitude showed around 3% fluctuation in RPM. Hence, propeller cavitation has been analyzed in 3% higher RPM to calculate the possible change in pressure pulses and cavitation.

2.5. Pressure pulse calculation

Pressure pulses have been computed using HULLFPP [21] which calculates field point potential induced by a cavitating propeller using a potential based boundary element method. Time series of cavity shapes, cavity volumes and pressure distribution on blades calculated by MPUF-3A are used as an input to this code. In the computations, the hull was assumed to be a flat plate at a distance of 30% of the propeller diameter from the blade tip. Tip clearance of 30% is commonly seen on ships.

In the propeller design methodology, prediction of pressure pulses plays an important role. The propeller geometry should be such that the level of pressure pulses is below the specified threshold. The method proposed by Holden et al. [22] is often used to analyze pressure pulses in the initial design stage. This method is based on numerous experimental studies and experiences with full-scale pressure pulses. The applicability of Holden's method for

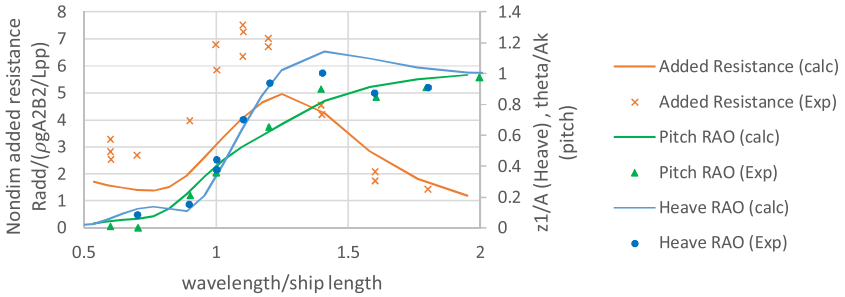

Fig. 3. Added resistance and ship motions calculation compared with the experimental measurements.

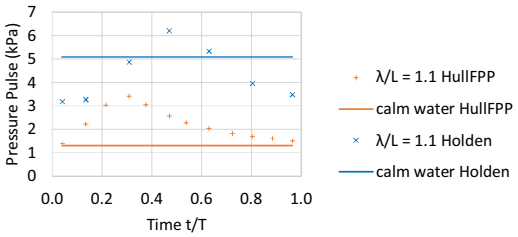

Fig. 4. Comparison of pressure pulses calculated using Holden method and HULLFPP code.

the analysis of propeller in waves has been tested by comparing the results with more accurate HULLFPP calculations. A comparison of pressure pulses predicted by both methods has been presented in Fig. 4.

In Fig. 4, it is evident that pressure pulses predicted by Holden's method are much higher than those predicted by HULLFPP. Moreover, the trend of variation in pressure pulses in different wake fields is different in two cases, as seen for $\lambda/L = 1.1$. Therefore, analysis using a simple method like Holden's might not be a good idea. A more detailed analysis like the one using HULLFPP is required to capture the effects of minor variations in wake structure. An explanation for the large over-prediction by Holden's method compared to HULLFPP might be that it is based on data from old propellers, typically with little skew.

2.6. Calculation of unsteady wave pressure

Propeller cavitation can get affected by the change in cavitation number caused by ship motions as well as dynamic wave pressure. To study this effect, the total pressure was calculated at the location of the propeller shaft, considering the instantaneous depth of propeller and the phase of the passing wave. The total pressure was then used in the calculation of cavitation number for analyzing time-varying cavitation and pressure pulses in waves.

3. Analysis

Initially, the propeller was analyzed in the calm water wake field to observe the cavitation pattern and pressure pulses in calm water condition. The influence of the factors affecting propeller in waves (i.e. wake variation, ship motions, dynamic wave pressure, speed loss and RPM fluctuations) on cavitation and pressure pulses has been studied. Cavitation bucket diagram has been studied to observe the effect of these factors on lift coefficient and cavitation number. The analysis has been divided into three parts where the influence of each factor has been considered separately.

1. Wake variation and change in cavitation number due to ship motions and waves
2. Increased loading due to speed loss
3. RPM fluctuations due to engine propeller interactions and average wake variation

3.1. Effect of wake variation and change in cavitation number

The KVLCC2 propeller has been analyzed using MPUF at multiple time intervals in the presence of three different regular waves. In order to observe the effect of wake variation alone, the propeller immersion was assumed constant at 15.1 m depth, equal to that in calm water. The maximum amount of cavitation in each case can be seen in Fig. 5. In calm water, the blade position at which maximum cavitation occurs has been plotted. However, in the presence of waves, cavitation depends not only on the location of the blade but also on the phase of the passing wave. Maximum cavitation with respect to blade position as well as time instant (or wave phase) can be seen in Fig. 5.

It can be seen from Fig. 5 that for three wavelengths, maximum cavitation occurred at different blade positions although the location of cavitation on the blade was similar. Maximum cavitation is observed in the case of $\lambda/L = 1.1$ (i.e. when the wavelength is close to ship length) at the instant when the stern of the ship is moving down causing low wake velocities in the upper part of the propeller disc close to the centerline. Here, it is important to note that the maximum cavitation in the presence of waves is occurring at one blade location at one instant in a single wave encounter period. The maximum cavitation seen in one full rotation of the blade varies as the wave passes, it can be as low as that shown in Fig. 6. It was also observed that in calm water, cavity is present on a couple of blades simultaneously for a significant amount of time whereas in other cases, as the cavity on one blade vanishes, the next blade starts cavitating. This may have an effect on the behavior of pressure pulses.

In addition to the effect of wake variation, change in cavitation number can also affect propeller cavitation and pressure pulses. In the presence of waves, varying propeller immersion due to ship motions and dynamic wave pressure lead to a change in cavitation number. Therefore, the propeller has been analyzed to see the combined effect of variation in cavitation number and wake variation on the cavitation and pressure pulses.

The total pressure, including the dynamic pressure, at the location of the propeller, was expressed in terms of an equivalent height of water column. The propeller was analyzed in wakes at different time instances at calculated equivalent propeller depth. Therefore,

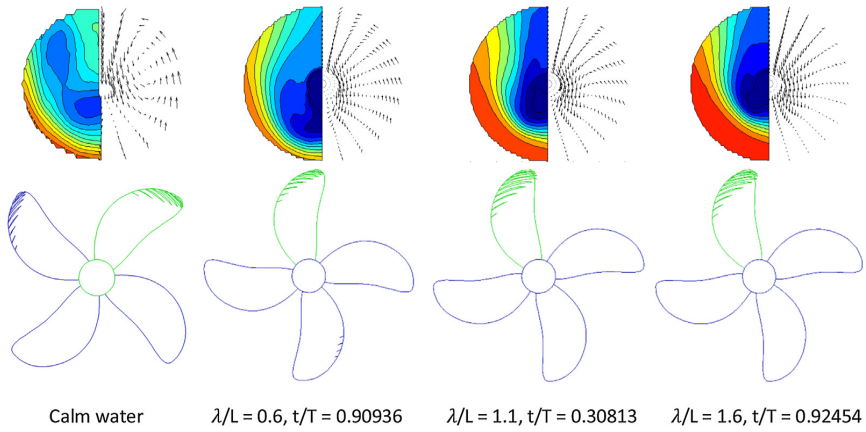

Fig. 5. Maximum suction side cavitation seen in each wavelength considering only wake change compared to cavitation in calm water wake.

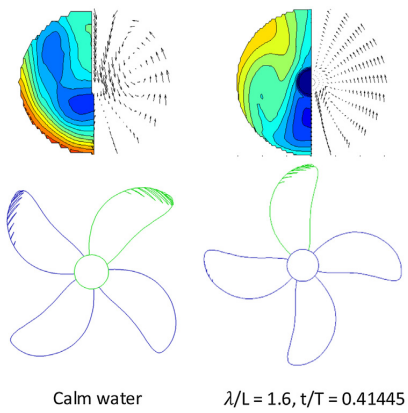

Fig. 6. Minimum suction side cavitation seen in the presence of wave among all three waves considering only wake change.

comparing the cavitation and pressure pulses using fixed cavitation number with that using varying cavitation number will show the effect of a change in cavitation number in waves.

As in the earlier case, the cavitating propeller has been presented at the angle and time instant of maximum cavitation in each wave

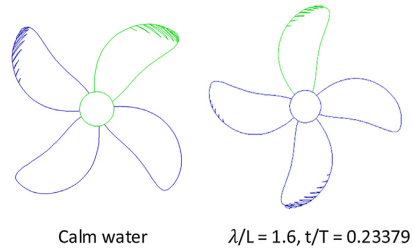

Fig. 8. Minimum suction side cavitation seen in the presence of wave among all three waves considering wake change, ship motions and dynamic wave pressure.

in Fig. 7. Comparing maximum cavitation in λ/L = 1.1 and 1.6 in Fig. 7 with Fig. 5, it seems that including the variation in cavitation number reduces the maximum volume of cavitation. This is because the variation in cavitation number is favourable for the instances of unfavorable wake variation. In other words, the worst possible wake in waves occurs at a cavitation number higher than that in calm water. Whereas, in λ/L = 0.6, the amount of cavitation is higher when the variation of cavitation number is taken into account. The amount of cavitation varies as the wave passes, the minimum cavitation among three wave conditions can be observed in Fig. 8. In this case, although the blade at 12 O'clock position shows minimum cavitation, blade at 6 O'clock position has higher cavitation. This

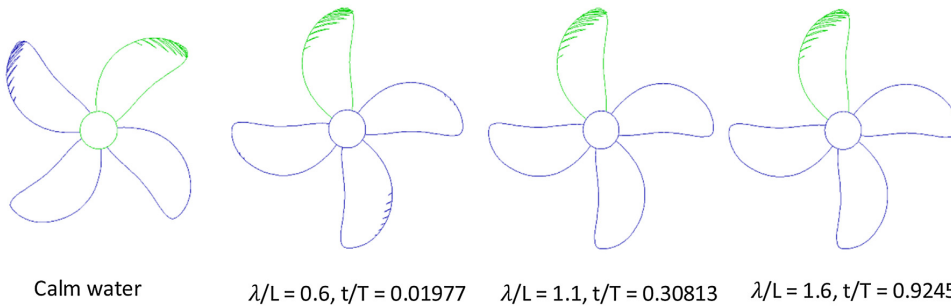

Fig. 7. Maximum suction side cavitation seen in each wave considering wake change, ship motions and dynamic wave pressure.

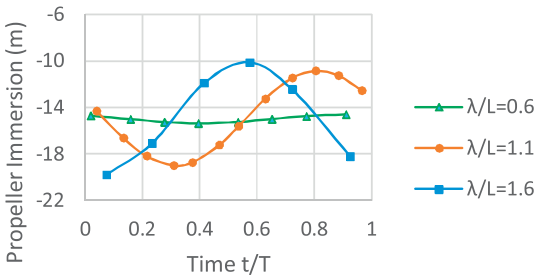

Fig. 9. Variation of propeller immersion in waves measured from calm water line (Propeller immersion in calm water is 15.1 m).

happens when the stern of the ship is moving up (note Fig. 9), causing low wake velocities in the lower part of propeller disc close to the centerline. Hence, propeller blade starts cavitating even when it is at 6 O'clock position.

To compare the cavitation in calm water with that in waves, it would be more appropriate to compare the time history of cavitation volume in calm water with that in waves. Therefore, cavitation volume on a single blade has been plotted as a function of blade position in the calm water and different times in each wave condition. Cavitation volumes with constant cavitation number have been presented in Figs. 10–12 and those considering the variation in cavitation number have been plotted in Figs. 13–15 .

First, coming to the computations at fixed cavitation number. In $\lambda/L = 0.6$, at all times, maximum cavitation is lower than the amount of cavitation in calm water. Whereas, in $\lambda/L = 1.1$ and $\lambda/L = 1.6$ maximum cavitation volume is as high as twice the amount of maximum cavitation in calm water. However, this happens only for one time instance. In most other cases, the amount of cavitation is either comparable or lower than the calm water cavitation. In cases $\lambda/L = 1.1$ and $\lambda/L = 1.6$ cavitation sometimes appears on the blade at 6 O'clock position which is not seen in the calm water and the $\lambda/L = 0.6$ case. In cases of $\lambda/L = 1.1$, $t/T = 0.46890$

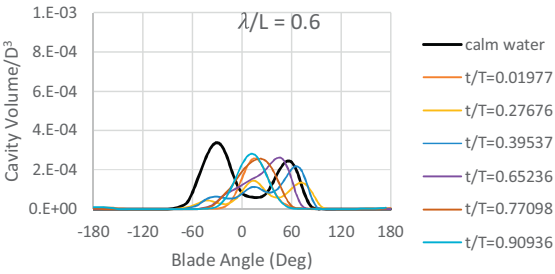

Fig. 10. Cavitation volume variation in $\lambda/L = 0.6$ at different times as wave passes considering only wake change.

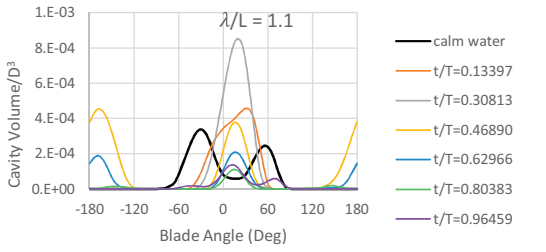

Fig. 11. Cavitation volume variation in $\lambda/L = 1.1$ at different times as wave passes considering only wake change.

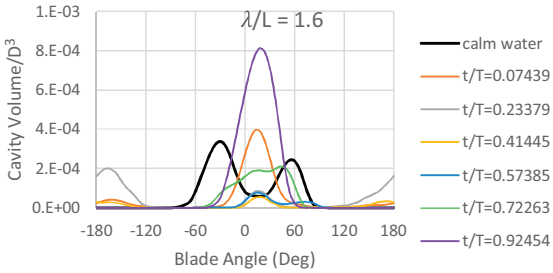

Fig. 12. Cavitation volume variation in $\lambda/L = 1.6$ at different times as wave passes, considering only wake change.

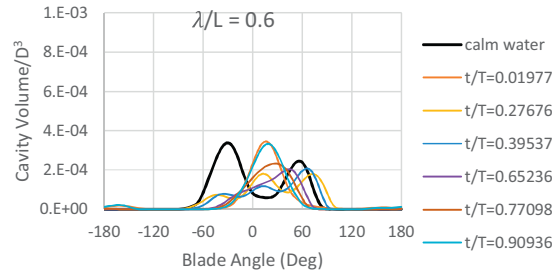

Fig. 13. Cavitation volume variation in $\lambda/L = 0.6$ at different times as wave passes, considering wake change, ship motions and dynamic wave pressure.

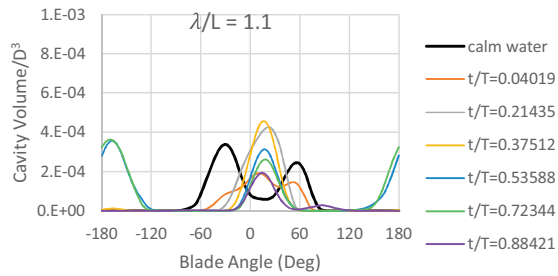

Fig. 14. Cavitation volume variation in $\lambda/L = 1.1$ at different times as wave passes, considering wake change, ship motions and dynamic wave pressure.

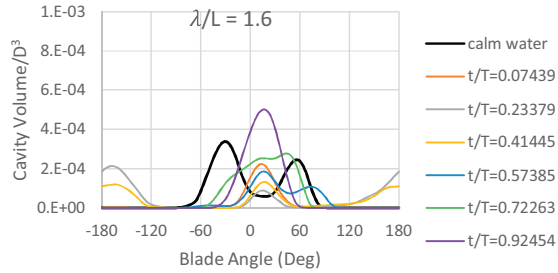

Fig. 15. Cavitation volume variation in $\lambda/L = 1.6$ at different times as wave passes, considering wake change, ship motions and dynamic wave pressure.

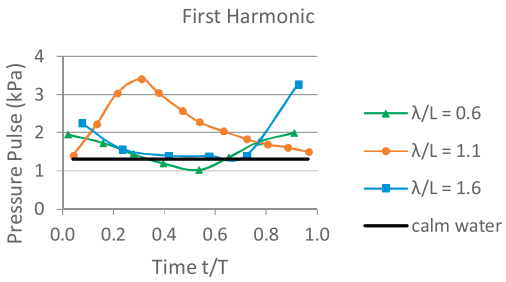

Fig. 16. First harmonic amplitude of pressure pulses in waves considering only wake change.

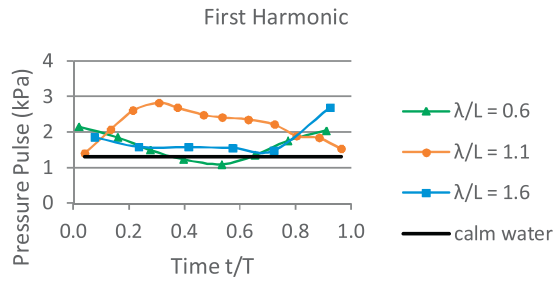

Fig. 19. First harmonic amplitude of pressure pulses in waves considering wake change, ship motions and wave dynamic pressure.

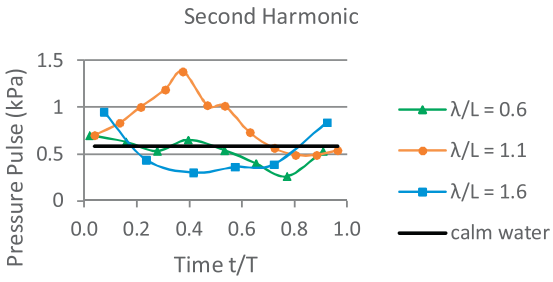

Fig. 17. Second harmonic amplitude of pressure pulses in waves considering only wake change.

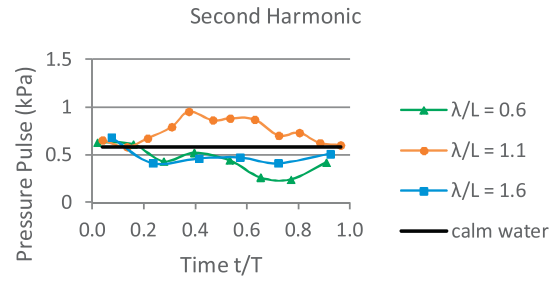

Fig. 20. Second harmonic amplitude of pressure pulses in waves considering wake change, ship motions and wave dynamic pressure.

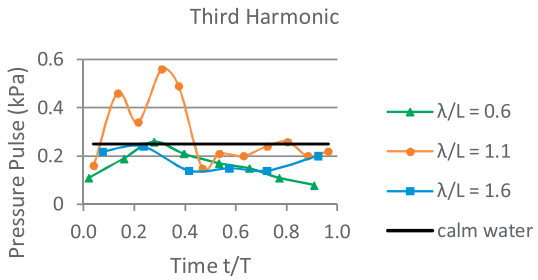

Fig. 18. Third harmonic amplitude of pressure pulses in waves considering only wake change.

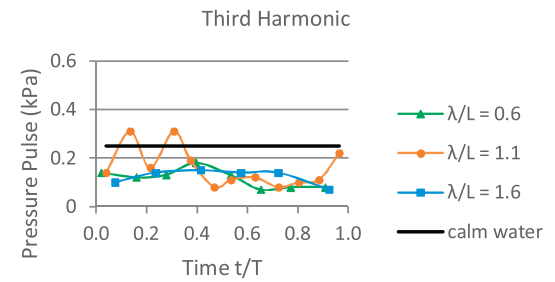

Fig. 21. Third harmonic amplitude of pressure pulses in waves considering wake change, ship motions and wave dynamic pressure.

and $\lambda/L = 1.6$, $t/T = 0.23379$, the volume of cavitation is higher at 6 O'clock position than at 12 O'clock position. These are the instances when the stern of the ship is moving upwards as noted earlier.

Cavity volume variation considering variation in cavitation number has been plotted in Figs. 13–15. Comparing these plots with Figs. 10–12, it can be observed that maximum cavitation volume is lower by about 45% in $\lambda/L = 1.1$ and by about 38% in $\lambda/L = 1.6$ when the effect of variation in cavitation number is included. Therefore, the change in cavitation number due to waves and ship motions seems to favor the propeller performance for these wavelengths. Whereas, for $\lambda/L = 0.6$, the maximum cavitation volume is 18% higher when the cavitation number variation is included. Considering all the factors affecting propeller in waves, only in a few time instances, the cavitation volume is larger than the maximum cavitation volume in calm water. Thus, waves do not significantly affect average cavitation volume.

In all the cases, the pattern of the cavity volume varies in a much different way than in the calm water case. In calm water, the cavity volume variation shows double peaks whereas, in the presence of waves, cavity volume has just a single maximum in most of the cases. This, as explained earlier, is due to low-speed area developed close to propeller centerline due to the motion of the stern. This behavior suggests that pressure pulses are affected by operation in waves as they primarily depend on cavity volume variation and distance to the hull. Therefore, it is important to see how pressure pulses are affected in the presence of waves.

Pressure pulses were analyzed in waves and in calm water using HULLFPP as already mentioned. Variation of the first, second and third harmonics in waves has been compared with those in calm water. Usually, the amplitude of the first harmonic i.e. pressure pulses of blade pass frequency is highest and most significant from the hull vibration point of view. Pressure pulses in calm water

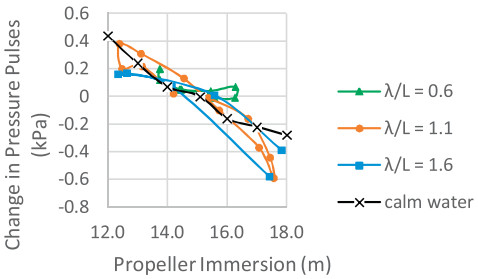

Fig. 22. Variation of pressure pulses with change in propeller immersion (Propeller immersion in calm water is 15.1 m).

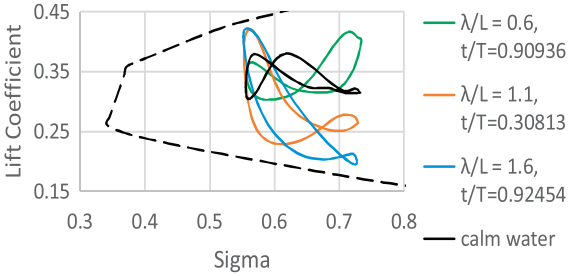

Fig. 23. Variation in lift coefficient of blade section at 0.7R at the instance of maximum cavitation in each wave considering only wake change.

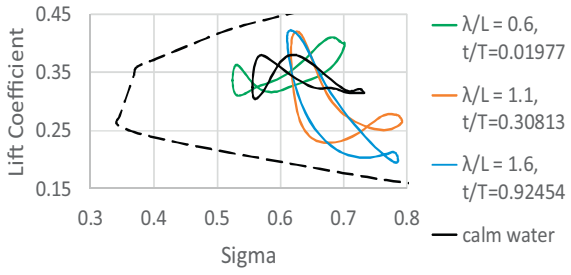

Fig. 24. Variation in lift coefficient of blade section at 0.7R at the instance of maximum cavitation in each wave considering wake change, ship motions and dynamic wave pressure.

and in waves considering constant cavitation number have been compared in Fig. 16. For λ/L = 1.1 and 1.6, the first harmonic of pressure pulses is higher than in calm water for almost all time instances. Maximum pressure pulses in these wave conditions are more than double of those in calm water. In the case of λ/L = 0.6, pressure pulses are higher than calm water for 50% of the time. Thus, it is clear that wake variation does significantly affect pressure pulses.

Coming to second and third harmonic of pressure pulses, they are considerably higher than calm water value only for λ/L = 1.1 as seen in Figs. 17 and 18. Moreover, for λ/L = 1.1 the maximum value of the second harmonic is close to the first harmonic amplitude of pressure pulses in calm water. For the other waves, the second and third harmonic pressure pulses are either comparable or lower than the calm water value.

In Figs. 19–21, pressure pulses considering the effect of wake variation, ship motions, and dynamic wave pressure have been plotted. In the case of waves with λ/L = 1.1 and 1.6 maximum values of first harmonic of pressure pulses is lower than that observed using wake change alone, which is in line with the change in cavitation volume as discussed above. However, pressure pulses in Fig. 19 are higher than that in Fig. 16 for approximately 50% of the times in all three waves. The maximum 0.4 kPa increase in the first harmonic of pressure pulses is observed due to the effect of variation in the cavitation number (in the case of λ/L = 1.6, t/T = 0.57385).

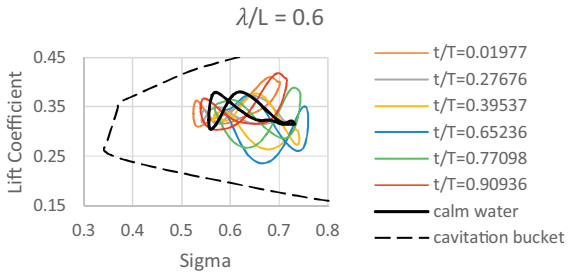

Fig. 25. Variation in lift coefficient of blade section at 0.7R at different times as wave passes in λ/L = 0.6 considering wake change, ship motions and dynamic wave pressure.

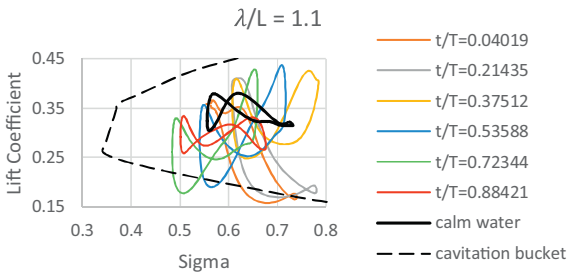

Fig. 26. Variation in lift coefficient of blade section at 0.7R at different times as wave passes in λ/L = 1.1 considering wake change, ship motions and dynamic wave pressure.

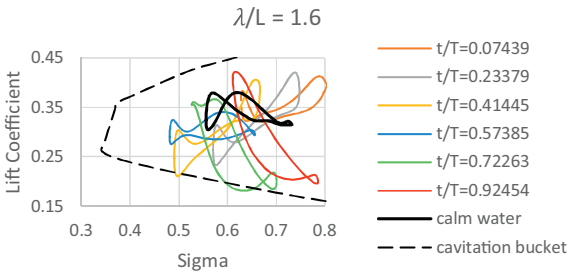

Fig. 27. Variation in lift coefficient of blade section at 0.7R at different times as wave passes in λ/L = 1.6 considering wake change, ship motions and dynamic wave pressure.

The second harmonic of the pressure pulses is higher than the calm water value only for λ/L = 1.1 while in other waves, it is lower than in calm water. For third harmonic, hardly any time instances show higher pressure pulses than calm water. Thus, considering first, second and third harmonic of pressure pulses in waves, wave condition λ/L = 1.1 seems critical for the analysis of propeller in the presence of waves.

To separate the effect of variation in cavitation number from the effect of wake change, change in the first harmonic of pressure pulses are plotted in Fig. 22 against equivalent propeller immersion. Change in pressure pulses has been calculated as the difference between the pressure pulses computed with fixed and with varying cavitation number i.e. difference between the level of pressure pulses in Figs. 16 and 19. The maximum increase of about 0.4 kPa is observed due to the effect of variation in cavitation number.

The propeller was analyzed in calm water wake at different immersions to compare the rate of change of pressure pulses with respect to propeller immersion in calm water with that in waves. From Fig. 22 it is seen that increase in pressure pulses due to change in propeller immersion is similar in calm water wake as well as in wake in the presence of waves. Therefore, possible increase in pressure pulses due to combined effect of waves and ship motions can be approximated by analyzing the propeller in calm water wake by varying the propeller immersion.

The lift coefficient obtained from MPUF-3A calculations has been plotted against cavitation number (sigma) for one full rotation of the blade section at 0.7R, thus forming a loop. Cavitation bucket obtained from Xfoil calculations has also been plotted for this propeller blade section. Operating loops in calm water as well as at the instant of maximum cavitation in each wavelength can be seen in Fig. 23 along with the cavitation bucket. Comparing the operating loops and Xfoil calculations with MPUF results, there is a slight discrepancy since calm water operating loop is well inside the cavitation bucket predicted by Xfoil hence the section at 0.7R should be free of any cavitation in calm water whereas MPUF computations show the presence of cavitation at that section. This can be due to calculations being for 2D flow in Xfoil and 3D flow in MPUF. Therefore, the cavitation bucket should only be considered for the approximate estimation of the cavitation-free zone. The aim of plotting the operating loops is to compare the variation in cavitation number and lift coefficient in different wakes.

In this case, the propeller depth was assumed constant, so the change in sigma is only due to change in instantaneous depth of the propeller blade as it rotates. Therefore, variation in sigma is similar in all the cases. However, the variation of lift coefficient changes drastically in the presence of waves, also the variation is much larger in λ/L = 1.1 and 1.6 than in calm water. Hence, if propeller sections are designed considering only the calm water wake, performance could become much worse in waves.

Similar Xfoil analysis considering the variation in cavitation number (due to varying propeller immersion) in addition to wake change (=angle of attack variation) at the instance of maximum cavitation has been presented in Fig. 24. Comparing it with Fig. 23, variation in sigma can be seen in addition to variation in lift coefficient. It can be observed that operating loops for wavelength ratios 1.1 and 1.6 have shifted towards higher sigma. This leads to a slight reduction in cavitation and pressure pulses (observed earlier) as cavitation bucket is slightly wider at higher sigma.

In addition to the instant of maximum cavitation, the behavior of operation loops should be examined at other time instances to know the behavior of the operating loop as the wave passes. Therefore, Xfoil analysis has been carried out at different time instances in each wave as seen in Figs. 25–27. Wake variation, as well as variation in propeller immersion, has been considered in this analysis.

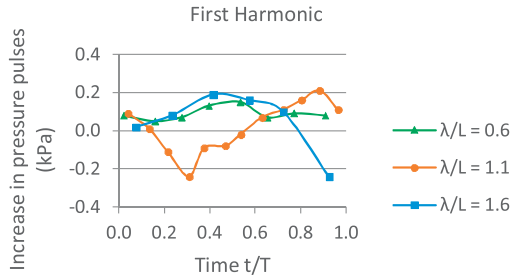

Fig. 28. Increase in pressure pulses as a result of increased load on the propeller caused by the added resistance.

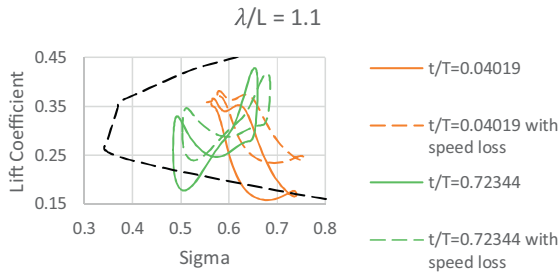

Fig. 29. Comparison of variation in lift coefficient of blade section at 0.7R with and without speed loss.

Comparing Fig. 24 with Fig. 26, it can be observed that the instance of maximum cavitation volume is not necessarily the worst condition for the propeller blade. Even though pressure side cavitation is not seen in the MPUF analysis at any time instance, Xfoil analysis tells us that the propeller operates very close to having pressure side sheet cavitation at some time-instances. (Cavitation bucket is only approximate as noted earlier. It has been provided as a reference to the comparison of different operating loops.) The maximum deviation from the calm water operating loop is seen in λ/L = 1.1. In this wave, maximum increase in suction side cavitation has been observed. Moreover, the propeller is more prone to pressure side cavitation as well as bubble cavitation at certain time instances in this wave as compared to calm water condition.

For the studied propeller, most of the operating points lie within the cavitation bucket, even in the presence of waves. This could be due to the general experience of the propeller designers about required margins for operation in waves and off design conditions, as they did not have the information about wake field in waves at the time of designing the propeller. However, there are no clear guidelines regarding cavitation margins to avoid performance drop in waves, and when designing another propeller for another ship, the resulting propeller performance in waves might be less favourable.

3.2. *Effect of increased loading*

Added resistance due to waves leads to increased propeller load. This is likely to increase the amount of cavitation on the propeller.

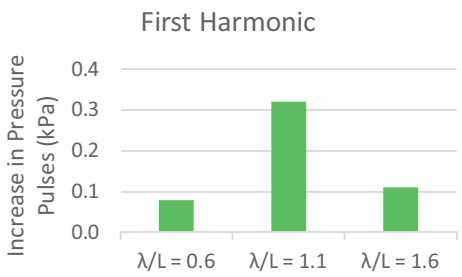

Fig. 30. Increase in pressure pulses due to RPM fluctuations in waves.

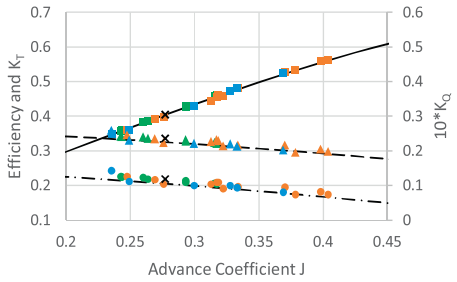

Fig. 33. Propeller efficiency, K_T and K_Q in the presence of waves along with propeller open water data. Propeller open-water efficiency, K_T and K_Q have been shown using solid, dash-dot and dashed lines respectively. Efficiency, K_T and K_Q in waves has been denoted by square, circle and triangle respectively. (λ/L = 0.6–Green; λ/L = 1.1–Orange; λ/L = 1.6–Blue). Performance in calm water wake has been denoted by cross mark.

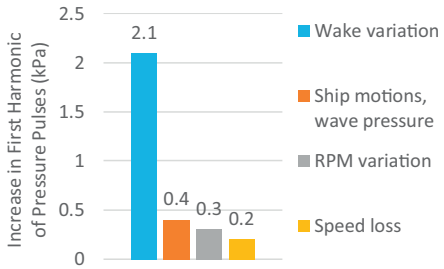

Fig. 31. Comparison of maximum increase in the first harmonic of pressure pulses due to different factors in the presence of waves.

Moreover, pressure pulses are likely to change if there is a significant variation in the cavitation pattern. Hence, the sensitivity of cavitation and pressure pulses towards the increased propeller loading has been studied.

As ship motions depend on ship speed, wake variation will also change for different ship speed. However, in the absence of wake data at reduced speed, wake variation at design speed has also been used at reduced ship speed. The ship speed has been calculated in irregular waves of peak frequency 0.090, 0.067 and 0.055 Hz, corresponding to λ/L = 0.6, 1.1 and 1.6 respectively with significant wave amplitude of 3m. Ship speed obtained using constant propeller RPM is 11.9, 11.3 and 11.6 knots for the three wave conditions. The propeller has been analyzed in each wave condition using the corresponding wake variation and ship speed. Propeller depth was assumed constant. The only difference between the computations in section 3.1 (with constant cavitation number) and these computations is the speed of the ship.

Increase in pressure pulses has been computed by comparing the pressure pulses in this analysis with those calculated considering wake change only (Fig. 16). As seen in Fig. 28, pressure pulses increased at maximum about 0.2 kPa due to increased load. The maximum cavitation volume increased by about 10%. However, in some cases, maximum cavitation volume and pressure pulses decreased even after increasing the propeller load. This was observed in the instances of wake variation that caused high pressure pulses (λ/L = 1.1, t/T = 0.30813and λ/L = 1.6, t/T = 0.92454). It was observed that the cavity is present for larger range of blade angles in the presence of speed loss or increased loading, but maximum cavitation volume is lower. However, decrease in the maximum cavitation volume is very small.

Variation in lift coefficient and cavitation number were also plotted to observe the effect of speed loss on operating loops. As seen in Fig. 29 operating loops shift towards higher lift coefficient due to speed loss, which is expected since blade angle of attack increases due to decreased advance coefficient of the propeller as the ship speed reduces. The increased angle of attack leads to higher propeller loading. Note that the increase in lift coefficient is greater for the points at lower lift coefficient. Also, the operating loops shift towards higher sigma as the ship speed is reduced. Therefore, due to speed loss, the probability of pressure side cavitation reduces. The presence of waves will often be accompanied by speed loss thus, lowering the risk of pressure side cavitation, which looks imminent in Fig. 26.

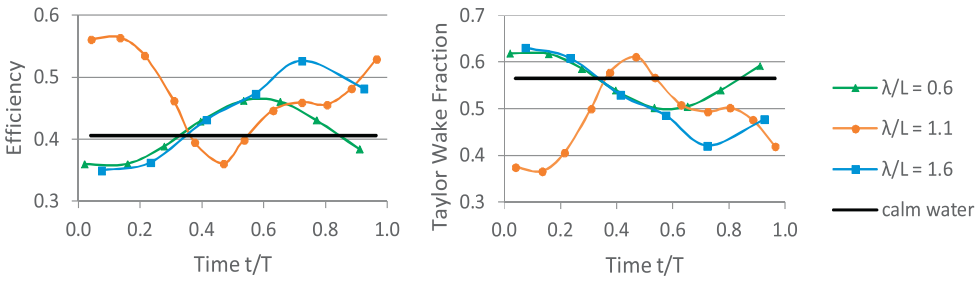

Fig. 32. Variation in efficiency and Taylor wake fraction at different times in the presence of waves considering only wake variation.

3.3. Effect of RPM fluctuations

As the ship travels in waves, wake fluctuates due to combined effect of waves and ship motions. This leads to varying propeller torque and therefore varying loads on the engine. Propeller RPM fluctuations depend on the engine control system, system inertia, and load variations. This RPM fluctuation might alter the cavitation pattern and pressure pulses. It was observed that RPM fluctuation is in phase with variation in the average wake. Whereas variation in pressure pulses is a function of wake distribution rather than the average wake.

RPM fluctuation was calculated using engine-propeller coupled simulations, as described in section 2.4. In the presence of waves, the propeller speed was seen to fluctuate between 74 to 78 RPM at a constant ship speed of 15.5 knots. The propeller has been analyzed at the instant of 78 RPM in the corresponding wake. The instances of maximum propeller speed occur at t/T = 0.39537, 0.46890 and 0.72263 in λ/L = 0.6, 1.1 and 1.6 respectively. Pressure pulses in these conditions were compared with those in the same instance of the wake but at 76 RPM, which is design RPM. About 0.3 kPa increase in the first harmonic of pressure pulses can be observed in Fig. 30. However, this increase is small as compared to increase in pressure pulses due to wake change in waves.

3.4. Summary of the factors affecting the pressure pulses in waves

The effect of wake change, ship motions, wave dynamic pressure, speed loss and RPM variation has been observed on cavitation and pressure pulses. All these effects have been considered in the presence of waves of 3 m wave amplitude to be able to compare the influence of these effects. Fig. 31 compares the maximum increase in the first harmonic of pressure pulse due to all four effects. The largest increase in pressure pulses is due to wake variation in waves. Effects of ship motions, RPM fluctuation, and speed loss are relatively small. Since wake variation is having a significant impact on the propeller performance, it should be taken into account while designing the propeller.

Also, note that considering the effect of wake variation in propeller design procedure is much more difficult than considering the effect of ship motions, added resistance and RPM fluctuations. Since obtaining reliable wake in waves is a challenging task in itself.

3.5. Efficiency variation in waves

As wake varies significantly in waves, propeller efficiency also varies with time. The propeller has been analyzed in different wakes in waves at design RPM, constant cavitation number, and design ship speed. Variation in propeller efficiency due to wake variation has been plotted in Fig. 32. When K_T, K_Q and efficiency in the presence of waves is plotted against the corresponding advance coefficients, data-points follow propeller open water curves as observed in Fig. 33. From this, we can conclude that the efficiency is primarily affected by the average change in wake fraction and not much by wake distribution. Whereas cavitation and pressure pulses are directly related to wake distribution, and they depend less on average wake at least in the vicinity of operating point, as we have argued earlier.

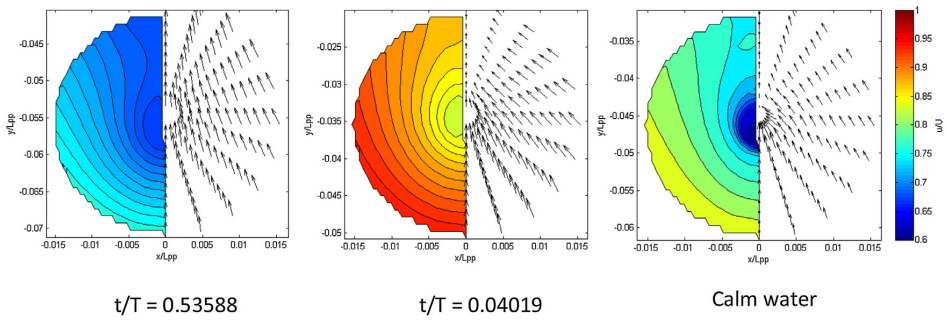

Fig. 34. Potential calm water wake and wake in λ/L = 1.1 at a couple of instances.

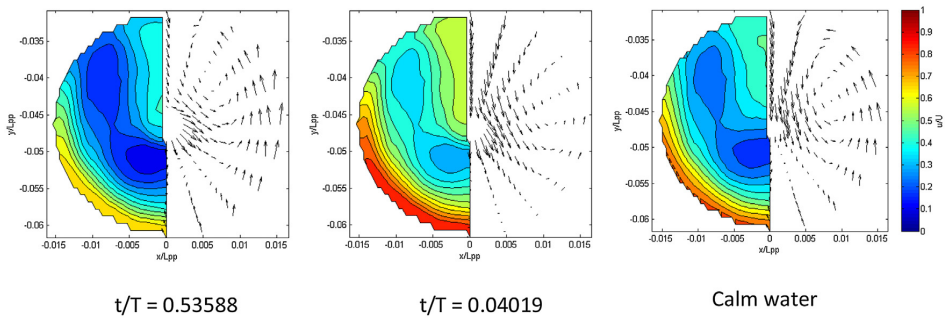

Fig. 35. Wakes in wave λ/L = 1.1 obtained using potential flow calculations at a couple of instances.

In addition to the wake variation in waves, wake fraction averaged over one wave encounter period is lower than the calm water Taylor wake fraction due to the pitching motion of ship leading to increased propeller inflow as described by Faltinsen et al. [23].

Since average wake is different in the presence of waves, this can affect the choice of optimum propeller diameter and RPM. Choosing the optimum diameter for the wake in waves can lead to better propeller efficiency in realistic operating condition rather than in calm water. Doing so, propeller efficiency may reduce in calm water but the vessel will perform better in waves. A further study is required to quantify total gain in efficiency considering different weather conditions.

3.6. Computation of wake in waves

From the presented analysis, it is evident that the propeller should be analyzed not just in calm water but also in waves. Moreover, propeller optimization should also consider the operation in realistic weather conditions, since calm water is rather an exception at sea. However, to achieve this, the first step would be to obtain the wake distribution in waves, as wake variation has more impact than the other effects of waves on the propeller. Currently, it is not a standard practice to obtain wake in waves. Thus, to analyze and optimize a propeller in the presence of waves, we need to have a tool or a method to calculate wake in waves.

The variation of spatially averaged wake in waves can be divided into two factors: (a) Mean change in wake due to pitching motion of ship, as explained by Faltinsen et al. [23] and (b) Wake fluctuation due to induced particle velocities caused by incoming waves and surge motion of ship, as discussed by Ueno et al. [24]. Both these factors are caused by potential effects. Therefore, although wake itself is a viscous phenomenon, wake change could be primarily due to potential effects. Chevalier and Kim [6], Jessup and Boswell [25] have studied cavitation of a propeller operating in waves by calculating wake velocities using potential flow calculations. Thus, we will proceed to check if potential flow calculations are suitable for finding the change in wake distribution due to waves for our current case vessel.

We checked if potential flow calculations can be used to estimate the change of wake distribution due to waves using the Shipflow software. First, the KVLCC2 hull was simulated in calm water to obtain the potential wake. The hull was then analyzed using Shipflow Motions to get the potential wake in waves. Potential wakes in calm water and in waves can be seen in Fig. 34. The potential calm water wake has been subtracted from the calm water wake distribution and potential wake in a particular wave has been added to it to get total wake in a wave. Wake distribution obtained using this procedure can be seen in Fig. 35 at a couple of instances in wave $\lambda/L = 1.1$. It can be observed that wake obtained using this method does not resemble the wake distribution obtained from CFD computations as seen in Fig. 1. One of the reasons is that the difference between potential wake in waves and in calm water is almost constant over the plane of propeller disc. Hence, wake variation obtained using this methodology adds or subtracts a constant value from the calm water wake. Therefore, contours of wake plots remain almost unaltered while just the level of contours changes.

Thus, it seems that viscous effects play a more significant role in wake variation than previously thought; partly due to the relatively high block coefficient of KVLCC2 hull. Therefore, any potential flow calculation method must be expected to fail to capture these effects, and therefore would fail to capture important wake features like wake peak. Hence, potential flow methods do not seem to be suited for calculation of the change of wake distribution due to waves, at least in the case of high block coefficient single-screw ships. However, it would be interesting to perform similar investigations for slender ships and twin-screw vessels.

4. Discussion

The analysis shows that the average amount of cavitation seen in the presence of waves is not significantly different from that in the calm water, even though the distribution of wake is very different. However, pressure pulses show a significant increase. Pressure pulses are proportional to the second derivative of the cavity volume. Therefore, higher cavity volume variations in the presence of waves lead to higher pressure pulses.

It was observed that average wake and wake distribution both change in the presence of waves. Little or no correlation is observed between the variation of Taylor wake fraction in Fig. 32 and the variation of pressure pulses in Fig. 16. Therefore, pressure pulses vary primarily due to change in wake distribution rather than variation in the average wake.

The Xfoil analysis gives a clear picture of worst possible operating conditions in waves. However, these conditions would vary depending on vessel design. Hence, instead of solely relying on the experience of propeller designers for the cavitation margins, it would be beneficial to have data of wake variation in at least one wavelength. Having wake data at least in one wavelength would be very useful, especially in the case of automated propeller optimization as described by Vesting [26], where the experience of the propeller designers is often missing.

In this study, the cavitation in different cases has been compared in terms of its volume. It is important also to look at the erosiveness of cavitation in waves compared to calm water. Since smaller volumes of cavitation can still be more erosive and therefore create more damage to the propeller.

Investigations in this paper are based on one hull and propeller design. We know that when it comes to propeller design and wake variation, each ship will have a different propeller and wake variation. Hence, in order to draw any generalized conclusions, more ships should be studied to check the general validity of our findings. Also, other wave conditions should also be analyzed e.g. irregular waves and following waves. Moreover, full-scale experimental measurements of pressure pulses in waves are required to confirm what is seen in the simulations, since there are complexities involved while going from model scale to full scale, like scale effects for wake variation and for the propeller itself. In spite of all this, the analysis in this paper strongly suggests that the conditions could become much worse in waves and much different from what is seen in calm water. When these conditions become clearer, it would be possible to extend the boundaries of propeller optimization by considering the conditions in the presence of waves.

5. Conclusions

The influence of operation in waves on the propeller performance, in terms of efficiency, cavitation extent and pressure pulses, has been investigated in this paper, using KVLCC2 as a case. The effect of wake change, ship motions, wave dynamic pressure, speed loss and RPM variation has been considered. It is found that the variation of wake distribution in waves has by far the largest impact on the propeller performance and the greatest change occurs for waves that have a length approximately equal to the ship length. However, getting wake data for operation in waves is hard. Also, the number of wake fields to be considered in a propeller design

must be very limited – current practice is to consider only the calm water wake field at the design speed. Thus, we recommend that the wake field in a regular wave of wavelength to ship length ratio $\lambda/L = 1.1$ is taken into account in the design, in addition to the calm water wake field. Knowing the wake distribution in worst intended operating condition can help us maximize the propeller efficiency while still avoiding the unwanted effects of cavitation and pressure pulses.

As our study has considered only one ship and propeller design, we recommend extending the study to more ship designs. Also, the effect of irregular waves and different wave headings on the wake distribution should be investigated.

Acknowledgements

The authors would like to thank Professor Frederick Stern from the University of Iowa for providing the wake data in waves used to analyze propeller in different conditions. We also thank Professor Bjørnar Pettersen for helping us obtain the wake data. This work is funded by the project 'Low Energy and Emission Design of Ships' (LEEDS, NFR 216432/O70) where the Research Council of Norway is the main sponsor. We are grateful to Rolls-Royce Hydrodynamic Research Centre along with the University Technology centers of Rolls Royce at NTNU and Chalmers University of Technology for their support. We would also like to show our gratitude to Professor Carl-Eric Janson from Chalmers University of Technology for helping us with the Shipflow computations.

Appendix A.

See Fig. A1 and A2.

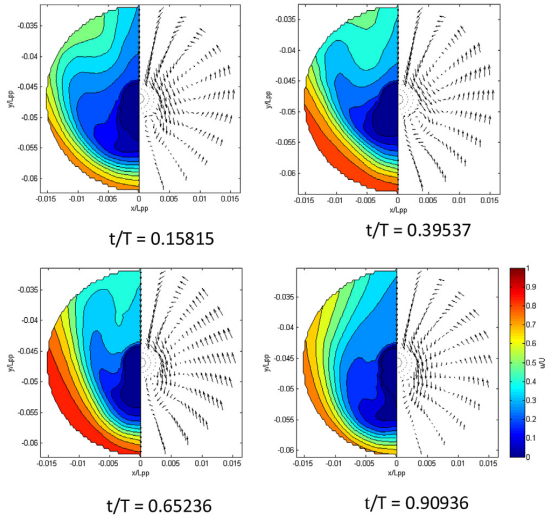

Fig. A1. Wake in the presence of wave having wavelength ratio $\lambda/L = 0.6$.

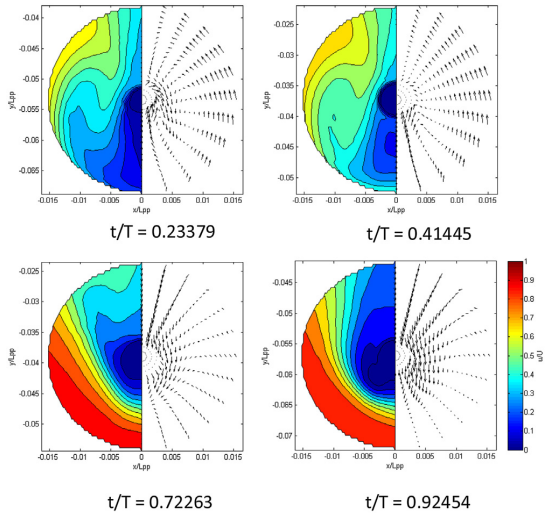

Fig. A2. Wake in the presence of wave having wavelength ratio $\lambda/L = 1.6$.

References

[1] D.I. Moor, D.C. Murdey, Motions and Propulsion of Single Screw Models in Head Seas, Part II, Trans. RINA 112 (1970) 121–164.
[2] S. Nakamura, S. Naito, Propulsive performance of a container ship in waves, J. Soc. Naval Archit. Jpn. (1975) 158.
[3] B.J. Guo, S. Steen, G.B. Deng, Seakeeping prediction of KVLCC2 in head waves with RANS, Appl. Ocean Res. 35 (2012) 56–67.
[4] Y. Hayashi, Phase-Averaged 3D PIV Flow Field Measurement for KVLCC2 Model in Waves: M. Sc Thesis (in Japanese), Osaka University, 2012.
[5] A.B. Albers, W.V. Gent, Unsteady wake velocities due to waves and motions measured on a ship model in head waves, 15th Symposium on Naval Hydrodynamics (1985).
[6] Y. Chevalier, Y.H. Kim, Propeller Operating in a Seaway. PRADS'95, Seoul, Korea, 1995.
[7] S.D. Jessup, H.-C. Wang, Propeller Cavitation Prediction for a Ship in a Seaway. DTIC Document, 1996.
[8] ABS Guidance notes on ship vibration. Houston, TX 77060 USA April 2006 (Updated January 2015).
[9] VERITEC, Vibration Control in Ships, A.S. Veritec Marine Technology Consultants, Noise and Vibration Group, Høvik, Norway, 1985.
[10] A.Y. Odabasi, P.A. Fitzsimmons, Alternative methods for wake quality assessment, Int. Shipbuild. Prog. 25 (1978) 8.
[11] E. Huse, Effect of Afterbody Forms and Afterbody Fins on the Wake Distribution of Single-Screw Ships, Ship Research Inst of Norway, 1974.
[12] H. Sadat-Hosseini, P.-C. Wu, P.M. Carrica, H. Kim, Y. Toda, F. Stern, CFD verification and validation of added resistance and motions of KVLCC2 with fixed and free surge in short and long head waves, Ocean Eng. 59 (2013) 240–273.
[13] L. He, Y. Tian, S.A. Kinnas, MPUF-3A(Version 3.1) User's Manual and Documentation 11-1. Ocean Engineering, University of Texas at Austin, 2011.
[14] SIMMAN, http://www.simman2008.dk/KVLCC/KVLCC2/kvlcc2_geometry.html, 2008 (accessed 14.04.16).
[15] M. Drela, H. Youngren, XFOIL 6.99 user guide, MIT Aero & Astro, 2013.
[16] Flowtech, SHIPFLOW 6.1, Users Manual. 2015.
[17] T.A. Loukakis, P.D. Sclavounos, Some extensions of the classical approach to strip theory of ship motions, including the calculation of mean added forces and moments, J. Ship Res. 22 (1978) 1–19.
[18] P.C. Wu, A CFD Study on Added Resistance, Motions and Phase Averaged Wake Fields of Full Form Ship Model in Head Waves, Osaka University, 2013.
[19] B. Taskar, K.K. Yum, S. Steen, E. Pedersen, The effect of waves on engine-propeller dynamics and propulsion performance of ships, Ocean Eng. 122 (2016) 262–277.

[20] B. Taskar, K.K. Yum, E. Pedersen, S. Steen, Dynamics of a marine propulsion system with a diesel engine and a propeller subject to waves, in: 34th International Conference on Ocean, Offshore and Arctic (OMAE), St. John's, Newfoundland, Canada, 2015.
[21] H. Sun, S.A. Kinnas, HULLFPP, Hull Field Point Potential, User's Manual and Documentation, University of Texas, Austin, 2007.
[22] K.O. Holden, O. Fagerjord, R. Frostad, Early design-stage approach to reducing hull surface forces due to propeller cavitation, Society of Naval Architects and Marine Engineers, No.14, 1980.
[23] O.M. Faltinsen, K.J. Minsaas, N. Liapis, S.O. Skjordal, Prediction of resistance and propulsion of a ship in a seaway, 13th Symposium on Naval Hydrodynamics (1980).
[24] M. Ueno, Y. Tsukada, K. Tanizawa, Estimation and prediction of effective inflow velocity to propeller in waves, J. Mar. Sci. Technol. 18 (2013)339–348.
[25] S.D. Jessup, R.J. Boswell, The Effects of Hull Pitching Motions and Waves on Periodic Propeller Blade Loads, David W. Taylor Naval Ship Research and Development Center, 1982.
[26] F. Vesting, Marine Propeller Optimisation – Strategy and Algorithm Development, Chalmers University of Technology, Göteborg, 2015.

Paper 5

Effect of waves on cavitation and pressure pulses of a tanker with twin podded propulsion

Bhushan Taskar, Sverre Steen, Jonas Eriksson

Accepted for publication in the

Journal of Applied Ocean Research

http://dx.doi.org/10.1016/j.apor.2017.04.005

Effect of waves on cavitation and pressure pulses of a tanker with twin podded propulsion

Bhushan Taskar[a], Sverre Steen[a], Jonas Eriksson[b]

[a] Department of Marine Technology, Norwegian University of Science and Technology (NTNU), Trondheim, Norway

[b] Rolls-Royce Marine AS, Norway

Corresponding Author: Bhushan Taskar (bhushan.taskar@ntnu.no, Tel: +47 47167689)

Abstract

There is increasing interest in optimizing ships for the actual operating condition rather than just for calm water. In order to optimize the propeller designs for operations in waves, it is essential to study how the propeller performance is affected by operation in waves. The effect of various factors that influence the propeller is quantified in this paper using a 8000 dwt chemical tanker equipped with twin-podded propulsion as a case vessel. Propeller performance in waves in terms of cavitation, pressure pulses, and efficiency is compared with the performance in calm water. The influence of wake variation, ship motions, RPM fluctuations and speed loss is studied. Substantial increase in cavitation and pressure pulses due to wake variation in the presence of waves is found. It is found that the effect of other factors is relatively small and easier to take into account as compared to wake variation. Therefore, considering the wake variation at least in the critical wave condition (where the wavelength is close to ship length) in addition to calm water wake is recommended in order to ensure that the optimized propeller performs well both in calm water and in waves.

Keywords: Propulsion in Waves, Cavitation, Pressure Pulses, Marine Propeller, Propeller Performance in Waves, Propeller Design, Twin podded propulsion.

List of Variables

A	Wave amplitude
Cp	Pressure coefficient
D	Propeller diameter
J	Advance coefficient
K_T	Thrust coefficient
K_Q	Torque coefficient
L	Ship Length
P_0	Atmospheric pressure
P_v	Vapour pressure of water
R	Propeller radius
T	Wave encounter period
dB	Sound level
g	Acceleration due to gravity
h	Depth of propeller shaft
k	Wave number
n	Propeller rps
t	Time
Γ	Blade tip circulation
σ	Cavitation number
η	Total propeller efficiency
$\eta 0$	Openwater efficiency
ρ	Water density
λ	Wavelength

1. Introduction

Currently, there is growing demand in the industry to optimize ships for actual operating conditions rather than calm water conditions due to environmental concerns and the competition in the shipbuilding industry. Propeller designs, which are traditionally optimized in calm water, should be revisited to explore the possibility of performance improvement by optimizing them for operating in waves.

Propellers are usually designed using wake field and propulsion factors obtained in calm water condition. However, Moor *et al.* [1] found that the propulsion factors change in the presence of waves, a finding supported by many other studies[2-5]. Nakamura *et al.* [2] demonstrated that wake increases in the presence of waves due to pitching motion of the ship. Similar results, confirming substantial wake variation in waves were obtained in the RANS simulation carried out by Guo et al. [3]. Hayashi [6] observed the strong variation of wake in three different head waves using a model of KVLCC2 ship through PIV measurements. Chevalier *et al.* [7], Jessup *et al.* [8] studied the effect of waves on the cavitation inception of propeller operating in a seaway. A drop in the cavitation inception speed of the vessel was observed in the presence of waves.

Due to increasing demand for efficiency, it is no longer common to design propellers completely without cavitation. While allowing some cavitation to increase the efficiency, one should carefully avoid the detrimental effects of cavitation i.e. excessive pressure pulses and erosion. Pressure pulses generated due to cavitation can cause vibrations in the ship structure, thus affecting passenger comfort and in severe cases damage the hull structure. In merchant ships, bearing forces cause about 10% of propeller-induced vibration velocities, whereas pressure fluctuations or hull surface forces are responsible for approximately 90% of the vibrations [9]. Out of 47 ships surveyed for vibration problems, high pressure pulses were the source of the vibration problem in 80% of the cases. Cracks were also reported in the aft peak of 20 ships, which correlated with the amplitude of pressure pulses at blade pass frequency [10].

Propellers are normally wake adapted to achieve high efficiency while limiting the level of pressure pulses. Since it is found that operation in waves has a strong influence on the wake field [2-4], the performance of the propeller in the presence of waves should also be considered in the design process. Taskar *et al.* [11] performed one such investigation using KVLCC2 as a case vessel to study the effect of waves on cavitation and pressure pulses. Wake variations in three different head waves were considered for the analysis and a considerable increase in pressure pulses was observed in the presence of waves. Among various factors studied, wake variation had by far the largest influence on

the pressure pulses. The study reports the need to analyze different types of ships to draw more generalized conclusions about the importance of waves. For single screw ships with high block coefficient like KVLCC2, the wake is considerably affected by the presence of hull, while for twin-screw or twin podded vessels wake is less disturbed by the hull. Thus, it can be expected that the effect of waves on wake distribution will be less pronounced in these cases. Therefore, to check the extent to which twin podded propulsion gets affected by waves, an 8000 dwt chemical tanker with twin Azipull thrusters was chosen for this study.

Considering that the lowering of pressure pulses comes at the expense of efficiency, accurate estimation of pressure pulses in realistic operating conditions can help in maximizing the propeller efficiency while still keeping pressure pulses within acceptable limits also when operating in waves.

Effect of various factors affecting propeller performance in waves like wake change, ship motions, wave dynamic pressure, added resistance and RPM fluctuation is studied. Cavitation and pressure pulses are calculated in different wave conditions and compared with the cavitation and pressure pulses in calm water wake.

2. Methods and validation

2.1. Propeller Analysis Tools

The propeller design software PropCalc, used by Rolls-Royce, has been utilized. The propeller analysis in PropCalc is performed by the software MPuF-3A, which is based on vortex lattice theory [12]. Details about the propeller geometry are given in Table 1. The open-water thrust, torque, and efficiency obtained from MPuF-3A computations is compared with the data from the propeller open water tests, which were carried out in the towing tank of MARINTEK using a model propeller of diameter 199.15 mm. The comparison can be seen in Figure 1. There is a slight discrepancy in the thrust and torque coefficients at lower J values, which could be due to the well-known limitations of potential theory based calculations at high angles of attack. In addition, the pod was located downstream of the propeller in the experiments whilst the presence of pod is not included in MPuF calculations.

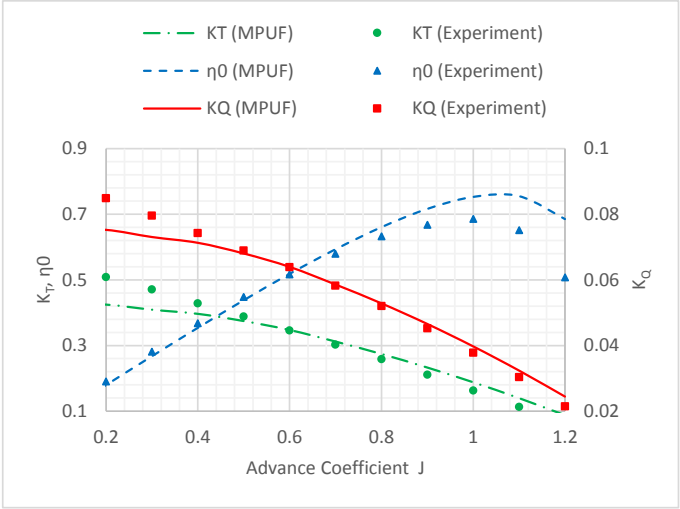

Figure 1 Comparison of MPuF-3A simulations with the experimental data for open water condition.

Table 1 Propeller Geometry

Diameter (D) (m)	3.3
No of blades	4
Hub diameter (m)	0.89
Rotational speed (RPM)	166
A_e/A_0	0.435
$(P/D)_{0.7}$	1.2
Skew (°)	18.6
Rake (°)	-10

2.2. Wake Data in the presence of Waves

The wake is normally determined only for the calm water condition; therefore, availability of wake data in waves is the major hurdle in analyzing the propeller in the presence of waves. Experimentally obtaining the model wake data in waves would need specialized equipment like PIV (Particle Image Velocimetry) in the towing tank. CFD simulations in the presence of waves are also computationally expensive. However, with increasing hardware capacity and software developments, such calculations are becoming increasingly viable. Results from the Tokyo workshop [13] show that reliable results can be achieved for ship motions in the presence of waves using different CFD software. Note that for the ship, propelled by twin pods, the flow around the hull is expected to be

less complex than with single screw ships where accurate predictions of, for example, bilge vortices are difficult. Therefore, the wake field, in this case, is also expected to be less demanding to predict compared with single screw ships.

Wake scaling issues can be avoided by simulating the full-scale ship in waves, which is certainly an advantage over model tests. Therefore, we decided to simulate the 8000 dwt chemical tanker in the presence of three different head waves at full-scale Reynolds number. Wavelengths were chosen such that different parts of the pitch RAO (response amplitude operator) can be covered, as wake is substantially affected by ship motions [11]. Simulations were performed at the design speed of the ship, which is 14 knots. The propeller was not included in the simulations, so only the nominal wake field was obtained. However, the pod was considered as a part of ship geometry and included in the computations, so that the effect of the pod on the wake variation was included. The ship main particulars are found in Table 2. The three different simulated conditions are specified in Table 3.

Table 2 Ship Particulars

Length between perpendiculars (m)	113.2
Length at water line (m)	117.2
Length overall (m)	118.3
Breadth at water line (m)	19
Depth (m)	15
Draft (m)	7.2
Displacement (m^3)	11546
Block coefficient (C_B)	0.7456
Design Speed (knots)	14

Table 3 Simulations Conditions

Ship speed [knot]	Froude number [-]	Wave amplitude [m]	λ/ L [-]	Encounter period [sec]
		1.53	0.6	7.55
14	0.212	1.28	1.1	5.89
		1.23	1.6	3.88

CFD modeling

Hydrodynamic ship simulations in waves with effect of viscosity included is not yet common practice at the design stage, since the viscosity is considered unimportant for ship motions in waves and because it is considered too computationally demanding and time-consuming to apply these methods to a time constrained design loop. In this case, the aim of the simulations was primarily to obtain wake change in the presence of waves, in which case the effect of viscosity is essential.

All simulations were performed in full scale using an Unsteady Reynolds Averaged Navier-Stokes, URANS, solver Star-CCM+, where the SST k-ω model was used for turbulence closure. An all-y+ wall treatment function was assigned to deal with the near-wall flow. The y+-target was of the order of 50-80. A Volume of Fluid, VOF, multiphase model was employed to calculate the flow motion in the two fluid phases, air and sea water. The waves were generated with a 5^{th} order approximation to the Stokes theory of waves. The response and motion of the ship in waves was managed by a Dynamic Fluid Body Interaction, DFBI, model. The motion of the ship was constrained to two degrees of freedom, heave and pitch. As for domain size, it is preferable to use as small domain as possible to minimize the cell count. However, it is also important to make sure that the boundaries of the domain are not so close that they can reflect back non-physical waves into the domain. According to [11], it is recommended that the inlet boundary should be located 1-2 ship lengths upstream of the hull and outlet boundary should be 3-5 ship lengths downstream to avoid any reflections from the boundary walls. Domain size used for the simulations can be seen in Figure 2. The computational domain was discretized by a predominantly hexahedral mesh with anisotropic mesh refinement. 80 cells per wavelength and 20 per wave amplitude resolve the wave zone. An overset mesh domain handles the ship motion with respect to the mesh. Details about the cell count and the number of cells in the background and overset mesh can be seen in Table 4. Surface mesh on the hull in the bow and stern region can be seen in Figure 3 and Figure 4 respectively. Overset and background mesh in the domain can be seen in Figure 5 and Figure 6. A refinement to capture diverging waves can be observed in Figure 6.

Table 4 Cell count for simulations in waves (in Million)

λ/ L	Background	Overset	Total
0.6	34.4	9.7	44.1
1.1	32.0	14.9	46.9
1.6	20.6	19.8	40.4

In a zone at the exit of the domain, waves are numerically damped out to minimize reflections. All simulations were performed with half of the hull along with symmetry boundary condition on the vertical plane going through the center of the ship. No slip condition was applied on the surface of the hull. A pressure outlet was used on the downstream boundary. On the rest of the boundaries, a velocity inlet condition was applied. The time step for the solver is set so that it fulfills the criteria needed to transport the wave through the domain maintaining a sharp air-water interface. It was also necessary to limit the time step due to the motion of the ship, and in all cases this criterion was limiting the time step. 2nd order numerical schemes were used for all flow equations as well as for time discretization.

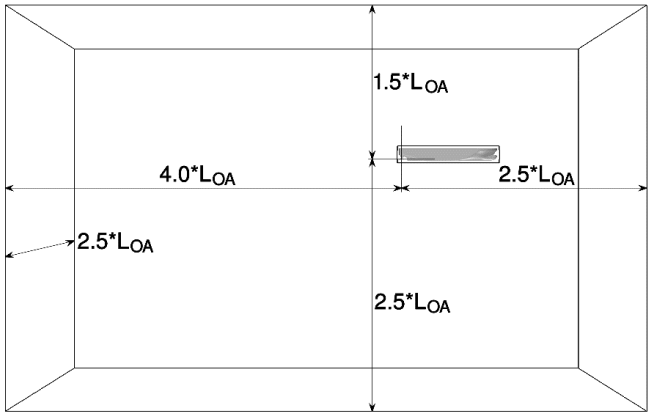

Figure 2 Simulation domain and boundaries.

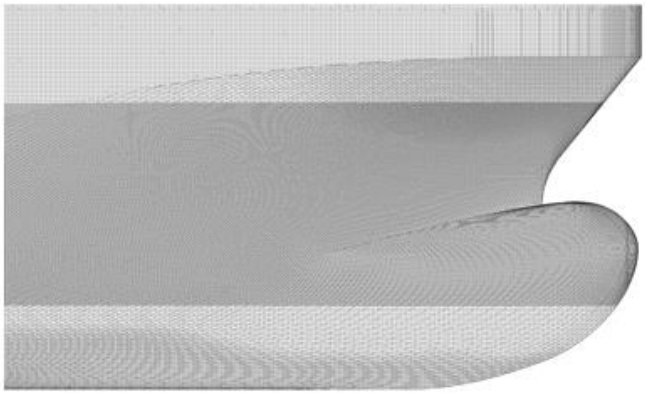

Figure 3 Surface mesh around bow region of the ship.

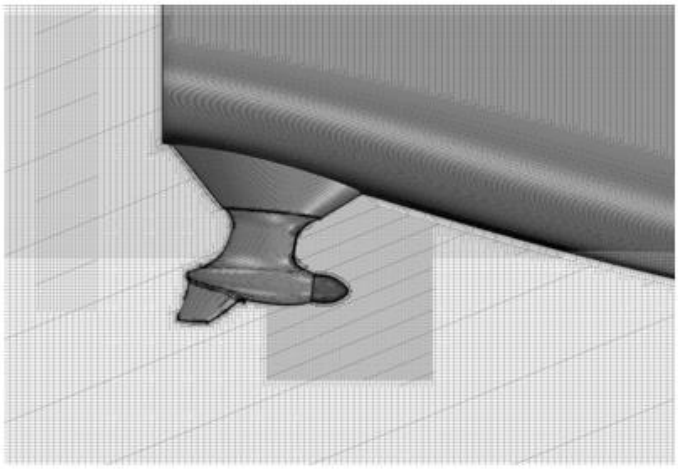

Figure 4 Surface mesh around the stern and pod of the ship.

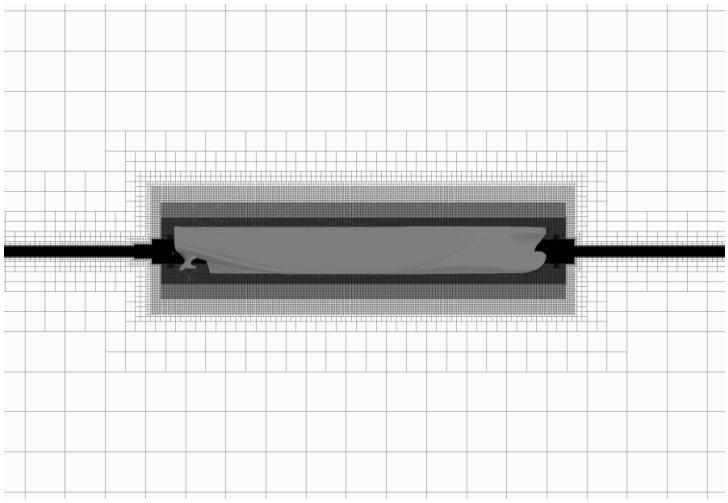

Figure 5 Vertical cross section of mesh in the simulation domain.

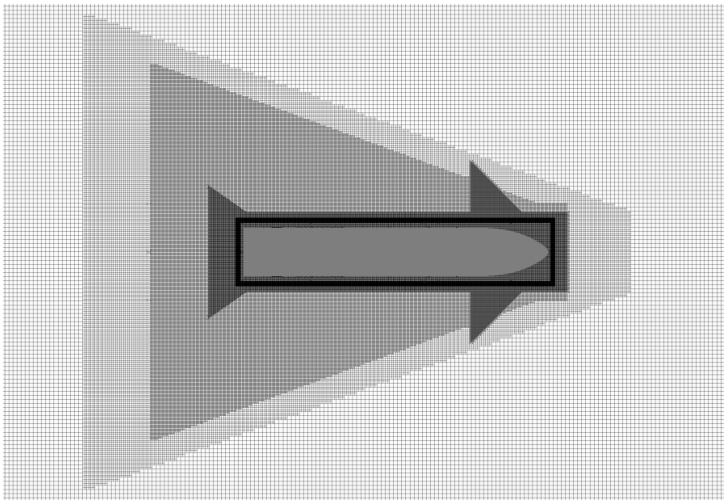

Figure 6 Horizontal cross section of mesh in the simulation domain.

Validation

CFD simulations were also run in calm water with the same mesh settings as in the presence of waves. Ship resistance, sinkage, and trim were compared with the experimental values from the model tests [14]. CFD computations show a good match with the full-scale predictions obtained using model tests.

Table 5 Comparison of results in calm water

	Experiment	CFD
Drag [kN]	207.05	210.8
Sinkage [m]	0.148	0.137
Trim [deg]	-0.23	-0.264

To validate the CFD computations in waves, ship motions obtained from the simulations were compared with motion RAOs (Response amplitude operators) obtained from potential flow calculations as well as available experimental results. Ship motion RAOs were calculated using linear strip theory, implemented in the ShipX Veres software [15]. Seakeeping tests were performed at MARINTEK [16] using the scaled model of 1:16.57. Heave and pitch were measured in the presence of waves corresponding to the full-scale wave amplitude of 1m. Comparison of heave and pitch motions, in terms of Response Amplitude Operators (RAO) obtained from CFD, ShipX Veres and experiments are presented in Figure 7 and Figure 8. Ship motions obtained from CFD simulations show a fairly good match with the experimental results and potential flow simulations. Propeller

ventilation due to limited submergence is a common problem for ships operating in high waves. In the current case, the calm water submergence ratio was h/R=3, where h is submergence of the propeller shaft and R is the propeller radius, while the minimum propeller submergence in waves was h/R=2. Therefore, propeller ventilation is not considered to be a problem here and not further considered in this study.

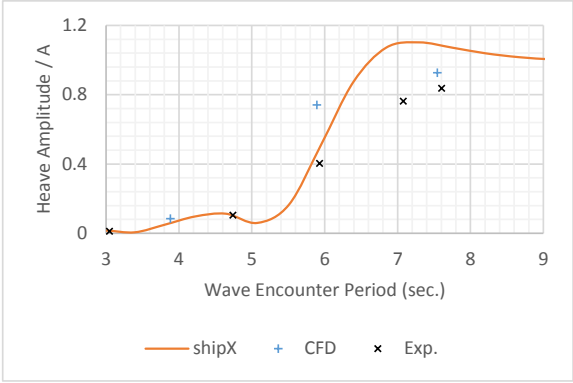

Figure 7 Comparison of heave motion response using CFD, experiments, and shipX calculations.

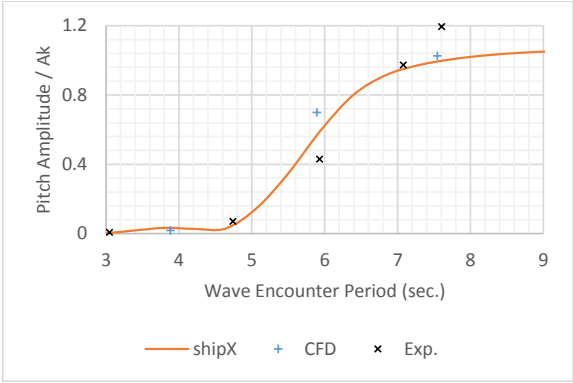

Figure 8 Comparison of pitch motion response using CFD, experiments, and ShipX calculations.

CFD Results

The aim of the CFD computations was to obtain the wake in the presence of waves. Wake data was extracted from the simulation after ship motions had stabilized in the computations. Wake data obtained in the presence of three different head waves are presented in Figure 9, Figure 10 and Figure 11. Even for the ship with twin azipull propulsion, where the effect of the hull on wake distribution is lower than that compared to the single screw ship, the presence of waves seems to have a significant impact.

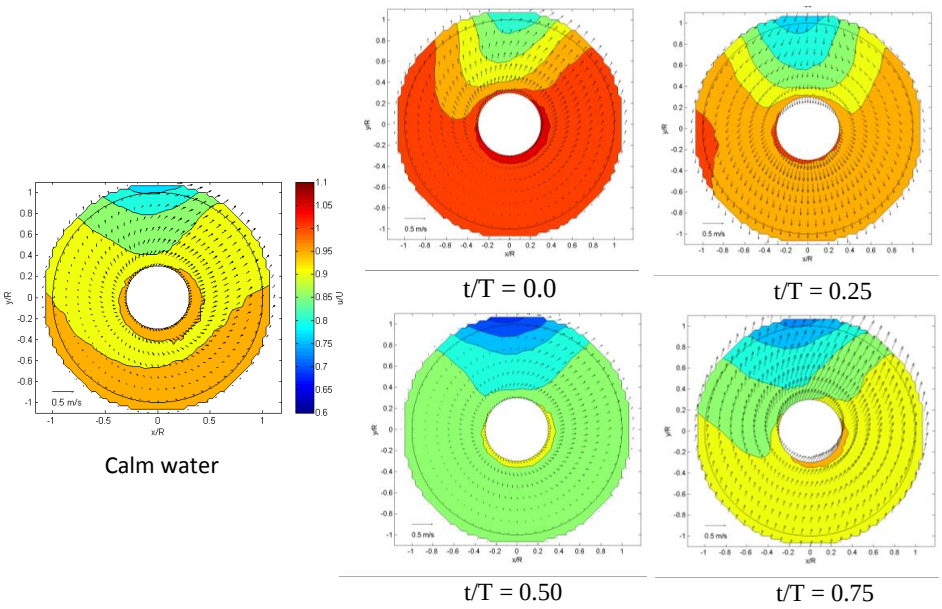

Figure 9 Wake in calm water compared to the wake in the presence of wave having wavelength ratio λ/L=1.6.

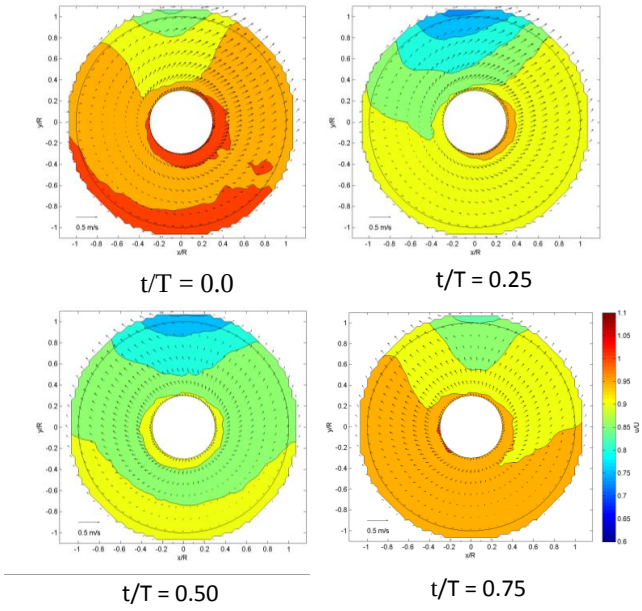

Figure 10 Wake in the presence of wave having wavelength ratio λ/L = 0.6.

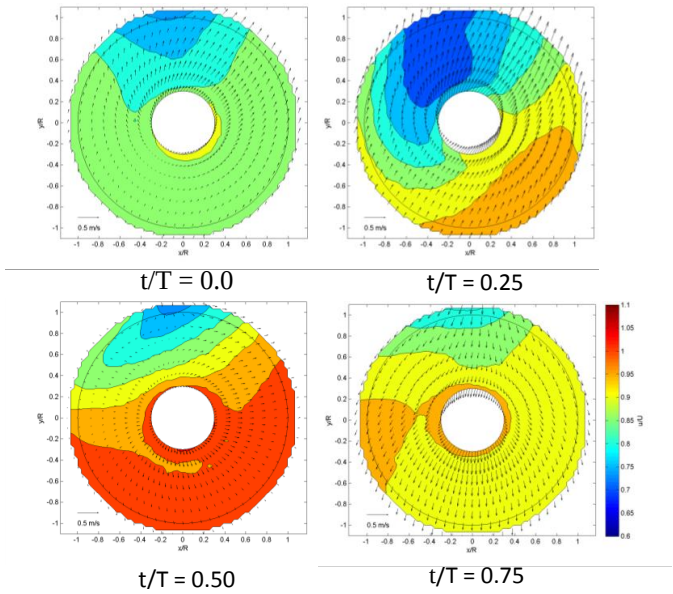

Figure 11 Wake in the presence of wave having wavelength ratio λ/L = 1.1.

2.3. Calculation of speed loss

Self-propulsion tests were performed at MARINTEK [16] for the case vessel considered in this paper. Speed loss was calculated in the presence of regular as well as irregular waves. Irregular waves were created using a JONSWAP spectrum with the value of the peakedness function (gamma) equal to 3.3. In the presence of irregular waves with significant waveheight 2m and peak period of 8.8 seconds, ship speed reduced by 1 knot at constant power setting. Speed loss was 3 knots for 4m significant waveheight and 11 seconds peak period. Since CFD simulations were performed at regular wave amplitudes ranging from 1.23m to 1.53m, it would have been appropriate to consider speed loss in the waves corresponding to 3m significant waveheight. In the absence of experimental data in this particular condition, propeller cavitation and pressure pulses were calculated at both 12 and 13 knots, which corresponds to 1 and 2 knots of speed loss. Irregular waves were considered for the calculation of speed loss to avoid getting unrealistically low ship speeds since added resistance in regular waves is often much larger than that in irregular waves.

2.4. Calculation of propeller RPM fluctuation

Engine load fluctuates due to time varying wake in waves, which leads to fluctuations in the engine RPM. The amount of fluctuation depends on the inertia of engine, propeller and shaft, control system and the wake variation [17]. In the absence of engine-propeller model for the propulsion system of this particular vessel, the amount of RPM fluctuation has to be approximated. This approximation is done by computing the change of torque due to the change of wake in waves, keeping RPM constant. Then, the change in RPM needed to produce the same change in torque is determined keeping wake constant.

In order to validate this methodology, the case of KVLCC2 was considered. Torque variations due to wake variation were taken from [18] to calculate RPM fluctuations using the method described above. Results were compared with RPM fluctuations calculated in [17] using engine-propeller coupled model. The above method predicts 4% fluctuations in RPM whereas fluctuations using engine-propeller coupled model are close to 3%. Thus, it is concluded that the approximate method to calculate RPM fluctuations used here gives slightly conservative results.

Applying this method to the current case vessel, propeller RPM was found to fluctuate by 2.4%, 4.2% and 3% in λ/L= 0.6, 1.1 and 1.6 respectively. Therefore, the propeller was analyzed at maximum RPMs i.e. 170, 173 and 170 RPM, which correspond to an instant of highest average wake velocity (at t/T=0, 0.51 and 0) in λ/L= 0.6, 1.1 and 1.6 respectively. Simulations reported in [17] show that the RPM fluctuates in phase with the average wake velocity meaning that RPM is largest when the average propeller inflow is largest. Although the current vessel and the propulsion system is much different from the one used by Taskar *et al.* [17], this conclusion can still be valid,since wake varies much slower than the propeller RPM. Hence the changes due to wake variation can be assumed to be quasi-steady from the propulsion system point of view.

2.5. Pressure Pulse calculation

Pressure pulses have been calculated using HullFPP [19]. The time history of cavity volume variation, obtained from unsteady propeller calculations in MPuF-3A, is used to derive field point potential induced by the cavitating propeller. The diffraction potential on the hull is solved using a potential theory based boundary element method to obtain the solid boundary factor. The fluctuating pressure on the hull is then determined by multiplying free-space pressures by the solid boundary factor. Pressure pulse calculations using HullFPP have been compared with experimental results by Hwang *et al.* [20]. In the current analysis, pressure pulses were computed on a flat plate at a distance of 30% of the propeller diameter from the blade tip.

2.6. Calculation of unsteady wave pressure

Ship motions affect the propeller submergence and therefore the hydrostatic pressure at the propeller, and passing waves can alter the ambient pressure around the propeller. Both effects influence the cavitation. The total pressure was calculated at the location of the propeller shaft, considering propeller submergence as well as dynamic wave pressure. Propeller submergence was calculated based on heave, pitch, and wave elevation. The phase of the passing wave was considered for the calculation of dynamic wave pressure. The total pressure thus obtained was converted to effective propeller immersion in calm water condition.

3. Analysis

The aim of this study is to find out the effect of waves on cavitation and pressure pulses due to waves and ship motions. Therefore, the effect of different factors affecting the propeller performance was studied. Variation in cavitation and pressure pulses was analyzed due to the influence of wake variation, ship motions, RPM fluctuations and speed loss due to added resistance. Each of these factors was separately studied to calculate their order of importance on the propeller performance so that the factors affecting the most can be taken into account while designing the propellers. The effect of each factor is studied in the following sections.

3.1. Effect of wake variation and change in cavitation number

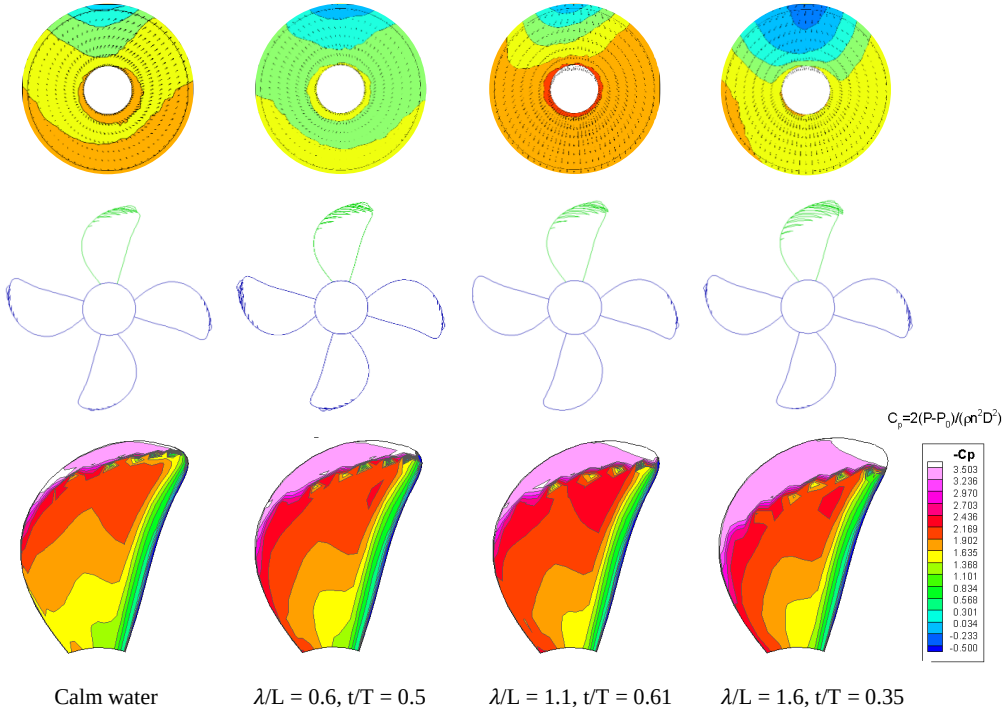

Figure 12 Maximum suction side cavitation seen in each wavelength considering only wake change compared to cavitation in calm water wake.

The propeller was analyzed in calm water and at different times in each wave condition. The wake was assumed quasi-steady for the analysis; since the frequency of propeller rotation is much larger than the encounter frequency of waves. In the analysis, propeller depth was kept constant even in the presence of waves to separately observe the effect of wake change.

Propeller cavitation and pressure distribution on the blade at 12 O'clock position is presented in Figure 12 at the instant of maximum cavitation in each wave condition. In all cases, the maximum cavitation is seen at 12 O'clock position of the propeller blade and it is larger than the cavitation in the calm water wake. This difference in the amount of cavitation is due to wake variation as wake varies considerably in waves. Among three wave conditions λ/L=1.6 causes a maximum increase in the amount of cavitation followed by λ/L=1.1 and 0.6 respectively. Also, note that in addition to the cavitation at 12 O'clock blade position, the cavitation volumes seen at other blade locations also vary substantially due to wake variation. Therefore, not just the volume but the pattern of cavitation volume variation with respect to the blade position gets affected due to wake change in waves.

Substantial variation in the pressure distribution on the propeller blade can be observed. Especially close to leading edge of the blade, -Cp is higher in waves than that in calm water wake.

The maximum cavitation occurs at a single instance in time. Therefore, to visualize the variation of cavitation patterns the propeller goes through in one wave encounter period, the minimum cavitation at 12 O'clock position in each case is shown in Figure 13. The minimum cavitation in λ/L=1.1 and 1.6 is comparable to the cavitation in calm water wake however in λ/L=0.6 it is lower that in calm water. Therefore, in λ/L=1.1 and 1.6 average cavitation on propeller blades over one wave encounter period is larger than the cavitation volume in calm water. Pressure distribution in calm water and λ/L=1.6 is almost identical. Whereas in λ/L=0.6 and 1.1, the distribution of -Cp is similar and less severe as compared to the calm water case.

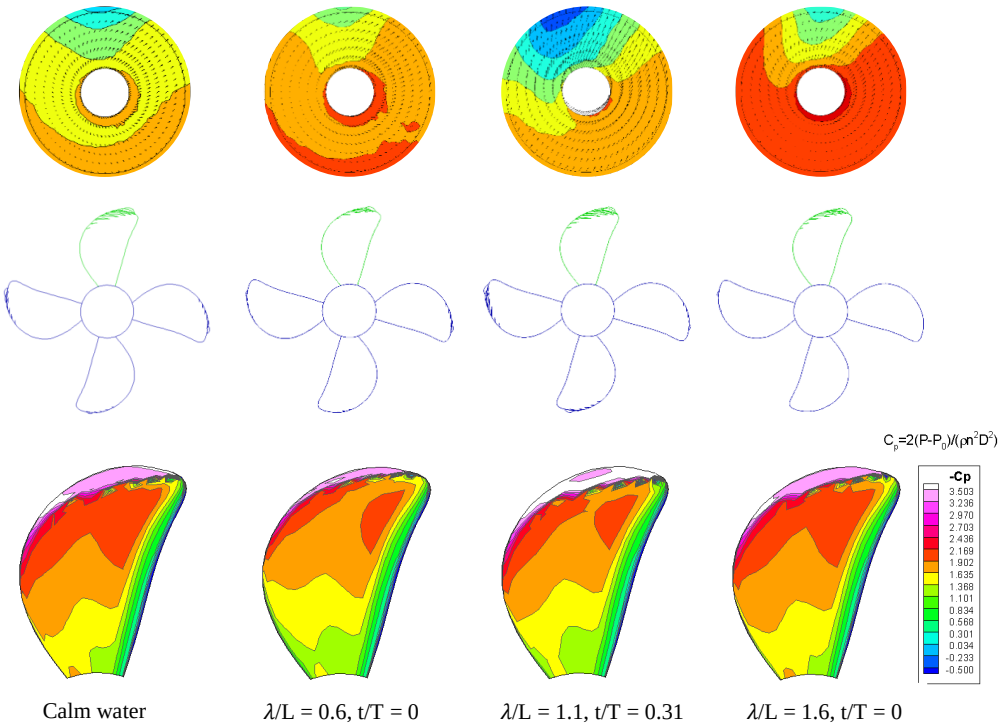

Figure 13 Minimum suction side cavitation seen in the presence of wave among all three waves considering only wake change.

In addition to the wake change, propeller immersion varies in waves due to ship motion, leading to a change in ambient pressure. Therefore, the propeller was analyzed in different wake fields taking into consideration the effect of ship motions and wave dynamic pressure by changing effective propeller immersion. Unlike in the earlier case, the cavitation number was varied along with the wake variation.

The maximum cavitation in each wave condition is shown in Figure 14. Comparing Figure 14 with Figure 12, the maximum cavitation decreases in λ/L=1.6. However, it increases in the other two cases. Therefore, in λ/L=1.6 the wake distribution corresponding to the maximum cavitation occurs at higher cavitation number due to the presence of waves whereas the opposite is true for λ/L=0.6 and 1.1. After considering the effect of varying propeller submergence, the maximum cavitation occurs at the same time instant in λ/L=1.1 and 1.6, while in λ/L=0.6 it is seen at a different time instant.

Cavitation number is defined as follows:

$$\sigma = \frac{P_0 + \rho g h - P_v}{0.5 \rho n^2 D^2}$$

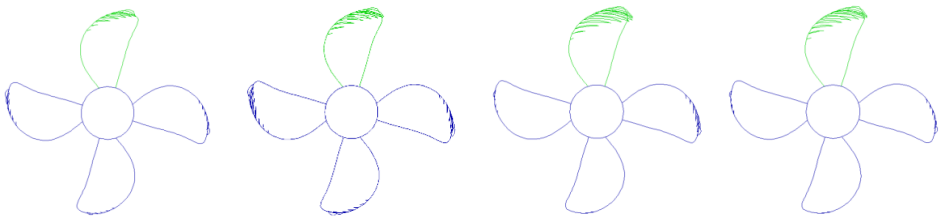

Figure 14 Maximum suction side cavitation seen in each wave considering wake change, ship motions, and dynamic wave pressure.

To study the variation of cavitation with respect to blade angle at different time instances, cavitation volumes have been plotted as function of blade angle in calm water and waves with and without varying the cavitation number. Cavity volume variations at fixed cavitation number in regular head waves λ/L=0.6, 1.1 and 1.6 can be seen in Figure 15, Figure 16 and Figure 17 respectively. In λ/L=0.6, the maximum cavitation volume is lower than that in calm water wake for most of the time. In λ/L=1.1 and 1.6, larger variations in cavity volume over a wave-passage, as well as cavity volume variation at different blade angles are found. In λ/L=1.6 cavity volume variations are far greater than for the other two cases. The maximum cavitation volumes in λ/L=0.6, 1.1 and 1.6 are higher than those in calm water by 28%, 68%, and 202% respectively. That means in λ/L=1.6, maximum cavitation volume reaches almost three times the cavitation volume seen in calm water wake. Additionally, in some of the cases, the cavity volume varies in a different way than in calm water wake (λ/L=1.1, t/T=0.1; λ/L=1.6, t/T=0.59). As the cavitation number has been kept constant in these simulations, the effect is only due to wake variation. Therefore, from the cavitation point of view, wake in wavelength λ/L=1.6 is most critical, followed by λ/L=1.1 and 0.6. Interestingly, heave and pitch

motions are largest in λ/L=1.6 followed by λ/L=1.1 and 0.6, which suggests that the ship motions are important for wake variations. The difference between thrust and torque coefficients considering cavitating and non-cavitating propeller calculations was insignificant in spite of large increase in cavity volumes. This means that even if cavity volumes increase significantly due to waves, they are not large enough to affect the thrust and torque.

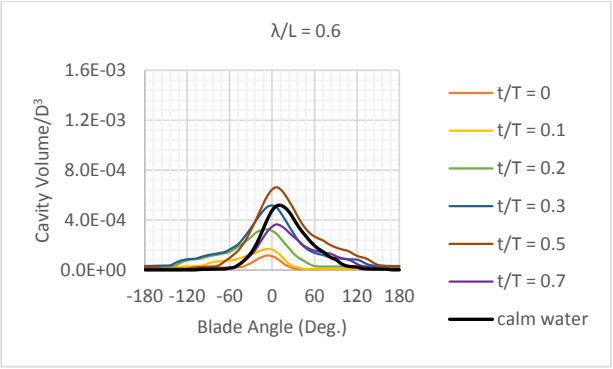

Figure 15 Cavity volume variation in λ/L = 0.6 at different times due to wake variation.

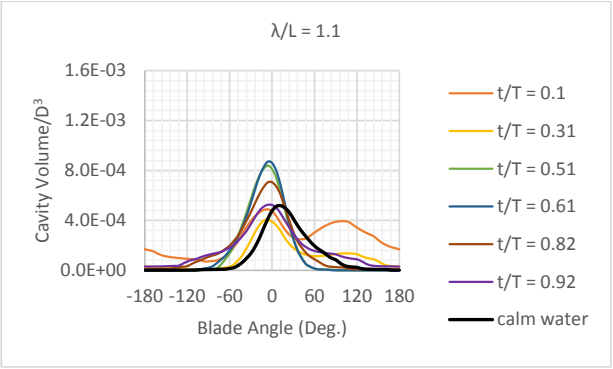

Figure 16 Cavity volume variation in λ/L = 1.1 at different times due to wake variation.

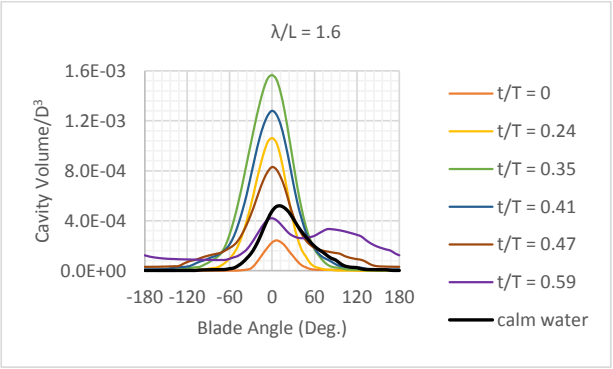

Figure 17 Cavity volume variation in λ/L = 1.6 at different times due to wake variation.

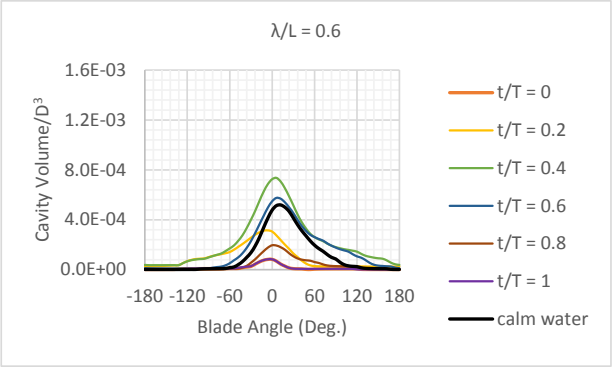

Figure 18 Cavity volume variation in λ/L = 0.6 at different times due to wake variation, ship motions and dynamic wave pressure.

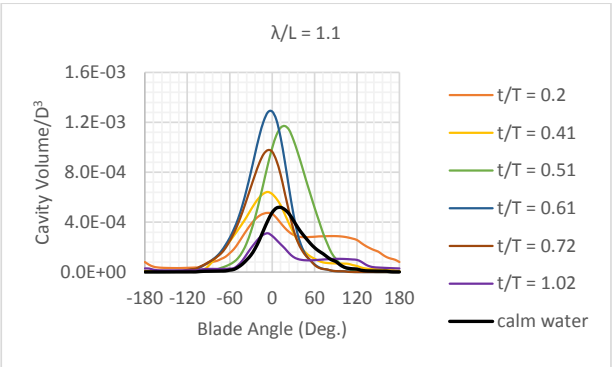

Figure 19 Cavity volume variation in λ/L = 1.1 at different times due to wake variation, ship motions and dynamic wave pressure.

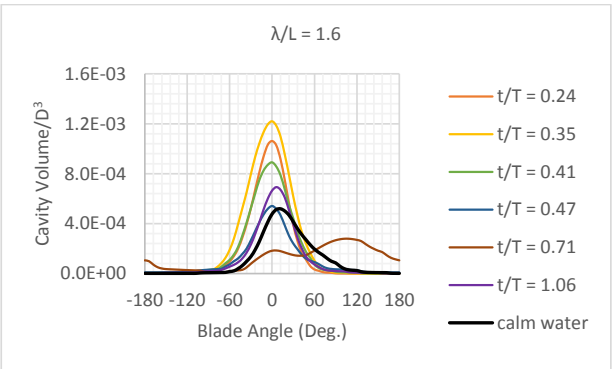

Figure 20 Cavity volume variation in λ/L = 1.6 at different times due to wake variation, ship motions and dynamic wave pressure.

Cavity volume variation considering also the effect of a change in cavitation number in addition to the wake change is plotted in Figure 18, Figure 19 and Figure 20 for λ/L=0.6, 1.1 and 1.6 respectively. Comparing Figure 15, Figure 16 and Figure 17 with Figure 18, Figure 19 and Figure 20 respectively, the maximum cavitation volume is higher in λ/L=0.6, 1.1 and lower in λ/L=1.6 when the cavitation number is varied along with the wake. After considering the effects of change in propeller immersion due to ship motions and wave dynamic pressure the maximum cavitation volume was higher than that in calm water by 42%, 148% and 135% in λ/L=0.6, 1.1 and 1.6 respectively. Therefore, λ/L=1.1 turns out to be the critical operating condition as far as the cavitation volume is concerned.

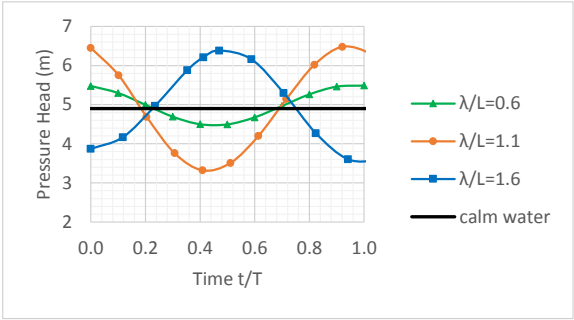

Figure 21 Variation in pressure head at the location of propeller shaft in the presence of waves.

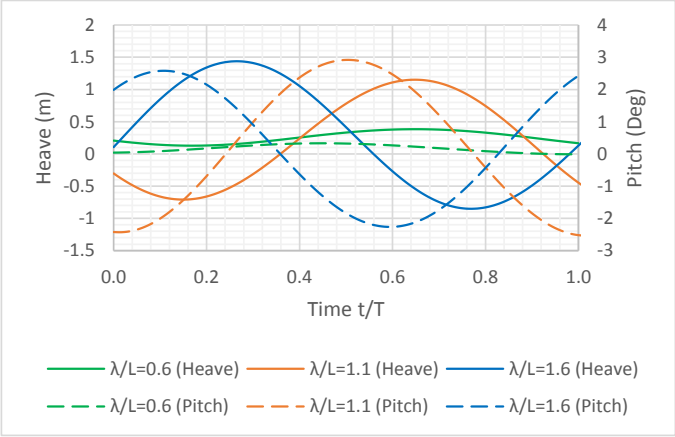

Figure 22 Phases of heave and pitch at different times in three waves (Heave: downwards is positive; Pitch: bow down is positive).

Wake distributions leading to high cavitation in λ/L=1.6 occur at higher propeller immersion whereas the opposite is true in the case of λ/L=1.1 (Figure 21).

Considerable cavity volume variation makes it necessary to investigate the level of pressure pulses in the presence of waves; since pressure pulses are proportional to the second derivative of cavity volume [21]. Pressure pulses were computed with and without considering the effect of a change in cavitation number due to ship motion and wave dynamic pressure. Pressure pulses in the first, second and third harmonic of blade pass frequency are plotted in Figure 23, Figure 24 and Figure 25 at fixed cavitation number. The first harmonic of blade pass frequency is usually the highest and the most important from the hull vibration point of view. All three harmonic amplitudes of pressure pulses are substantially higher in λ/L=1.1 and 1.6 as compared to pressure pulses in calm water wake. In these two wave conditions, pressure pulses are higher than calm water pressure pulses for most of the wave encounter period; in fact, the minimum pressure pulses are of similar magnitude as in calm water wake. This trend is consistent for all three harmonic amplitudes. Therefore, wake variation does significantly affect the propeller performance in the presence of waves.

Higher pressure pulses in λ/L=1.1 and 1.6 correspond to the increase of wake peak in the nominal wake. Especially, the magnitude of the wake peak with respect to average wake seems to play an important role; which is as per the expectations [22]. Nominal wakes at the instances of high pressure pulses are such that the blade at 12 O'clock position experiences higher load as compared to the other blades as observed in Figure 12. Interestingly, maximum pressure pulses in λ/L=1.1 and 1.6 correlate well with the phases of heave and pitch motions (from Figure 22 and Figure 23). Which means, in λ/L=1.1, maximum pressure pulses are seen close to t/T=0.6 and heave motion is also maximum around t/T=0.6. Similar is true for λ/L=1.6.

Only in the case of λ/L=0.6, alteration in the level of pressure pulses is relatively small; the magnitude of pressure pulses fluctuates around the value in calm water wake. The increase in the cavitation volume is also comparatively small in this case as seen earlier. Therefore, wake change in λ/L=0.6 has little effect on cavitation and pressure pulses.

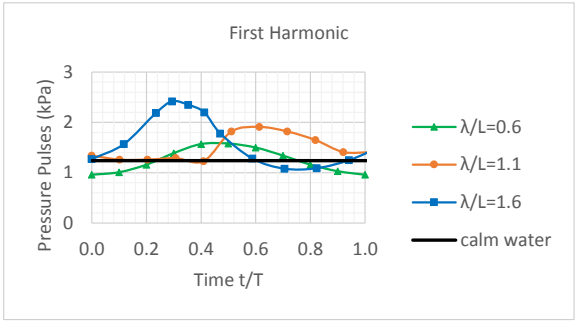

Figure 23 First harmonic amplitude of pressure pulses in waves considering wake variation.

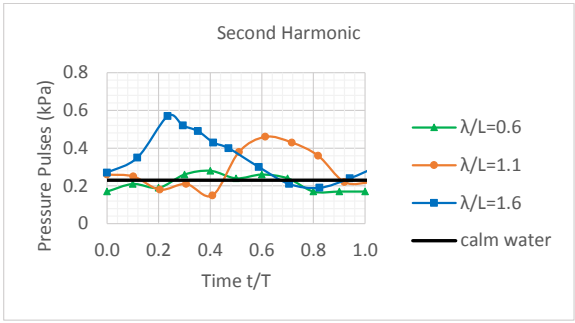

Figure 24 Second harmonic amplitude of pressure pulses in waves considering wake variation.

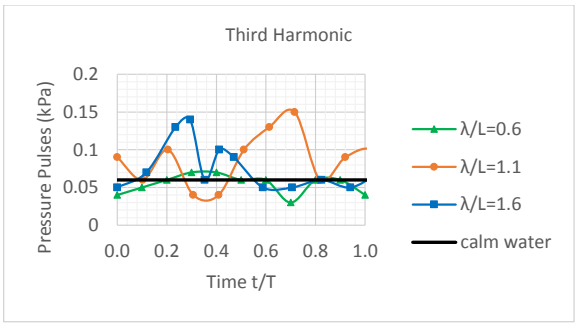

Figure 25 Third harmonic amplitude of pressure pulses in waves considering wake variation.

It is interesting to note that pressure pulses vary due to variation in wake distribution and not because of the change in average wake when ship motions are significant i.e. in λ/L = 1.1 and 1.6. Variation in Taylor wake fraction and variation of thrust and torque coefficient in the presence of waves are plotted in Figure 26 and Figure 27 respectively. Variation in Taylor wake fraction and pressure pulses is not synchronous except in the case of λ/L=0.6, where ship motions are much smaller than the other two cases, causing minor deviations in wake distribution. Therefore, in λ/L=0.6 the first harmonic of

pressure pulses vary due to average wake rather than wake distribution, since a clear correlation between wake fraction and first harmonic amplitude of pressure pulses is evident.

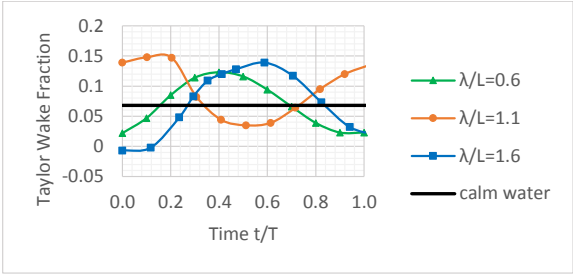

Figure 26 Average wake variation in waves.

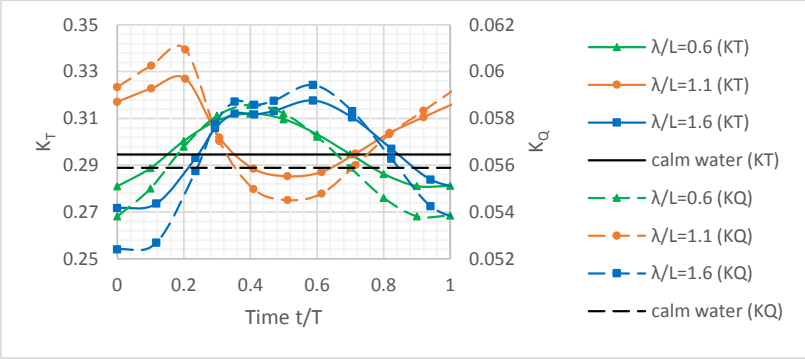

Figure 27 Variation of thrust and torque coefficient in the presence of waves due to wake variation

Pressure pulses considering the effect of a change in propeller immersion and the dynamic pressure due to wave are plotted in Figure 28, Figure 29 and Figure 30. As for cavitation volumes, maximum pressure pulses increase in λ/L=0.6 and 1.1 after including variation in cavitation number, whereas they decrease in the case of λ/L=1.6. Still, the level of pressure pulses is significantly larger than the calm water pressure pulses in all three harmonic amplitudes except in the case of λ/L=0.6.

Pressure pulses created in λ/L=1.1 and 1.6 are equally larger than that in calm water wake except in the case of third harmonic amplitude where pressure pulses are greater in λ/L=1.6. The first harmonic of pressure pulses in λ/L=0.6, 1.1 and 1.6 increase at maximum by 30%, 81%, and 77% respectively. Second and third harmonic amplitudes are notably higher than those in calm water wake. Therefore, the combined effect of wake variation and change in cavitation number has a noteworthy influence on the level of pressure pulses.

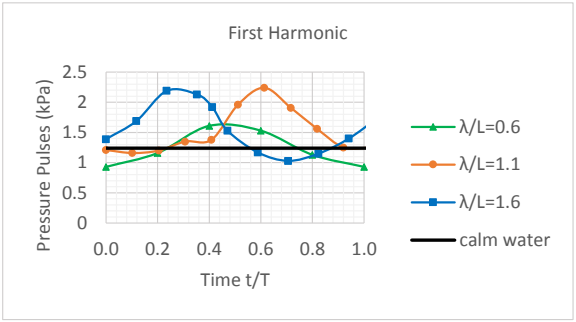

Figure 28 First harmonic amplitude of pressure pulses in waves considering wake variation, ship motions, and dynamic wave pressure.

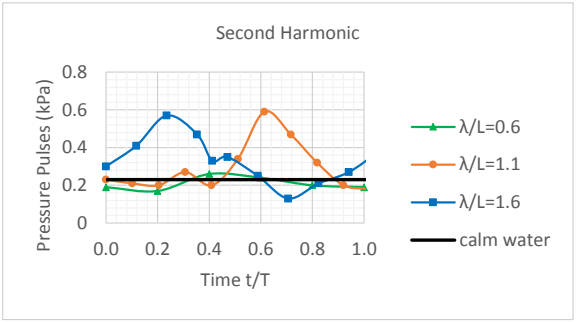

Figure 29 Second harmonic amplitude of pressure pulses in waves considering wake variation, ship motions, and dynamic wave pressure.

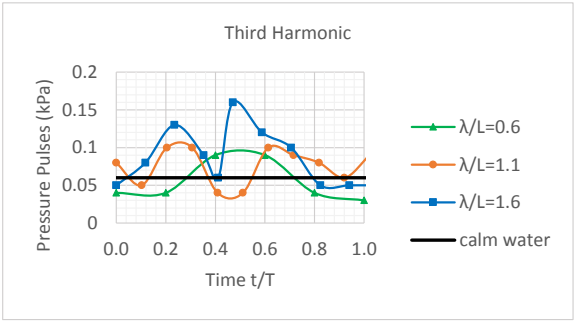

Figure 30 Third harmonic amplitude of pressure pulses in waves considering wake variation, ship motions, and dynamic wave pressure.

To separate the effect of the varying cavitation number, the difference in the level of pressure pulses in Figure 28 and Figure 23 is plotted in Figure 31 with the corresponding change in propeller depth. Pressure pulses are also computed at different propeller depths in calm water wake. Propeller immersion is the effective depth of the propeller shaft such that the variation of cavitation number

due to wave dynamic pressure is also taken into account. The rate of change of pressure pulses with respect to the propeller immersion is comparable in all cases. Calm water propeller immersion is 4.9m, which varies from 3.5m to 6.5m in the presence of waves, causing a corresponding change in pressure pulses ranging from 0.28 kPa to -0.28 kPa. Comparing Figure 31 with Figure 23 shows that the change in pressure pulses due to wake variation alone is much larger than the change of pressure pulses due to depth variation. Moreover, the effect of a change in propeller depth can be estimated by ship motions and the rate of change of pressure pulses by simulating the propeller in calm water wake at different immersions whereas considering the effect of wake variation is much more complicated.

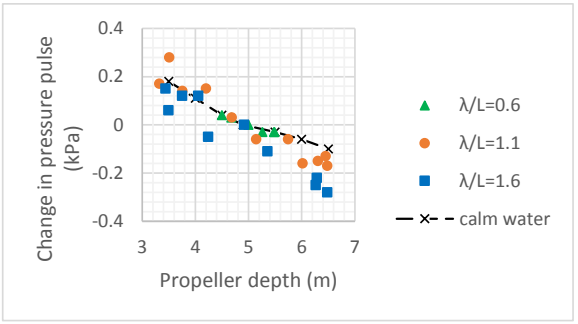

Figure 31 Variation in the first harmonic amplitude of pressure pulses due to change in effective propeller depth (Propeller immersion in calm water is 4.9m).

Pressure pulses of blade pass frequency and higher harmonics are often responsible for hull vibration and hull damage close to the propeller. However, noise created by the tip vortex has high frequency, and might cause inboard noise detrimental for crew and passenger comfort. Noise due to tip vortex can be estimated using the tip vortex index (TVI) defined by Raestad [23]. Since TVI is a function of tip circulation, circulation at blade section r/R=0.997 at 12 O'clock blade position is compared in the presence of waves at different time intervals. The variation in tip circulation can be seen in Figure 32, where a similar amount of increase in tip circulation is observed in λ/L=0.6 and 1.6 while in λ/L=1.1, the variation is rather small. The maximum tip circulation in in λ/L=0.6 and 1.6 is greater than that in calm water by 13% and 14% respectively. On average, tip circulation in these two conditions is larger than calm water tip circulation whereas it is lower in the case of λ/L=1.1. Interestingly, the trend in the variation of tip circulation is different from the trend seen in cavitation and pressure pulses where the changes in λ/L=1.1 and 1.6 were much larger as compared to λ/L=0.6.

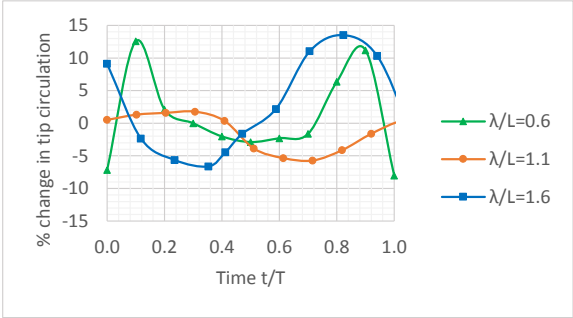

Figure 32 Change in the propeller tip circulation at 12 O'clock position of the propeller blade at different time intervals in waves as compared to the tip circulation in calm water wake.

In order to know if the amount of change in tip circulation can considerably alter the noise level, the possible increase in the inboard noise should be estimated. Noise level at a certain inboard location can be related to the tip vortex index (TVI) as given by [23].

$$\mathrm{dB_{ref}} = 20\log(TVI.n^2.D^2) + 20\log \mathrm{C_1} + 10\log \mathrm{C_2} \quad (1)$$

$$\text{also, TVI} \propto \Gamma^2 \quad (2)$$

where Γ is blade tip circulation at 12 O'clock position.

Therefore, difference in noise level in the presence of waves as compared to calm water can be written as:

$$\mathrm{dB_{wave}} - \mathrm{dB_{calm}} = 20\log\left(\frac{\Gamma_{\mathrm{wave}}}{\Gamma_{\mathrm{calm}}}\right)^2 \quad (3)$$

Using Eq. (3) and the results in Figure 32, it is found that the noise level can rise by up to 2 dB due to the change in tip circulation observed in waves.

3.2. Effect of increased loading

The ship speed will decrease in the presence of head waves, mainly due to added resistance on the hull. Change in speed will in principle affect the wake variations, both due to changes in motions and in generation of wake in general. Due to the computational expense, the CFD calculations were only performed at the design speed of 14 knots. Therefore, the propeller has been analyzed at 12 and 13 knots in the same set of wake variations observed in the presence of waves at the design speed of the ship, using the same propeller RPM as used in the design speed condition. Speed loss increases the loading on the propeller blades, thus affecting the amount of cavitation. Therefore, increase in the level of pressure pulses due to speed loss in different waves has been studied. The propeller was also analyzed in the calm water wake distribution found for 14 knots at 12 knots speed to compare the rate

of change of pressure pulses for different wake distributions as a function of speed loss. The differences in the first harmonic amplitude of pressure pulses obtained at the design speed of 14 knots and reduced speeds of 12 and 13 knots in various wake distributions are presented in Figure 33. The maximum increase in the first harmonic amplitude of pressure pulses due to a speed loss of 2 knots is around 0.58 kPa, and roughly half that value for a speed loss of one knot. Increase in pressure pulses due to speed loss is similar in calm water and waves. Therefore, even if wakes in waves are not available, it is possible to approximate the potential increase in pressure pulses by calculating the speed loss and using the resulting increase in propeller loading.

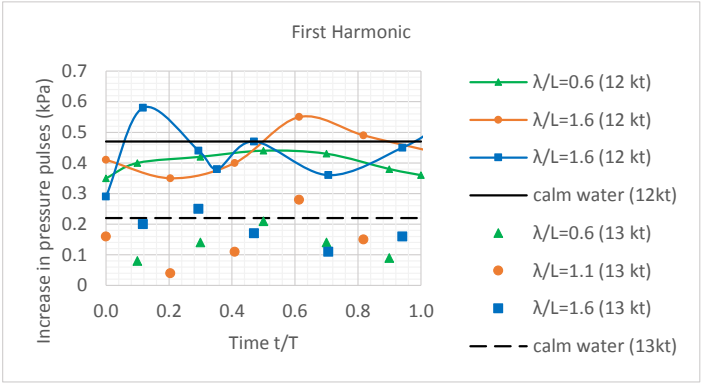

Figure 33 Increase in first harmonic pressure pulses as a result of increased load on the propeller caused by speed loss of 1 and 2 knots, while keeping RPM unchanged.

3.3. Effect of RPM fluctuations

The propeller was analyzed at the instant of maximum average wake velocity (meaning minimum Taylor wake fraction) in each wave condition, which corresponds to the instance of maximum RPM. The simulations were performed considering wakes corresponding to those time instances and maximum increase in RPM, estimated based on the method explained earlier. Pressure pulses thus obtained at higher RPM were compared with those obtained in respective wakes at design RPM. Simulations were also performed in calm water wake at highest RPM observed among three wave conditions that is 4.2%. The increase in all three harmonics of pressure pulses in three wave conditions and calm water have been plotted in Figure 34. The increase in first harmonic amplitude is most significant in all four cases, with the maximum increase seen in λ/L=1.1 (Note that maximum increase in RPM was observed in this case). The level of increase in first and second harmonic amplitude is comparable in calm water wake and different wave conditions. Therefore, like in the case of increased propeller loading due to speed loss, also the effect of RPM fluctuation can be estimated by simulating

the propeller in calm water wake at higher RPM. Change in third harmonic amplitude is small in all four cases.

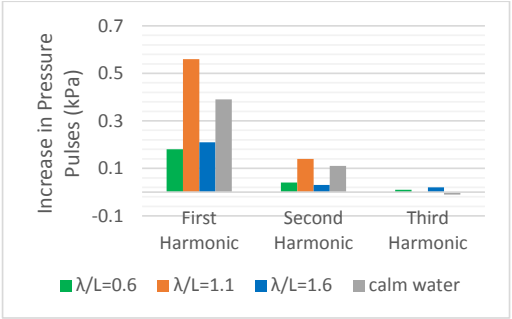

Figure 34 Increase in pressure pulses due to RPM fluctuations in three waves and calm water.

3.4. Summary of the factors affecting the pressure pulses in waves

The maximum increase in the first, second and third harmonic of pressure pulses due to different factors is compared in Figure 35. Wake variation has by far the largest influence on all the three harmonics of pressure pulses followed by almost equal influence due to RPM variation and speed loss. The increase in pressure pulses due to wake change is as high as the level of pressure pulses in calm water. The effect of a change in cavitation number due to ship motions and dynamic wave pressure is relatively small on the first harmonic, while the effect is comparable to that due to RPM variation and speed loss on second and third harmonic amplitudes.

RPM variation and ship motions increase the pressure pulses at some time intervals while decreasing at other times, since propeller immersion and RPM oscillates around the mean value. Interestingly, in λ/L=1.1 and 1.6 where ship motions are considerable, propeller immersion and Taylor wake fraction vary in phase; meaning that the propeller immersion is maximum when Taylor wake fraction is also at its peak. This can be observed by comparing Figure 21 and Figure 26. Consequently, the occurrence of lowest propeller immersion coincides with the highest propeller RPM (because of lowest Taylor wake fraction) both of which contribute to increase in pressure pulses. In λ/L=0.6, exact opposite is true thus the effect of ship motions on pressure pulses would tend to cancel the effect of RPM fluctuation; however in this case, changes in pressure pulses due to ship motions are small.

From the propeller design point of view, obtaining the wake variation in waves is a challenging task in itself as already mentioned. Therefore, considering the currently available tools, it is difficult to take into account the effect of wake variation in the propeller design. Significant change in the performance was observed both in this case and in the earlier investigations using a single screw ship [11]. Therefore, to limit the required computations while still capturing the main effects of waves in

propeller performance, it is recommended to obtain wake variation at least in the critical wave condition (wavelength close to ship length) to have an idea about the possible performance variations due to waves.

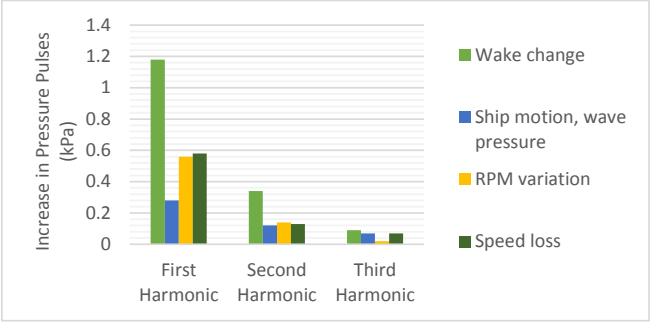

Figure 35 Comparison of maximum increase in pressure pulses due to different factors in the presence of waves.

3.5. Efficiency variation in waves

As wake varies substantially in waves, its effect on propeller efficiency should be investigated. Total propeller efficiency in three head waves has been plotted in Figure 36. It can be noted that total propeller efficiency varies significantly in the presence of waves. To investigate the cause of change in efficiency, propeller efficiency, thrust and torque coefficients in calm water and in waves have been plotted in Figure 37 along with propeller open water curves. Since efficiency, thrust and torque coefficients follow open water curves, it can be concluded that the efficiency is primarily affected by the average change in wake fraction and not much due to variation in nominal wake distribution. Whereas cavitation and pressure pulses are directly related to wake distribution, and they depend less on average wake as discussed earlier.

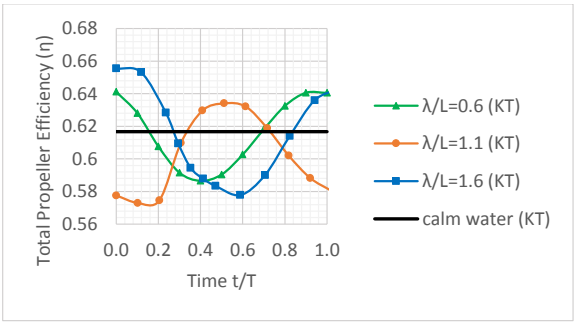

Figure 36 Variation in efficiency in the presence of waves due to wake variation.

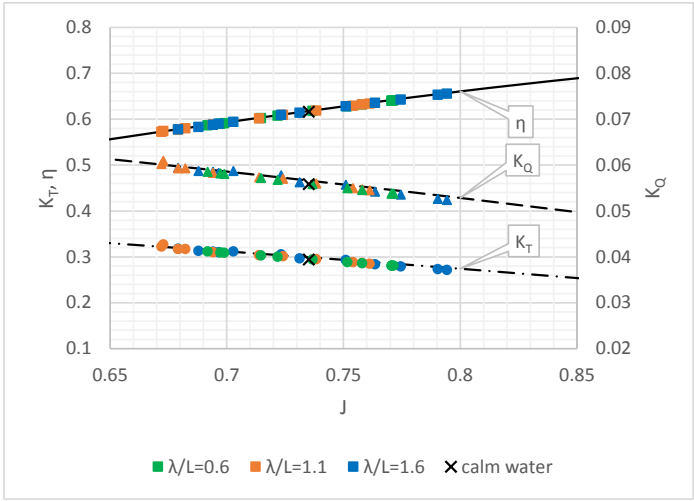

Figure 37 Propeller efficiency, K_T and K_Q in the presence of waves along with propeller open water data. Propeller open-water efficiency (η), K_T and K_Q are shown using solid, dash-dot and dashed lines respectively. Efficiency, K_T and K_Q in waves are denoted by square, circle and triangle respectively. (λ/L = 0.6–Green; λ/L = 1.1–Orange; λ/L = 1.6–Blue). Cross marks denote the performance in calm water wake.

4. Conclusions

Propeller performance of a 8000 dwt chemical tanker with twin Azipull propulsion has been assessed in the presence of waves regarding efficiency, cavitation, and pressure pulses. The effect of wake change, ship motions, wave dynamic pressure, speed loss, and RPM variation has been considered. It is found that the variation of wake distribution in waves has the largest impact on the propeller performance and the greatest change in cavitation and pressure pulses occurred for waves λ/L = 1.1 and 1.6; changes were relatively small in λ/L = 0.6.

A notable increase in pressure pulses was observed in the analysis of KVLCC2 propeller in the presence of waves [11]. It was believed that the high wake of a full-bodied single-screw ship also lead to strong wake variations due waves. Therefore, it was expected that wake change would be smaller in the case of the current twin-podded case vessel. However, noteworthy wake variations were detected due to waves and ship motions also for the current ship, as shown in section 2.2.

In the analysis reported in [11], wake variation led to higher pressure pulses. However, change in maximum cavitation volume was small. Also, cavity volume variations showed different patterns in the wake in calm water and waves. In the current analysis, both cavity volume and pressure pulses are larger in the presence of waves. However, the pattern of cavity volume variation is similar in calm

water and waves for most of the cases. Considering both studies, carried out on different types of hull and propeller designs, propeller performance does differ in the presence of waves. Therefore, analyzing the propeller performance in the presence of waves is recommended when designing the propeller.

While designing the propeller, there is a trade-off between the allowable level of pressure pulses and efficiency. Restricting the level of pressure pulses also limits the maximum efficiency that can be achieved. It is possible that in the absence of any knowledge about pressure pulses in a rough sea, a conservative estimate is applied thus leading to low pressure pulses at the cost of efficiency. Therefore, if pressure pulses in realistic operating conditions can be calculated, the further increase in the efficiency can be achieved while still avoiding detrimental effects due to waves. However, getting wake data for operation in waves is hard. Thus, we recommend that the wake field in a regular wave of a wavelength close to ship length should be taken into account in the design, in addition to the calm water wake field.

In the view of a substantial increase in the cavitation volumes in the presence of waves, further investigations are necessary to find out if the erosivity of the cavitation is getting affected due to wake change, since even a small amount of erosive cavitation can damage the propeller.

Acknowledgement

This work is funded by the project ‘Low Energy and Emission Design of Ships’ (LEEDS, NFR 216432/O70) where the Research Council of Norway is the main sponsor. We are grateful to Rolls-Royce Hydrodynamic Research Centre along with the University Technology centers of Rolls Royce at NTNU and Chalmers University of Technology for their support. We also thank Professor Bjørnar Pettersen from NTNU and Leif Vartdal from Rolls Royce Marine, Norway for insightful discussions and suggestions.

References

[1] Moor D.I., Murdey D.C. Motions and Propulsion of Single Screw Models in Head Seas, Part II. The Royal Institution of Naval Architects. 1970; Vol 112(2).

[2] Nakamura S., Naito S. Propulsive performance of a container ship in waves. J. Soc. Naval Archit. Jpn. 1975; Vol 158.

[3] Guo B.J., Steen S., Deng G.B. Seakeeping prediction of KVLCC2 in head waves with RANS. Applied Ocean Research. 2012; Vol 35: 56-67. http://dx.doi.org/10.1016/j.apor.2011.12.003

[4] Wu P.C. A CFD Study on Added Resistance, Motions and Phase Averaged Wake Fields of Full Form Ship Model in Head Waves [Doctoral Dissertation]: Osaka University; July 2013.

[5] Albers A.B., Gent W.v. Unsteady wake velocities due to waves and motions measured on a ship model in head waves. 15th Symposium on Naval Hydrodynamics, 1985.

[6] Hayashi Y. Phase-Averaged 3D PIV Flow Field Measurement for KVLCC2 Model in Waves [M. Sc. Thesis (in Japanese)]: Osaka University; 2012.

[7] Chevalier Y., Kim Y.H. Propeller Operating in a Seaway. PRADS'95, Seoul, Korea, 1995.

[8] Jessup S.D., Wang H.-C. Propeller Cavitation Prediction for a Ship in a Seaway. DTIC Document; 1996.

[9] ABS. Guidance notes on ship vibration. Houston, USA; April 2006 (Updated January 2015).

[10] VERITEC. Vibration control in ships. Høvik, Norway: A.S. Veritec Marine Technology Consultants, Noise and Vibration Group; 1985.

[11] Taskar B., Steen S., Bensow R.E., Schröder B. Effect of waves on cavitation and pressure pulses. Applied Ocean Research. 2016; Vol 60: 61-74. http://dx.doi.org/10.1016/j.apor.2016.08.009

[12] He L., Tian Y., Kinnas S.A. MPUF-3A (Version 3.1) User's Manual and Documentation 11-1. Ocean Engineering, University of Texas at Austin; 2011.

[13] Larsson L., Stern F., Visonneau M., Hino T., Hirata N., Kim J. Proceedings, Tokyo 2015 Workshop on CFD in Ship Hydrodynamics2015.

[14] Alterskjær S.A. R&D8000 phase I, calm water tests with 3 different fore ships. MARINTEK; 2010.

[15] Fathi D.E. ShipX Vessel Responses (VERES), User's Manual. MARINTEK; 2016.

[16] Alterskjær S.A. R&D8000 phase I, head sea tests with 3 different fore ships. MARINTEK; 2011.

[17] Taskar B., Yum K.K., Steen S., Pedersen E. The effect of waves on engine-propeller dynamics and propulsion performance of ships. Ocean Engineering. 2016; Vol 122: 262-277. http://dx.doi.org/10.1016/j.oceaneng.2016.06.034

[18] Taskar B., Steen S. Analysis of Propulsion Performance of KVLCC2 in Waves. Fourth International Symposium on Marine Propulsors, Austin, Texas, USA, 2015.

[19] Sun H., Kinnas S.A. HULLFPP, Hull Field Point Potential, User's Manual and Documentation. University of Texas, Austin; 2007.

[20] Hwang Y., Sun H., kinnas S.A. Prediction of Hull Pressure Fluctuations Induced by Single and Twin Propellers. Propellers/Shafting '06 Symposium, SNAME, Williamsburg, VA. , 2006.

[21] Carlton J.S. Marine propellers and propulsion (Third Edition). Oxford: Butterworth-Heinemann; 2012.

[22] Odabasi A.Y., Fitzsimmons P.A. Alternative Methods for Wake Quality Assessment. International Shipbuilding Progress. 1978; Vol 25: 8 p.

[23] Raestad A.E. Tip vortex index-an engineering approach to propeller noise prediction. The Naval Architect, July/August 1996.

Previous PhD theses published at the Department of Marine Technology

Norwegian University of Science and Technology

Previous PhD theses published at the Departement of Marine Technology (earlier: Faculty of Marine Technology) NORWEGIAN UNIVERSITY OF SCIENCE AND TECHNOLOGY

Report No.	Author	Title
	Kavlie, Dag	Optimization of Plane Elastic Grillages, 1967
	Hansen, Hans R.	Man-Machine Communication and Data-Storage Methods in Ship Structural Design, 1971
	Gisvold, Kaare M.	A Method for non-linear mixed -integer programming and its Application to Design Problems, 1971
	Lund, Sverre	Tanker Frame Optimalization by means of SUMT-Transformation and Behaviour Models, 1971
	Vinje, Tor	On Vibration of Spherical Shells Interacting with Fluid, 1972
	Lorentz, Jan D.	Tank Arrangement for Crude Oil Carriers in Accordance with the new Anti-Pollution Regulations, 1975
	Carlsen, Carl A.	Computer-Aided Design of Tanker Structures, 1975
	Larsen, Carl M.	Static and Dynamic Analysis of Offshore Pipelines during Installation, 1976
UR-79-01	Brigt Hatlestad, MK	The finite element method used in a fatigue evaluation of fixed offshore platforms. (Dr.Ing. Thesis)
UR-79-02	Erik Pettersen, MK	Analysis and design of cellular structures. (Dr.Ing. Thesis)
UR-79-03	Sverre Valsgård, MK	Finite difference and finite element methods applied to nonlinear analysis of plated structures. (Dr.Ing. Thesis)
UR-79-04	Nils T. Nordsve, MK	Finite element collapse analysis of structural members considering imperfections and stresses due to fabrication. (Dr.Ing. Thesis)
UR-79-05	Ivar J. Fylling, MK	Analysis of towline forces in ocean towing systems. (Dr.Ing. Thesis)
UR-80-06	Nils Sandsmark, MM	Analysis of Stationary and Transient Heat Conduction by the Use of the Finite Element Method. (Dr.Ing. Thesis)
UR-80-09	Sverre Haver, MK	Analysis of uncertainties related to the stochastic modeling of ocean waves. (Dr.Ing. Thesis)
UR-81-15	Odland, Jonas	On the Strength of welded Ring stiffened cylindrical Shells primarily subjected to axial Compression
UR-82-17	Engesvik, Knut	Analysis of Uncertainties in the fatigue Capacity of

		Welded Joints
UR-82-18	Rye, Henrik	Ocean wave groups
UR-83-30	Eide, Oddvar Inge	On Cumulative Fatigue Damage in Steel Welded Joints
UR-83-33	Mo, Olav	Stochastic Time Domain Analysis of Slender Offshore Structures
UR-83-34	Amdahl, Jørgen	Energy absorption in Ship-platform impacts
UR-84-37	Mørch, Morten	Motions and mooring forces of semi submersibles as determined by full-scale measurements and theoretical analysis
UR-84-38	Soares, C. Guedes	Probabilistic models for load effects in ship structures
UR-84-39	Aarsnes, Jan V.	Current forces on ships
UR-84-40	Czujko, Jerzy	Collapse Analysis of Plates subjected to Biaxial Compression and Lateral Load
UR-85-46	Alf G. Engseth, MK	Finite element collapse analysis of tubular steel offshore structures. (Dr.Ing. Thesis)
UR-86-47	Dengody Sheshappa, MP	A Computer Design Model for Optimizing Fishing Vessel Designs Based on Techno-Economic Analysis. (Dr.Ing. Thesis)
UR-86-48	Vidar Aanesland, MH	A Theoretical and Numerical Study of Ship Wave Resistance. (Dr.Ing. Thesis)
UR-86-49	Heinz-Joachim Wessel, MK	Fracture Mechanics Analysis of Crack Growth in Plate Girders. (Dr.Ing. Thesis)
UR-86-50	Jon Taby, MK	Ultimate and Post-ultimate Strength of Dented Tubular Members. (Dr.Ing. Thesis)
UR-86-51	Walter Lian, MH	A Numerical Study of Two-Dimensional Separated Flow Past Bluff Bodies at Moderate KC-Numbers. (Dr.Ing. Thesis)
UR-86-52	Bjørn Sortland, MH	Force Measurements in Oscillating Flow on Ship Sections and Circular Cylinders in a U-Tube Water Tank. (Dr.Ing. Thesis)
UR-86-53	Kurt Strand, MM	A System Dynamic Approach to One-dimensional Fluid Flow. (Dr.Ing. Thesis)
UR-86-54	Arne Edvin Løken, MH	Three Dimensional Second Order Hydrodynamic Effects on Ocean Structures in Waves. (Dr.Ing. Thesis)
UR-86-55	Sigurd Falch, MH	A Numerical Study of Slamming of Two-Dimensional Bodies. (Dr.Ing. Thesis)
UR-87-56	Arne Braathen, MH	Application of a Vortex Tracking Method to the Prediction of Roll Damping of a Two-Dimension Floating Body. (Dr.Ing. Thesis)

UR-87-57	Bernt Leira, MK	Gaussian Vector Processes for Reliability Analysis involving Wave-Induced Load Effects. (Dr.Ing. Thesis)
UR-87-58	Magnus Småvik, MM	Thermal Load and Process Characteristics in a Two-Stroke Diesel Engine with Thermal Barriers (in Norwegian). (Dr.Ing. Thesis)
MTA-88-59	Bernt Arild Bremdal, MP	An Investigation of Marine Installation Processes – A Knowledge - Based Planning Approach. (Dr.Ing. Thesis)
MTA-88-60	Xu Jun, MK	Non-linear Dynamic Analysis of Space-framed Offshore Structures. (Dr.Ing. Thesis)
MTA-89-61	Gang Miao, MH	Hydrodynamic Forces and Dynamic Responses of Circular Cylinders in Wave Zones. (Dr.Ing. Thesis)
MTA-89-62	Martin Greenhow, MH	Linear and Non-Linear Studies of Waves and Floating Bodies. Part I and Part II. (Dr.Techn. Thesis)
MTA-89-63	Chang Li, MH	Force Coefficients of Spheres and Cubes in Oscillatory Flow with and without Current. (Dr.Ing. Thesis
MTA-89-64	Hu Ying, MP	A Study of Marketing and Design in Development of Marine Transport Systems. (Dr.Ing. Thesis)
MTA-89-65	Arild Jæger, MH	Seakeeping, Dynamic Stability and Performance of a Wedge Shaped Planing Hull. (Dr.Ing. Thesis)
MTA-89-66	Chan Siu Hung, MM	The dynamic characteristics of tilting-pad bearings
MTA-89-67	Kim Wikstrøm, MP	Analysis av projekteringen for ett offshore projekt. (Licenciat-avhandling)
MTA-89-68	Jiao Guoyang, MK	Reliability Analysis of Crack Growth under Random Loading, considering Model Updating. (Dr.Ing. Thesis)
MTA-89-69	Arnt Olufsen, MK	Uncertainty and Reliability Analysis of Fixed Offshore Structures. (Dr.Ing. Thesis)
MTA-89-70	Wu Yu-Lin, MR	System Reliability Analyses of Offshore Structures using improved Truss and Beam Models. (Dr.Ing. Thesis)
MTA-90-71	Jan Roger Hoff, MH	Three-dimensional Green function of a vessel with forward speed in waves. (Dr.Ing. Thesis)
MTA-90-72	Rong Zhao, MH	Slow-Drift Motions of a Moored Two-Dimensional Body in Irregular Waves. (Dr.Ing. Thesis)
MTA-90-73	Atle Minsaas, MP	Economical Risk Analysis. (Dr.Ing. Thesis)
MTA-90-74	Knut-Aril Farnes, MK	Long-term Statistics of Response in Non-linear Marine Structures. (Dr.Ing. Thesis)
MTA-90-75	Torbjørn Sotberg, MK	Application of Reliability Methods for Safety Assessment of Submarine Pipelines. (Dr.Ing.

		Thesis)
MTA-90-76	Zeuthen, Steffen, MP	SEAMAID. A computational model of the design process in a constraint-based logic programming environment. An example from the offshore domain. (Dr.Ing. Thesis)
MTA-91-77	Haagensen, Sven, MM	Fuel Dependant Cyclic Variability in a Spark Ignition Engine - An Optical Approach. (Dr.Ing. Thesis)
MTA-91-78	Løland, Geir, MH	Current forces on and flow through fish farms. (Dr.Ing. Thesis)
MTA-91-79	Hoen, Christopher, MK	System Identification of Structures Excited by Stochastic Load Processes. (Dr.Ing. Thesis)
MTA-91-80	Haugen, Stein, MK	Probabilistic Evaluation of Frequency of Collision between Ships and Offshore Platforms. (Dr.Ing. Thesis)
MTA-91-81	Sødahl, Nils, MK	Methods for Design and Analysis of Flexible Risers. (Dr.Ing. Thesis)
MTA-91-82	Ormberg, Harald, MK	Non-linear Response Analysis of Floating Fish Farm Systems. (Dr.Ing. Thesis)
MTA-91-83	Marley, Mark J., MK	Time Variant Reliability under Fatigue Degradation. (Dr.Ing. Thesis)
MTA-91-84	Krokstad, Jørgen R., MH	Second-order Loads in Multidirectional Seas. (Dr.Ing. Thesis)
MTA-91-85	Molteberg, Gunnar A., MM	The Application of System Identification Techniques to Performance Monitoring of Four Stroke Turbocharged Diesel Engines. (Dr.Ing. Thesis)
MTA-92-86	Mørch, Hans Jørgen Bjelke, MH	Aspects of Hydrofoil Design: with Emphasis on Hydrofoil Interaction in Calm Water. (Dr.Ing. Thesis)
MTA-92-87	Chan Siu Hung, MM	Nonlinear Analysis of Rotordynamic Instabilities in Highspeed Turbomachinery. (Dr.Ing. Thesis)
MTA-92-88	Bessason, Bjarni, MK	Assessment of Earthquake Loading and Response of Seismically Isolated Bridges. (Dr.Ing. Thesis)
MTA-92-89	Langli, Geir, MP	Improving Operational Safety through exploitation of Design Knowledge - an investigation of offshore platform safety. (Dr.Ing. Thesis)
MTA-92-90	Sævik, Svein, MK	On Stresses and Fatigue in Flexible Pipes. (Dr.Ing. Thesis)
MTA-92-91	Ask, Tor Ø., MM	Ignition and Flame Growth in Lean Gas-Air Mixtures. An Experimental Study with a Schlieren System. (Dr.Ing. Thesis)
MTA-86-92	Hessen, Gunnar, MK	Fracture Mechanics Analysis of Stiffened Tubular Members. (Dr.Ing. Thesis)

MTA-93-93	Steinebach, Christian, MM	Knowledge Based Systems for Diagnosis of Rotating Machinery. (Dr.Ing. Thesis)
MTA-93-94	Dalane, Jan Inge, MK	System Reliability in Design and Maintenance of Fixed Offshore Structures. (Dr.Ing. Thesis)
MTA-93-95	Steen, Sverre, MH	Cobblestone Effect on SES. (Dr.Ing. Thesis)
MTA-93-96	Karunakaran, Daniel, MK	Nonlinear Dynamic Response and Reliability Analysis of Drag-dominated Offshore Platforms. (Dr.Ing. Thesis)
MTA-93-97	Hagen, Arnulf, MP	The Framework of a Design Process Language. (Dr.Ing. Thesis)
MTA-93-98	Nordrik, Rune, MM	Investigation of Spark Ignition and Autoignition in Methane and Air Using Computational Fluid Dynamics and Chemical Reaction Kinetics. A Numerical Study of Ignition Processes in Internal Combustion Engines. (Dr.Ing. Thesis)
MTA-94-99	Passano, Elizabeth, MK	Efficient Analysis of Nonlinear Slender Marine Structures. (Dr.Ing. Thesis)
MTA-94-100	Kvålsvold, Jan, MH	Hydroelastic Modelling of Wetdeck Slamming on Multihull Vessels. (Dr.Ing. Thesis)
MTA-94-102	Bech, Sidsel M., MK	Experimental and Numerical Determination of Stiffness and Strength of GRP/PVC Sandwich Structures. (Dr.Ing. Thesis)
MTA-95-103	Paulsen, Hallvard, MM	A Study of Transient Jet and Spray using a Schlieren Method and Digital Image Processing. (Dr.Ing. Thesis)
MTA-95-104	Hovde, Geir Olav, MK	Fatigue and Overload Reliability of Offshore Structural Systems, Considering the Effect of Inspection and Repair. (Dr.Ing. Thesis)
MTA-95-105	Wang, Xiaozhi, MK	Reliability Analysis of Production Ships with Emphasis on Load Combination and Ultimate Strength. (Dr.Ing. Thesis)
MTA-95-106	Ulstein, Tore, MH	Nonlinear Effects of a Flexible Stern Seal Bag on Cobblestone Oscillations of an SES. (Dr.Ing. Thesis)
MTA-95-107	Solaas, Frøydis, MH	Analytical and Numerical Studies of Sloshing in Tanks. (Dr.Ing. Thesis)
MTA-95-108	Hellan, Øyvind, MK	Nonlinear Pushover and Cyclic Analyses in Ultimate Limit State Design and Reassessment of Tubular Steel Offshore Structures. (Dr.Ing. Thesis)
MTA-95-109	Hermundstad, Ole A., MK	Theoretical and Experimental Hydroelastic Analysis of High Speed Vessels. (Dr.Ing. Thesis)
MTA-96-110	Bratland, Anne K., MH	Wave-Current Interaction Effects on Large-Volume Bodies in Water of Finite Depth. (Dr.Ing. Thesis)
MTA-96-111	Herfjord, Kjell, MH	A Study of Two-dimensional Separated Flow by a Combination of the Finite Element Method and

		Navier-Stokes Equations. (Dr.Ing. Thesis)
MTA-96-112	Æsøy, Vilmar, MM	Hot Surface Assisted Compression Ignition in a Direct Injection Natural Gas Engine. (Dr.Ing. Thesis)
MTA-96-113	Eknes, Monika L., MK	Escalation Scenarios Initiated by Gas Explosions on Offshore Installations. (Dr.Ing. Thesis)
MTA-96-114	Erikstad, Stein O., MP	A Decision Support Model for Preliminary Ship Design. (Dr.Ing. Thesis)
MTA-96-115	Pedersen, Egil, MH	A Nautical Study of Towed Marine Seismic Streamer Cable Configurations. (Dr.Ing. Thesis)
MTA-97-116	Moksnes, Paul O., MM	Modelling Two-Phase Thermo-Fluid Systems Using Bond Graphs. (Dr.Ing. Thesis)
MTA-97-117	Halse, Karl H., MK	On Vortex Shedding and Prediction of Vortex-Induced Vibrations of Circular Cylinders. (Dr.Ing. Thesis)
MTA-97-118	Igland, Ragnar T., MK	Reliability Analysis of Pipelines during Laying, considering Ultimate Strength under Combined Loads. (Dr.Ing. Thesis)
MTA-97-119	Pedersen, Hans-P., MP	Levendefiskteknologi for fiskefartøy. (Dr.Ing. Thesis)
MTA-98-120	Vikestad, Kyrre, MK	Multi-Frequency Response of a Cylinder Subjected to Vortex Shedding and Support Motions. (Dr.Ing. Thesis)
MTA-98-121	Azadi, Mohammad R. E., MK	Analysis of Static and Dynamic Pile-Soil-Jacket Behaviour. (Dr.Ing. Thesis)
MTA-98-122	Ulltang, Terje, MP	A Communication Model for Product Information. (Dr.Ing. Thesis)
MTA-98-123	Torbergsen, Erik, MM	Impeller/Diffuser Interaction Forces in Centrifugal Pumps. (Dr.Ing. Thesis)
MTA-98-124	Hansen, Edmond, MH	A Discrete Element Model to Study Marginal Ice Zone Dynamics and the Behaviour of Vessels Moored in Broken Ice. (Dr.Ing. Thesis)
MTA-98-125	Videiro, Paulo M., MK	Reliability Based Design of Marine Structures. (Dr.Ing. Thesis)
MTA-99-126	Mainçon, Philippe, MK	Fatigue Reliability of Long Welds Application to Titanium Risers. (Dr.Ing. Thesis)
MTA-99-127	Haugen, Elin M., MH	Hydroelastic Analysis of Slamming on Stiffened Plates with Application to Catamaran Wetdecks. (Dr.Ing. Thesis)
MTA-99-128	Langhelle, Nina K., MK	Experimental Validation and Calibration of Nonlinear Finite Element Models for Use in Design of Aluminium Structures Exposed to Fire. (Dr.Ing. Thesis)
MTA-99-	Berstad, Are J., MK	Calculation of Fatigue Damage in Ship Structures.

129		(Dr.Ing. Thesis)
MTA-99-130	Andersen, Trond M., MM	Short Term Maintenance Planning. (Dr.Ing. Thesis)
MTA-99-131	Tveiten, Bård Wathne, MK	Fatigue Assessment of Welded Aluminium Ship Details. (Dr.Ing. Thesis)
MTA-99-132	Søreide, Fredrik, MP	Applications of underwater technology in deep water archaeology. Principles and practice. (Dr.Ing. Thesis)
MTA-99-133	Tønnessen, Rune, MH	A Finite Element Method Applied to Unsteady Viscous Flow Around 2D Blunt Bodies With Sharp Corners. (Dr.Ing. Thesis)
MTA-99-134	Elvekrok, Dag R., MP	Engineering Integration in Field Development Projects in the Norwegian Oil and Gas Industry. The Supplier Management of Norne. (Dr.Ing. Thesis)
MTA-99-135	Fagerholt, Kjetil, MP	Optimeringsbaserte Metoder for Ruteplanlegging innen skipsfart. (Dr.Ing. Thesis)
MTA-99-136	Bysveen, Marie, MM	Visualization in Two Directions on a Dynamic Combustion Rig for Studies of Fuel Quality. (Dr.Ing. Thesis)
MTA-2000-137	Storteig, Eskild, MM	Dynamic characteristics and leakage performance of liquid annular seals in centrifugal pumps. (Dr.Ing. Thesis)
MTA-2000-138	Sagli, Gro, MK	Model uncertainty and simplified estimates of long term extremes of hull girder loads in ships. (Dr.Ing. Thesis)
MTA-2000-139	Tronstad, Harald, MK	Nonlinear analysis and design of cable net structures like fishing gear based on the finite element method. (Dr.Ing. Thesis)
MTA-2000-140	Kroneberg, André, MP	Innovation in shipping by using scenarios. (Dr.Ing. Thesis)
MTA-2000-141	Haslum, Herbjørn Alf, MH	Simplified methods applied to nonlinear motion of spar platforms. (Dr.Ing. Thesis)
MTA-2001-142	Samdal, Ole Johan, MM	Modelling of Degradation Mechanisms and Stressor Interaction on Static Mechanical Equipment Residual Lifetime. (Dr.Ing. Thesis)
MTA-2001-143	Baarholm, Rolf Jarle, MH	Theoretical and experimental studies of wave impact underneath decks of offshore platforms. (Dr.Ing. Thesis)
MTA-2001-144	Wang, Lihua, MK	Probabilistic Analysis of Nonlinear Wave-induced Loads on Ships. (Dr.Ing. Thesis)
MTA-2001-145	Kristensen, Odd H. Holt, MK	Ultimate Capacity of Aluminium Plates under Multiple Loads, Considering HAZ Properties. (Dr.Ing. Thesis)
MTA-2001-146	Greco, Marilena, MH	A Two-Dimensional Study of Green-Water

		Loading. (Dr.Ing. Thesis)
MTA-2001-147	Heggelund, Svein E., MK	Calculation of Global Design Loads and Load Effects in Large High Speed Catamarans. (Dr.Ing. Thesis)
MTA-2001-148	Babalola, Olusegun T., MK	Fatigue Strength of Titanium Risers – Defect Sensitivity. (Dr.Ing. Thesis)
MTA-2001-149	Mohammed, Abuu K., MK	Nonlinear Shell Finite Elements for Ultimate Strength and Collapse Analysis of Ship Structures. (Dr.Ing. Thesis)
MTA-2002-150	Holmedal, Lars E., MH	Wave-current interactions in the vicinity of the sea bed. (Dr.Ing. Thesis)
MTA-2002-151	Rognebakke, Olav F., MH	Sloshing in rectangular tanks and interaction with ship motions. (Dr.Ing. Thesis)
MTA-2002-152	Lader, Pål Furset, MH	Geometry and Kinematics of Breaking Waves. (Dr.Ing. Thesis)
MTA-2002-153	Yang, Qinzheng, MH	Wash and wave resistance of ships in finite water depth. (Dr.Ing. Thesis)
MTA-2002-154	Melhus, Øyvin, MM	Utilization of VOC in Diesel Engines. Ignition and combustion of VOC released by crude oil tankers. (Dr.Ing. Thesis)
MTA-2002-155	Ronæss, Marit, MH	Wave Induced Motions of Two Ships Advancing on Parallel Course. (Dr.Ing. Thesis)
MTA-2002-156	Økland, Ole D., MK	Numerical and experimental investigation of whipping in twin hull vessels exposed to severe wet deck slamming. (Dr.Ing. Thesis)
MTA-2002-157	Ge, Chunhua, MK	Global Hydroelastic Response of Catamarans due to Wet Deck Slamming. (Dr.Ing. Thesis)
MTA-2002-158	Byklum, Eirik, MK	Nonlinear Shell Finite Elements for Ultimate Strength and Collapse Analysis of Ship Structures. (Dr.Ing. Thesis)
IMT-2003-1	Chen, Haibo, MK	Probabilistic Evaluation of FPSO-Tanker Collision in Tandem Offloading Operation. (Dr.Ing. Thesis)
IMT-2003-2	Skaugset, Kjetil Bjørn, MK	On the Suppression of Vortex Induced Vibrations of Circular Cylinders by Radial Water Jets. (Dr.Ing. Thesis)
IMT-2003-3	Chezhian, Muthu	Three-Dimensional Analysis of Slamming. (Dr.Ing. Thesis)
IMT-2003-4	Buhaug, Øyvind	Deposit Formation on Cylinder Liner Surfaces in Medium Speed Engines. (Dr.Ing. Thesis)
IMT-2003-5	Tregde, Vidar	Aspects of Ship Design: Optimization of Aft Hull with Inverse Geometry Design. (Dr.Ing. Thesis)
IMT-	Wist, Hanne Therese	Statistical Properties of Successive Ocean Wave

2003-6		Parameters. (Dr.Ing. Thesis)
IMT-2004-7	Ransau, Samuel	Numerical Methods for Flows with Evolving Interfaces. (Dr.Ing. Thesis)
IMT-2004-8	Soma, Torkel	Blue-Chip or Sub-Standard. A data interrogation approach of identity safety characteristics of shipping organization. (Dr.Ing. Thesis)
IMT-2004-9	Ersdal, Svein	An experimental study of hydrodynamic forces on cylinders and cables in near axial flow. (Dr.Ing. Thesis)
IMT-2005-10	Brodtkorb, Per Andreas	The Probability of Occurrence of Dangerous Wave Situations at Sea. (Dr.Ing. Thesis)
IMT-2005-11	Yttervik, Rune	Ocean current variability in relation to offshore engineering. (Dr.Ing. Thesis)
IMT-2005-12	Fredheim, Arne	Current Forces on Net-Structures. (Dr.Ing. Thesis)
IMT-2005-13	Heggernes, Kjetil	Flow around marine structures. (Dr.Ing. Thesis
IMT-2005-14	Fouques, Sebastien	Lagrangian Modelling of Ocean Surface Waves and Synthetic Aperture Radar Wave Measurements. (Dr.Ing. Thesis)
IMT-2006-15	Holm, Håvard	Numerical calculation of viscous free surface flow around marine structures. (Dr.Ing. Thesis)
IMT-2006-16	Bjørheim, Lars G.	Failure Assessment of Long Through Thickness Fatigue Cracks in Ship Hulls. (Dr.Ing. Thesis)
IMT-2006-17	Hansson, Lisbeth	Safety Management for Prevention of Occupational Accidents. (Dr.Ing. Thesis)
IMT-2006-18	Zhu, Xinying	Application of the CIP Method to Strongly Nonlinear Wave-Body Interaction Problems. (Dr.Ing. Thesis)
IMT-2006-19	Reite, Karl Johan	Modelling and Control of Trawl Systems. (Dr.Ing. Thesis)
IMT-2006-20	Smogeli, Øyvind Notland	Control of Marine Propellers. From Normal to Extreme Conditions. (Dr.Ing. Thesis)
IMT-2007-21	Storhaug, Gaute	Experimental Investigation of Wave Induced Vibrations and Their Effect on the Fatigue Loading of Ships. (Dr.Ing. Thesis)
IMT-2007-22	Sun, Hui	A Boundary Element Method Applied to Strongly Nonlinear Wave-Body Interaction Problems. (PhD Thesis, CeSOS)
IMT-2007-23	Rustad, Anne Marthine	Modelling and Control of Top Tensioned Risers. (PhD Thesis, CeSOS)
IMT-2007-24	Johansen, Vegar	Modelling flexible slender system for real-time simulations and control applications
IMT-2007-25	Wroldsen, Anders Sunde	Modelling and control of tensegrity structures.

		(PhD Thesis, CeSOS)
IMT-2007-26	Aronsen, Kristoffer Høye	An experimental investigation of in-line and combined inline and cross flow vortex induced vibrations. (Dr. avhandling, IMT)
IMT-2007-27	Gao, Zhen	Stochastic Response Analysis of Mooring Systems with Emphasis on Frequency-domain Analysis of Fatigue due to Wide-band Response Processes (PhD Thesis, CeSOS)
IMT-2007-28	Thorstensen, Tom Anders	Lifetime Profit Modelling of Ageing Systems Utilizing Information about Technical Condition. (Dr.ing. thesis, IMT)
IMT-2008-29	Refsnes, Jon Erling Gorset	Nonlinear Model-Based Control of Slender Body AUVs (PhD Thesis, IMT)
IMT-2008-30	Berntsen, Per Ivar B.	Structural Reliability Based Position Mooring. (PhD-Thesis, IMT)
IMT-2008-31	Ye, Naiquan	Fatigue Assessment of Aluminium Welded Box-stiffener Joints in Ships (Dr.ing. thesis, IMT)
IMT-2008-32	Radan, Damir	Integrated Control of Marine Electrical Power Systems. (PhD-Thesis, IMT)
IMT-2008-33	Thomassen, Paul	Methods for Dynamic Response Analysis and Fatigue Life Estimation of Floating Fish Cages. (Dr.ing. thesis, IMT)
IMT-2008-34	Pákozdi, Csaba	A Smoothed Particle Hydrodynamics Study of Two-dimensional Nonlinear Sloshing in Rectangular Tanks. (Dr.ing.thesis, IMT/ CeSOS)
IMT-2007-35	Grytøyr, Guttorm	A Higher-Order Boundary Element Method and Applications to Marine Hydrodynamics. (Dr.ing.thesis, IMT)
IMT-2008-36	Drummen, Ingo	Experimental and Numerical Investigation of Nonlinear Wave-Induced Load Effects in Containerships considering Hydroelasticity. (PhD thesis, CeSOS)
IMT-2008-37	Skejic, Renato	Maneuvering and Seakeeping of a Singel Ship and of Two Ships in Interaction. (PhD-Thesis, CeSOS)
IMT-2008-38	Harlem, Alf	An Age-Based Replacement Model for Repairable Systems with Attention to High-Speed Marine Diesel Engines. (PhD-Thesis, IMT)
IMT-2008-39	Alsos, Hagbart S.	Ship Grounding. Analysis of Ductile Fracture, Bottom Damage and Hull Girder Response. (PhD-thesis, IMT)
IMT-2008-40	Graczyk, Mateusz	Experimental Investigation of Sloshing Loading and Load Effects in Membrane LNG Tanks Subjected to Random Excitation. (PhD-thesis, CeSOS)
IMT-2008-41	Taghipour, Reza	Efficient Prediction of Dynamic Response for Flexible amd Multi-body Marine Structures. (PhD-

		thesis, CeSOS)
IMT-2008-42	Ruth, Eivind	Propulsion control and thrust allocation on marine vessels. (PhD thesis, CeSOS)
IMT-2008-43	Nystad, Bent Helge	Technical Condition Indexes and Remaining Useful Life of Aggregated Systems. PhD thesis, IMT
IMT-2008-44	Soni, Prashant Kumar	Hydrodynamic Coefficients for Vortex Induced Vibrations of Flexible Beams, PhD thesis, CeSOS
IMT-2009-45	Amlashi, Hadi K.K.	Ultimate Strength and Reliability-based Design of Ship Hulls with Emphasis on Combined Global and Local Loads. PhD Thesis, IMT
IMT-2009-46	Pedersen, Tom Arne	Bond Graph Modelling of Marine Power Systems. PhD Thesis, IMT
IMT-2009-47	Kristiansen, Trygve	Two-Dimensional Numerical and Experimental Studies of Piston-Mode Resonance. PhD-Thesis, CeSOS
IMT-2009-48	Ong, Muk Chen	Applications of a Standard High Reynolds Number Model and a Stochastic Scour Prediction Model for Marine Structures. PhD-thesis, IMT
IMT-2009-49	Hong, Lin	Simplified Analysis and Design of Ships subjected to Collision and Grounding. PhD-thesis, IMT
IMT-2009-50	Koushan, Kamran	Vortex Induced Vibrations of Free Span Pipelines, PhD thesis, IMT
IMT-2009-51	Korsvik, Jarl Eirik	Heuristic Methods for Ship Routing and Scheduling. PhD-thesis, IMT
IMT-2009-52	Lee, Jihoon	Experimental Investigation and Numerical in Analyzing the Ocean Current Displacement of Longlines. Ph.d.-Thesis, IMT.
IMT-2009-53	Vestbøstad, Tone Gran	A Numerical Study of Wave-in-Deck Impact usin a Two-Dimensional Constrained Interpolation Profile Method, Ph.d.thesis, CeSOS.
IMT-2009-54	Bruun, Kristine	Bond Graph Modelling of Fuel Cells for Marine Power Plants. Ph.d.-thesis, IMT
IMT 2009-55	Holstad, Anders	Numerical Investigation of Turbulence in a Sekwed Three-Dimensional Channel Flow, Ph.d.-thesis, IMT.
IMT 2009-56	Ayala-Uraga, Efren	Reliability-Based Assessment of Deteriorating Ship-shaped Offshore Structures, Ph.d.-thesis, IMT
IMT 2009-57	Kong, Xiangjun	A Numerical Study of a Damaged Ship in Beam Sea Waves. Ph.d.-thesis, IMT/CeSOS.
IMT 2010-58	Kristiansen, David	Wave Induced Effects on Floaters of Aquaculture Plants, Ph.d.-thesis, CeSOS.

IMT 2010-59	Ludvigsen, Martin	An ROV-Toolbox for Optical and Acoustic Scientific Seabed Investigation. Ph.d.-thesis IMT.
IMT 2010-60	Hals, Jørgen	Modelling and Phase Control of Wave-Energy Converters. Ph.d.thesis, CeSOS.
IMT 2010- 61	Shu, Zhi	Uncertainty Assessment of Wave Loads and Ultimate Strength of Tankers and Bulk Carriers in a Reliability Framework. Ph.d. Thesis, IMT/ CeSOS
IMT 2010-62	Shao, Yanlin	Numerical Potential-Flow Studies on Weakly-Nonlinear Wave-Body Interactions with/without Small Forward Speed, Ph.d.thesis,CeSOS.
IMT 2010-63	Califano, Andrea	Dynamic Loads on Marine Propellers due to Intermittent Ventilation. Ph.d.thesis, IMT.
IMT 2010-64	El Khoury, George	Numerical Simulations of Massively Separated Turbulent Flows, Ph.d.-thesis, IMT
IMT 2010-65	Seim, Knut Sponheim	Mixing Process in Dense Overflows with Emphasis on the Faroe Bank Channel Overflow. Ph.d.thesis, IMT
IMT 2010-66	Jia, Huirong	Structural Analysis of Intect and Damaged Ships in a Collission Risk Analysis Perspective. Ph.d.thesis CeSoS.
IMT 2010-67	Jiao, Linlin	Wave-Induced Effects on a Pontoon-type Very Large Floating Structures (VLFS). Ph.D.-thesis, CeSOS.
IMT 2010-68	Abrahamsen, Bjørn Christian	Sloshing Induced Tank Roof with Entrapped Air Pocket. Ph.d.thesis, CeSOS.
IMT 2011-69	Karimirad, Madjid	Stochastic Dynamic Response Analysis of Spar-Type Wind Turbines with Catenary or Taut Mooring Systems. Ph.d.-thesis, CeSOS.
IMT - 2011-70	Erlend Meland	Condition Monitoring of Safety Critical Valves. Ph.d.-thesis, IMT.
IMT – 2011-71	Yang, Limin	Stochastic Dynamic System Analysis of Wave Energy Converter with Hydraulic Power Take-Off, with Particular Reference to Wear Damage Analysis, Ph.d. Thesis, CeSOS.
IMT – 2011-72	Visscher, Jan	Application of Particla Image Velocimetry on Turbulent Marine Flows, Ph.d.Thesis, IMT.
IMT – 2011-73	Su, Biao	Numerical Predictions of Global and Local Ice Loads on Ships. Ph.d.Thesis, CeSOS.
IMT – 2011-74	Liu, Zhenhui	Analytical and Numerical Analysis of Iceberg Collision with Ship Structures. Ph.d.Thesis, IMT.
IMT – 2011-75	Aarsæther, Karl Gunnar	Modeling and Analysis of Ship Traffic by Observation and Numerical Simulation. Ph.d.Thesis, IMT.

Imt – 2011-76	Wu, Jie	Hydrodynamic Force Identification from Stochastic Vortex Induced Vibration Experiments with Slender Beams. Ph.d.Thesis, IMT.
Imt – 2011-77	Amini, Hamid	Azimuth Propulsors in Off-design Conditions. Ph.d.Thesis, IMT.
IMT – 2011-78	Nguyen, Tan-Hoi	Toward a System of Real-Time Prediction and Monitoring of Bottom Damage Conditions During Ship Grounding. Ph.d.thesis, IMT.
IMT- 2011-79	Tavakoli, Mohammad T.	Assessment of Oil Spill in Ship Collision and Grounding, Ph.d.thesis, IMT.
IMT- 2011-80	Guo, Bingjie	Numerical and Experimental Investigation of Added Resistance in Waves. Ph.d.Thesis, IMT.
IMT- 2011-81	Chen, Qiaofeng	Ultimate Strength of Aluminium Panels, considering HAZ Effects, IMT
IMT- 2012-82	Kota, Ravikiran S.	Wave Loads on Decks of Offshore Structures in Random Seas, CeSOS.
IMT- 2012-83	Sten, Ronny	Dynamic Simulation of Deep Water Drilling Risers with Heave Compensating System, IMT.
IMT- 2012-84	Berle, Øyvind	Risk and resilience in global maritime supply chains, IMT.
IMT- 2012-85	Fang, Shaoji	Fault Tolerant Position Mooring Control Based on Structural Reliability, CeSOS.
IMT- 2012-86	You, Jikun	Numerical studies on wave forces and moored ship motions in intermediate and shallow water, CeSOS.
IMT- 2012-87	Xiang ,Xu	Maneuvering of two interacting ships in waves, CeSOS
IMT- 2012-88	Dong, Wenbin	Time-domain fatigue response and reliability analysis of offshore wind turbines with emphasis on welded tubular joints and gear components, CeSOS
IMT- 2012-89	Zhu, Suji	Investigation of Wave-Induced Nonlinear Load Effects in Open Ships considering Hull Girder Vibrations in Bending and Torsion, CeSOS
IMT- 2012-90	Zhou, Li	Numerical and Experimental Investigation of Station-keeping in Level Ice, CeSOS
IMT- 2012-91	Ushakov, Sergey	Particulate matter emission characteristics from diesel enignes operating on conventional and alternative marine fuels, IMT
IMT- 2013-1	Yin, Decao	Experimental and Numerical Analysis of Combined In-line and Cross-flow Vortex Induced Vibrations, CeSOS

IMT-2013-2	Kurniawan, Adi	Modelling and geometry optimisation of wave energy converters, CeSOS
IMT-2013-3	Al Ryati, Nabil	Technical condition indexes doe auxiliary marine diesel engines, IMT
IMT-2013-4	Firoozkoohi, Reza	Experimental, numerical and analytical investigation of the effect of screens on sloshing, CeSOS
IMT-2013-5	Ommani, Babak	Potential-Flow Predictions of a Semi-Displacement Vessel Including Applications to Calm Water Broaching, CeSOS
IMT-2013-6	Xing, Yihan	Modelling and analysis of the gearbox in a floating spar-type wind turbine, CeSOS
IMT-7-2013	Balland, Océane	Optimization models for reducing air emissions from ships, IMT
IMT-8-2013	Yang, Dan	Transitional wake flow behind an inclined flat plate-----Computation and analysis, IMT
IMT-9-2013	Abdillah, Suyuthi	Prediction of Extreme Loads and Fatigue Damage for a Ship Hull due to Ice Action, IMT
IMT-10-2013	Ramìrez, Pedro Agustìn Pèrez	Ageing management and life extension of technical systems- Concepts and methods applied to oil and gas facilities, IMT
IMT-11-2013	Chuang, Zhenju	Experimental and Numerical Investigation of Speed Loss due to Seakeeping and Maneuvering. IMT
IMT-12-2013	Etemaddar, Mahmoud	Load and Response Analysis of Wind Turbines under Atmospheric Icing and Controller System Faults with Emphasis on Spar Type Floating Wind Turbines, IMT
IMT-13-2013	Lindstad, Haakon	Strategies and measures for reducing maritime CO2 emissons, IMT
IMT-14-2013	Haris, Sabril	Damage interaction analysis of ship collisions, IMT
IMT-15-2013	Shainee, Mohamed	Conceptual Design, Numerical and Experimental Investigation of a SPM Cage Concept for Offshore Mariculture, IMT
IMT-16-2013	Gansel, Lars	Flow past porous cylinders and effects of biofouling and fish behavior on the flow in and around Atlantic salmon net cages, IMT
IMT-17-2013	Gaspar, Henrique	Handling Aspects of Complexity in Conceptual Ship Design, IMT
IMT-18-2013	Thys, Maxime	Theoretical and Experimental Investigation of a Free Running Fishing Vessel at Small Frequency of Encounter, CeSOS
IMT-19-2013	Aglen, Ida	VIV in Free Spanning Pipelines, CeSOS

IMT-1-2014	Song, An	Theoretical and experimental studies of wave diffraction and radiation loads on a horizontally submerged perforated plate, CeSOS
IMT-2-2014	Rogne, Øyvind Ygre	Numerical and Experimental Investigation of a Hinged 5-body Wave Energy Converter, CeSOS
IMT-3-2014	Dai, Lijuan	Safe and efficient operation and maintenance of offshore wind farms ,IMT
IMT-4-2014	Bachynski, Erin Elizabeth	Design and Dynamic Analysis of Tension Leg Platform Wind Turbines, CeSOS
IMT-5-2014	Wang, Jingbo	Water Entry of Freefall Wedged – Wedge motions and Cavity Dynamics, CeSOS
IMT-6-2014	Kim, Ekaterina	Experimental and numerical studies related to the coupled behavior of ice mass and steel structures during accidental collisions, IMT
IMT-7-2014	Tan, Xiang	Numerical investigation of ship's continuous- mode icebreaking in leverl ice, CeSOS
IMT-8-2014	Muliawan, Made Jaya	Design and Analysis of Combined Floating Wave and Wind Power Facilities, with Emphasis on Extreme Load Effects of the Mooring System, CeSOS
IMT-9-2014	Jiang, Zhiyu	Long-term response analysis of wind turbines with an emphasis on fault and shutdown conditions, IMT
IMT-10-2014	Dukan, Fredrik	ROV Motion Control Systems, IMT
IMT-11-2014	Grimsmo, Nils I.	Dynamic simulations of hydraulic cylinder for heave compensation of deep water drilling risers, IMT
IMT-12-2014	Kvittem, Marit I.	Modelling and response analysis for fatigue design of a semisubmersible wind turbine, CeSOS
IMT-13-2014	Akhtar, Juned	The Effects of Human Fatigue on Risk at Sea, IMT
IMT-14-2014	Syahroni, Nur	Fatigue Assessment of Welded Joints Taking into Account Effects of Residual Stress, IMT
IMT-1-2015	Bøckmann, Eirik	Wave Propulsion of ships, IMT
IMT-2-2015	Wang, Kai	Modelling and dynamic analysis of a semi-submersible floating vertical axis wind turbine, CeSOS
IMT-3-2015	Fredriksen, Arnt Gunvald	A numerical and experimental study of a two-dimensional body with moonpool in waves and current, CeSOS
IMT-4-2015	Jose Patricio Gallardo Canabes	Numerical studies of viscous flow around bluff bodies, IMT

IMT-5-2015	Vegard Longva	Formulation and application of finite element techniques for slender marine structures subjected to contact interactions, IMT
IMT-6-2015	Jacobus De Vaal	Aerodynamic modelling of floating wind turbines, CeSOS
IMT-7-2015	Fachri Nasution	Fatigue Performance of Copper Power Conductors, IMT
IMT-8-2015	Oleh I Karpa	Development of bivariate extreme value distributions for applications in marine technology,CeSOS
IMT-9-2015	Daniel de Almeida Fernandes	An output feedback motion control system for ROVs, AMOS
IMT-10-2015	Bo Zhao	Particle Filter for Fault Diagnosis: Application to Dynamic Positioning Vessel and Underwater Robotics, CeSOS
IMT-11-2015	Wenting Zhu	Impact of emission allocation in maritime transportation, IMT
IMT-12-2015	Amir Rasekhi Nejad	Dynamic Analysis and Design of Gearboxes in Offshore Wind Turbines in a Structural Reliability Perspective, CeSOS
IMT-13-2015	Arturo Jesùs Ortega Malca	Dynamic Response of Flexibles Risers due to Unsteady Slug Flow, CeSOS
IMT-14-2015	Dagfinn Husjord	Guidance and decision-support system for safe navigation of ships operating in close proximity, IMT
IMT-15-2015	Anirban Bhattacharyya	Ducted Propellers: Behaviour in Waves and Scale Effects, IMT
IMT-16-2015	Qin Zhang	Image Processing for Ice Parameter Identification in Ice Management, IMT
IMT-1-2016	Vincentius Rumawas	Human Factors in Ship Design and Operation: An Experiential Learning, IMT
IMT-2-2016	Martin Storheim	Structural response in ship-platform and ship-ice collisions, IMT
IMT-3-2016	Mia Abrahamsen Prsic	Numerical Simulations of the Flow around single and Tandem Circular Cylinders Close to a Plane Wall, IMT
IMT-4-2016	Tufan Arslan	Large-eddy simulations of cross-flow around ship sections, IMT

IMT-5-2016	Pierre Yves-Henry	Parametrisation of aquatic vegetation in hydraulic and coastal research,IMT
IMT-6-2016	Lin Li	Dynamic Analysis of the Instalation of Monopiles for Offshore Wind Turbines, CeSOS
IMT-7-2016	Øivind Kåre Kjerstad	Dynamic Positioning of Marine Vessels in Ice, IMT
IMT-8-2016	Xiaopeng Wu	Numerical Analysis of Anchor Handling and Fish Trawling Operations in a Safety Perspective, CeSOS
IMT-9-2016	Zhengshun Cheng	Integrated Dynamic Analysis of Floating Vertical Axis Wind Turbines, CeSOS
IMT-10-2016	Ling Wan	Experimental and Numerical Study of a Combined Offshore Wind and Wave Energy Converter Concept
IMT-11-2016	Wei Chai	Stochastic dynamic analysis and reliability evaluation of the roll motion for ships in random seas, CeSOS
IMT-12-2016	Øyvind Selnes Patricksson	Decision support for conceptual ship design with focus on a changing life cycle and future uncertainty, IMT
IMT-13-2016	Mats Jørgen Thorsen	Time domain analysis of vortex-induced vibrations, IMT
IMT-14-2016	Edgar McGuinness	Safety in the Norwegian Fishing Fleet – Analysis and measures for improvement, IMT
IMT-15-2016	Sepideh Jafarzadeh	Energy effiency and emission abatement in the fishing fleet, IMT
IMT-16-2016	Wilson Ivan Guachamin Acero	Assessment of marine operations for offshore wind turbine installation with emphasis on response-based operational limits, IMT
IMT-17-2016	Mauro Candeloro	Tools and Methods for Autonomous Operations on Seabed and Water Coumn using Underwater Vehicles, IMT
IMT-18-2016	Valentin Chabaud	Real-Time Hybrid Model Testing of Floating Wind Tubines, IMT
IMT-1-2017	Mohammad Saud Afzal	Three-dimensional streaming in a sea bed boundary layer, IMT
IMT-2-2017	Peng Li	A Theoretical and Experimental Study of Wave-induced Hydroelastic Response of a Circular Floating Collar, IMT
IMT-3-2017	Martin Bergström	A simulation-based design method for arctic maritime transport systems, IMT

IMT-4-2017	Bhushan Taskar	The effect of waves on marine propellers and propulsion, IMT